To Serpil Polat, Necati Polat and Dali

PLASTIC DEGRADATION USING GENETICALLY ENGINEERED MICROORGANISMS

A THESIS SUBMITTED TO

THE GRADUATE SCHOOL OF ENGINEERING AND SCIENCE

OF BILKENT UNIVERSITY

IN PARTIAL FULFILLMENT OF THE REQUIREMENTS FOR

THE DEGREE OF

MASTER OF SCIENCE

IN

MATERIALS SCIENCE AND NANOTECHNOLOGY

By

CEM DIRSE POLAT

JANUARY 2025

PLASTIC DEGRADATION USING GENETICALLY ENGINEERED MICROORGANISMS

By Cem Dirse Polat

January 2025

We certify that we have read this dissertation and that in our opinion it is fully adequate,
in scope and in quality, as a thesis for the degree of Master of Science.

_____
Urartu Özgür Şafak Şeker (Advisor)

_____
Bilge Baytekin

_____
İrem Erel Göktepe

Approved for the Graduate School of Engineering and Science:

_____

Orhan Arıkan
Director of the Graduate School

ABSTRACT

PLASTIC DEGRADATION USING GENETICALLY ENGINEERED MICROORGANISMS

Cem Dirse Polat

MSc in Materials Science and Nanotechnology

Advisor: Urartu Özgür Şafak Şeker

January, 2025

The usage of PET plastics in daily life have excessively increased in the last decade. The increased usage of PET is accompanied with the massive amount of PET waste accumulating rapidly. Environmental pollution caused by this waste has reached a critical point with pollutants being found even in the most remote parts of the world. Causing massive damage to ecosystems and even human health, PET plastic waste needs to be handled urgently. Although there are ongoing PET recycling and treatment efforts, the current methods in use are insufficient. The techniques currently used are either costly, leave a significant carbon footprint or are lacking in their ability to recycle microplastics. However, with the discovery of microorganisms which have the ability of degrading PET, biodegradation of PET products has emerged as a promising green alternative.

In this thesis we designed bacterial tools to utilize the PET hydrolyzing enzyme, PETase. For this purpose, living bacterial platforms were engineered. The first system employed *E. coli* as the host to display PETase on the cellular surface. With PETase molecules anchored on its surface, aiding in the stability and the activity of the enzyme, the system will be a useful tool for PET degradation. For the surface display system, the Ag43 autotransporter protein is used. The system was cloned, and expression was analyzed using immunocytochemistry labeling. The activity of the system was analyzed with chromatography and mass spectrometry. The second system proposed uses *E. coli* once again as a workhorse for PETase secretion, creating a simple yet effective tool for the bioremediation of PET. For secretion of the enzyme, the disruption of Braun's lipoprotein to create a leaky outer membrane is exploited. The system was cloned, and the cloning was verified. Also, the activity of native PETase was analyzed with HPLC and mass spectrometry. With this analysis, the PET degrading activity of PETase was confirmed.

Keywords: Synthetic Biology, PETase, PET Bioremediation, Bacterial Surface Display, Bacterial Protein Secretion

ÖZET

GENETİĞİ DEĞİŞTİRİLMİŞ MİKROORGANİZMA KULLANARAK PLASTİK DEGRADASYONU

Cem Dirse Polat

Malzeme Bilimi ve Nanoteknoloji, Yüksek Lisans

Tez Danışmanı: Urartu Özgür Şafak Şeker

Ocak, 2025

PET plastiklerin günlük hayatta kullanımı son on yılda aşırı derecede artmıştır. PET kullanımındaki bu artış, hızla biriken büyük miktarda PET atığını ortaya çıkarmıştır. Dünyanın en uzak bölgelerinde bile PET kirleticilerine rastlanması, bu atıkların neden olduğu çevre kirliliğinin ne denli kritik bir noktaya ulaştığını göstermektedir. Ekosistemlere ve insan sağlığına büyük zarar veren PET plastik atıklarının geri dönüştürülmesi acilen ele alınması gereken bir problemdir. Her ne kadar PET geri dönüşüm çabaları devam etse de, mevcut yöntemler yetersizdir. Günümüzde kullanılan teknikler ya maliyetlidir, önemli bir karbon ayak izi bırakır ya da mikroplastikleri geri dönüştürme konusunda yetersizdir. Ancak, PET'i parçalama yeteneğine sahip mikroorganizmaların keşfi ile birlikte, PET ürünlerinin biyolojik ayrışması umut verici bir yeşil alternatif olarak ortaya çıkmıştır.

Bu tezin amacı, PET biyoremediasyonu amacıyla PET hidrolize eden enzim olan PETaz'ın etkin şekilde ifade edilmesi ve taşınması için bir sistem tasarlamaktır. Bu amaç doğrultusunda, canlı bir bakteriyel platform tasarlanmıştır. Tasarlanan ilk system ile PETaz hücre yüzeyinde sergilenmiştir. PETaz moleküllerinin yüzeye bağlanmasıyla enzimin kararlılığı ve aktivitesine katkı sağlanacak ve bu canlı bakteriyel sistem PET ayrıştırılması için faydalı bir araç olacaktır. Yüzey sergileme sistemi için Ag43 ototransporter proteini kullanılmıştır. Sistem klonlanmış ve immünositokimya etiketleme yöntemiyle analiz edilmiştir, protein lokalizasyonu verifiye edilmiştir. Sistemin aktivitesi, kromatografi ve kütle spektrometresi ile incelenmiştir. Oluşturulan ikinci sistemde, enzimin salgılanması için, Braun'un lipoproteinini bozarak geçirgen bir dış membran oluşturulması sağlanmıştır. Sistem klonlanmış ve klonlama doğrulanmıştır. Ayrıca, doğal PETaz'ın aktivitesi HPLC, kütle spektrometresi ve elektron mikroskobu ile analiz edilmiştir. Bu analiz sayesinde PETaz'ın PET degradasyonu yapabildiği doğrulanmıştır.

Anahtar Kelimeler: Sentetik Biyoloji, PETaz Enzimi, PET Biyoremediasyonu, Bakteriyel Yüzey Gösterim, Bakteriyel Protein Salgılanması

ACKNOWLEDGEMENTS

First and foremost, I would like to start by thanking Dr. Urartu Şeker. As my thesis advisor, he offered unwavering support throughout this journey. He placed his trust in me, gave me the chance to work with the brilliant people in our lab and provided me with the perfect environment to succeed. I greatly admire his dedication to our craft and completing my master's education under his mentorship has been a privilege.

I am also thankful to my jury members, Dr. Bilge Baytekin and Dr. İrem Erel Göktepe for their valuable time and attention.

Next, I am grateful to all the SBL lab members that I have worked with. They helped me with every step along the way, whether it was with the brainstorming sessions for project proposals, help with experimental procedures, with the morale they gave me when things started to get tough, or just the occasional coffee breaks. I have felt their support from the beginning, and I am very honored that I get to call them my friends not just colleagues.

To my wonderful girlfriend Ceren, I am incredibly lucky to have someone so sweet, so understanding and so gracious. You have been along with me for the entire ride, the highest highs and lowest lows. You have backed me up and supported me each and every day and I sincerely believe that the hardship we have endured together brought us closer than ever. One more time, thank you.

Finally, to my mom and dad, I would like to express my deepest gratitude. You believed in me even in times when it got difficult for me to believe in myself. You (and obviously Dali) are the reason I never gave up. Thank you for always being with me, I could not have come this far without you.

TABLE OF CONTENTS

CHAPTER I: INTRODUCTION 1

1.1 The Problem of Plastic and Microplastic Pollution 1

1.2 Biotechnological Approach for the Remediation of PET 6

1.3 *Is*PETase and *Is*MHETase 7

1.4 Aim of the Study 10

CHAPTER II: MATERIALS AND METHODS 13

2.1 Cell Strains, Cell Maintenance, Cell Growth and Transformation 13

2.2 Construction of pET-22b(+) – PETase – 6xHis Vector 14

2.3 Construction of pET-22b(+) –PelB - 6xHis – Ag43 – PETase Vector 15

2.4 Construction of pET-22b(+) – pLacO MicL + pNTetO PETase Vector 16

2.5 Next-Generation Sequencing (NGS), Sanger Sequencing and *In Silico* Sequence Alignments 17

2.6 Expression, Purification and Quantification of PETase Enzyme 18

2.7 Coomassie Staining and Western Blotting of Purified PETase 21

2.8 Expression of Surface-Displayed PETase 23

2.9 Protein Precipitation and Western Blotting of Surface-Displayed PETase 23

2.10 Immunocytochemistry (ICC) Labeling of Surface Displayed PETase 24

2.11 p-NPB Assay for Purified PETase Enzyme Activity 25

2.12 PET Degradation Assay for PETase 26

2.13 PET Degradation Assay for Surface-Displayed PETase 28

2.14 Reverse Phase HPLC and LC/MS-QTOF Analysis of PET Degradation Assay Products 30

2.15 SEM Imaging of Enzyme Treated PET 31

CHAPTER III: RESULTS AND DISCUSSION 32

3.1 Cloning and Expression of PETase Protein 32

3.2 Analysis of PETase Activity 38

3.3 Visualization of Enzymatic PET Degradation 47

3.4 Cloning and Expression of Whole Cell System Displaying PETase Protein 49

3.5 Analysis of Whole Cell System Activity 55

3.6 Cloning of the iLOM-SS - PETase Construct 61
CHAPTER IV: CONCLUSION 64
BIBLIOGRAPHY 67
APPENDIX A 74
DNA SEQUENCES OF CONSTRUCTS 74
APPENDIX B 78
LIST OF PRIMERS 78
APPENDIX C 79
PLASMID MAPS OF CONSTRUCTS 79
APPENDIX D 81
SEQUENCING RESULTS 81
APPENDIX E 84
ADDITIONAL REACTION RECIPES 84
APPENDIX F 89
ADDITIONAL RESULTS 89

LIST OF TABLES

Table A. 1: Gene sequences used in this study. 74
Table B. 1: Primer sequences used in this study. 78
Table E. 1. Recipes of LB growth medium and LB agar 84
Table E. 2. Reagent amounts for Q5 Polymerase reactions. 84
Table E. 3. Thermal cycler settings for Q5 Polymerase reactions. 84
Table E. 4. Double restriction enzyme reaction set-up. 85
Table E. 5. Recipe for homemade Gibson assembly mixture (1.33X). 85
Table E. 6. Recipe for 5X Isothermal Buffer. 85
Table E. 7. Transformation and Storage (TSS) buffer recipe. 86
Table E. 8. Recipe for HisTrap Binding Buffer (pH 7.4). 86
Table E. 9. Recipe for HisTrap Elution Buffer (ph 7.4). 86
Table E. 10. Recipe for M9 Minimal Growth Media. 86
Table E. 11. Recipe for 50 mM Glycine-NaOH Buffer (pH 9.0). 87
Table E. 12. Setup for T4 ligation reaction. 87
Table E. 13. Recipe for Coomassie destaining solution 87
Table E. 14. Recipe for 1X Towbin Buffer. 87
Table E. 15. 1x TBST recipe. 88
Table E. 16. Recipe for 10x PBS (pH 7.4) 88

LIST OF FIGURES

Figure 1. Plastic produced globally by sector. Upwards of 250 million tons of waste are produced annually. Most plastic waste is landfilled (40%) [12].....2
Figure 2. 3D crystal structure of A) PETase and B) MHETase [61].....8
Figure 3. PET degradation pathway. PETase hydrolyses PET into BHET, MHET and TPA. MHETase hydrolyses MHET into TPA and EG. Illustration drawn using BioRender.com. 8
Figure 4. Illustration of the aim of the study. The two engineered constructs: A) The surface display of PETase on the surface of *E. coli*. The beta domain of Ag43 embeds itself to the outer membrane as a β barrel structure whereas PETase is attached via the alpha domain. B) The bacterial secretion of PETase. micL sRNA disrupts the expression of Braun's lipoprotein. The lack of Braun's lipoprotein creates a leaky outer membrane which allows for the free diffusion of PETase. Illustration drawn using BioRender.com.....12
Figure 5. Illustration of the PETase expression and isolation workflow. Cloned vectors are transformed into *E. coli* BL21 (DE3) cells, after overnight growth and the following IPTG induction protein is expressed. To extract the protein, cells are resuspended with appropriate buffer and are lysed. Lysed cells are filtered and PETase is purified using FPLC. Purified protein is later used in downstream applications. Illustration drawn using BioRender.com.....21
Figure 6. The principle of the pNPB assay. Illustration drawn using BioRender.com. 25
Figure 7. Illustration of isolated PETase activity assay. A) For the no refresh group samples, PET film and PETase solution are incubated for 10 days. After termination, samples are HPLC analyzed. B) For the enzyme refresh group samples, PET film and PETase solution incubated for a total of 10 days. Every 24 hours the solution is renewed with freshly isolated PETase. After termination, collected samples are HPLC analyzed. Illustration created in BioRender.com.....27

Figure 8. Illustration of surface displayed PETase activity assay. A) Assay for buffer group samples. Induced cells are suspended in 50 mM glycine-NaOH buffer and incubated with PET film. After 10 days, samples are collected for HPLC analysis. B) Assay for LB and M9 group samples. Induced cells are resuspended in respective media and incubated with PET film. Every 3 days fresh media is supplemented to the culture and samples are collected. Once the assay is terminated, samples are HPLC analyzed. Illustration created in BioRender.com. 29
Figure 9. Working principle of HPLC analysis. Samples collected from the activity assays are run through a C18 column where the mixture components are separated. The components are analyzed for absorbance at 240 nm which accounts for PET degradation products (TPA, MHET, BHET). Illustration created using BioRender.com. 30
Figure 10. Schematic illustration of the PETase expression construct. A polyhistidine tag is attached to PETase via a GS linker. Expression is under T7 promoter control. Illustration created using BioRender.com....32
Figure 11. PCR amplification of PETase. Expected band is 941 bp. Lane 1 is the 1 kb plus DNA ladder (NEB)....33
Figure 12. Restriction digestion to retrieve the pET-22b backbone. Expected band is 5298 bp. Lane 1 is the 1 kb plus DNA ladder (NEB). Dashed line indicates spliced gel image.....34
Figure 13. Western blot analysis of purified PETase. Lane 2 and lane 3 represent the elute from the FPLC protein isolation process. For lane 4, the same isolation process is applied to empty BL21 cells as a control group. PageRuler prestained protein ladder (Thermo Scientific) is used as the marker, lane 1.....35
Figure 14. Coomassie staining of isolated PETase. The isolate from the FPLC process can be viewed in lane 2. PageRuler prestained protein ladder (Thermo Scientific) is used as a protein marker, lane 1.....36
Figure 15. Enzyme vs Autohydrolysis results for the pnpB assay. 405 nm absorbances of the samples after treatment at different substrate concentrations. Enzyme

concentrations used is constant. Analysis of the statistical significance was determined with student's t-test. ns indicates no significance, * indicates $p \leq 0.05$. ..39
Figure 16. HPLC chromatogram of TPA standard dilutions. The TPA peaks are marked with a red arrow. 41
Figure 17. HPLC analysis of no refresh group samples. A) Chromatogram of no refresh group with 0 μg/ml PETase concentration (buffer only). B) Chromatogram of no refresh group with 50 μg/ml PETase concentration. C) Chromatogram of no refresh group with 150 μg/ml PETase concentration. D) Chromatograms in A, B and C are overlapped. Samples collected and analyzed after 10-day incubation. 42
Figure 18. HPLC analysis of refresh group samples. A) Samples collected at day 1. B) Samples collected at day 5. C) Samples collected at day 10. Negative control is PETase only (no substrate). Peaks of interested are mark with red arrows. 43
Figure 19. Mass spectrometry analysis of PET degradation products. A) Analysis of peaks at 9 min. B) Analysis of peaks at 10 min. C) Analysis of peaks at 11 min. Expected values are marked with red. 45
Figure 20. SEM images of treated PET film samples. A) PET film treated with 150 μg/ml every 24 hours. B) PET film treated with 50 μg/ml every 24 hours. C) PET film treated with 0 μg/ml (only 50 mM glycine-NaOH buffer) every 24 hours. D) Untreated PET film. 47
Figure 21. The schematic illustration of the Ag43-PETase expression construct. An N-terminal polyhistidine tag is linked to PETase via a GS linker. Flanking the his-tagged PETase, the pelB leader sequence can be found on the N-terminal. On the C-terminal, the Ag43 construct, passenger, and translocation domains, respectively, can be found. The expression cassette is under the control of the T7 promoter. 50
Figure 22. PCR amplification of PETase with overhangs. The expected band of 944 base pairs can be observed in lane 2. 1 kb plus DNA ladder (NEB) is used as a marker, lane 1.....50
Figure 23. Digestion results of pET-22b – pelB – 6His – sfGFP – Ag43 plasmid. The expected band of 8013 base pairs can be observed in lane 1. 1 kb plus DNA ladder (NEB) is used as a DNA marker, lane 2. 51

Figure 24. Western blot analysis of surface displayed PETase. Lane 2 is empty BL21 negative control. Lane 3 and 4 represents 0 IPTG negative control replicates. Lanes 5 and 6 represents 0.25 mM IPTG induced group replicates. Lanes 7 and 8 represent 0.5 mM IPTG induced group replicates. Lanes 9 and 10 represent 1 mM IPTG induced group replicates. PageRuler prestained protein ladder is used as the marker in lane 1. 52
Figure 25. ICC staining of induced Ag43-PETase cells. Top left: Brightfield imaging of cells. Top right: blue light excited, for DAPI visualization. Bottom left: red-yellow light excited, for Dylight550 visualization. Scale bars represent 50 μm. Bottom right: all images merged. 54
Figure 26. HPLC chromatogram for buffer group samples. Unknown bands of interest can be observed around the 10-minute mark. PET incubated with empty BL21 is used as the negative control group. 56
Figure 27. Mass spectrometry profile of the buffer group assay reaction products. ...57
Figure 28. Chromatograms resulting from the HPLC analysis of LB group samples. A) Samples collected during day 3. B) Samples collected during day 6. C) Samples collected during day 9. PET incubated with empty BL21 cells are used as negative control. In each sample, unknown peaks around 9-10-11 minutes can be observed which are the expected minutes for the peaks of PET degradation products. 57
Figure 29. Chromatograms resulting from the HPLC analysis of M9 group samples. A) Samples collected during day 3. B) Samples collected during day 6. C) Samples collected during day 9. PET incubated with empty BL21 cells are used as negative control. In each sample, unknown peaks around 9-10-11 minutes can be observed which are the expected minutes for the peaks of PET degradation products. 58
Figure 30. Mass spectrometry profiles of A) LB group and B) M9 group samples. Collected samples from day 3, day 6 and day 9 were mixed respectively for each group prior to analysis. 59
Figure 31. Schematic illustration of the micL-PETase construct. micL sRNA expression is under the control of pLacO while PETase expression is controlled by pTetO. PETase is tagged with a 6xHis tag and the secretion tag, pelB. 61

Figure 32. PCR amplification followed by XbaI and KpnI restriction digestion of PETase. GeneRuler 1 kb Plus DNA ladder (Thermo Scientific) is used as the marker in lane 1. 62
Figure 33. Double digestion of the pET-22b(+) – pLacO MicL + pNTetO sfGFP vector by XbaI and BamHI enzymes. 1 kb plus DNA ladder (NEB) is the marker used in lane 1. 62
Figure C. 1. Plasmid map illustration of pET – 22b(+) – PETase – 6xHis vector 79
Figure C. 2. Plasmid map illustration of pET-22b(+) –PelB - 6xHis – Ag43 – PETase vector. 79
Figure C. 3. Plasmid map illustration of pET-22b(+) – pLacO MicL + pNTetO PETase vector 80
Figure D. 1. Sequence alignment of pET22b - PETase - 6xHis construct. Alignment done in Geneious software. 81
Figure D. 2. Sanger sequencing result for pET-22b(+) –PelB - 6xHis – Ag43 – PETase. Alignment shows the sequencing of the insert, PETase. Alignment done and image retrieved from Benchling.com. 82
Figure D. 3. Sanger sequencing result for pET-22b(+) – pLacO MicL + pNTetO PETase. Alignment shows the sequencing of the insert, PETase. Alignment done and image retrieved from Benchling.com. 83
Figure F. 1. HPLC analysis of enzyme refresh group (50 μg/ml) assay. A-J are day 1 to 10 samples, respectively. K is all chromatograms overlapped. 89
Figure F. 2. HPLC analysis of enzyme refresh group (150 μg/ml) assay. A-J are day 1 to 10 samples, respectively. K is all chromatograms overlapped. 90

CHAPTER I: INTRODUCTION

1.1 The Problem of Plastic and Microplastic Pollution

The invention of synthetic polymers goes all the way back to 1869 when John Wesley Hyatt treated cellulose with the cyclic ketone, camphor. The celluloid plastic he discovered was the first of many to come [1]. This was revolutionary, as mankind now knew that they did not have to limit themselves with materials already existing in the nature. A massive breakthrough was in 1907 when Leo Baekeland discovered the plastic, Baekelite [2]. The polymer was ideal for a wide variety of uses, especially as an electrical and thermal insulator to be used in electrical circuits and kitchen gadgets. Following the early success of the newly invented synthetic polymers, the plastics era truly started. Polyethylene terephthalate (PET) was patented in 1941 by John Rex Whinfield and James Tennant Dickson [3], later the plastic was formed into the first PET bottle by Nathaniel Wyeth in 1973 [4].

The most commonly used plastic types during the last decade have been differentiated into 7 major groups: 1- Polyethylene terephthalate (PET), 2- High-density polyethylene (HDPE), 3- Polyvinyl chloride (PVC), 4- Low-density polyethylene (LDPE), 5- Polypropylene (PP), 6- Polystyrene (PS) and 7-Other Plastics. These synthetic plastics are versatile, robust, flexible, malleable and have insulating properties [5,6]. The many useful properties of synthetic plastics, their low cost and ease of manufacture have made them one of the most widely used and consumed materials currently available [6,7]. The versatility of plastics mean that they are a relevant part of almost every sector and

industry. The widespread usage of plastics has led to their massive mass production rates. In the 1950s the annual amount of manufactured plastics worldwide was estimated to be at 1.5 million metric tons [8]. In the 70s this number leaped to 50 million metric tons and currently it is estimated that upwards of 450 million metric tons are being produced each year [8,9]. Annual PET production is estimated to be around 30 million tons which accounts for around 6-8% of all plastic produced [8,10,11].

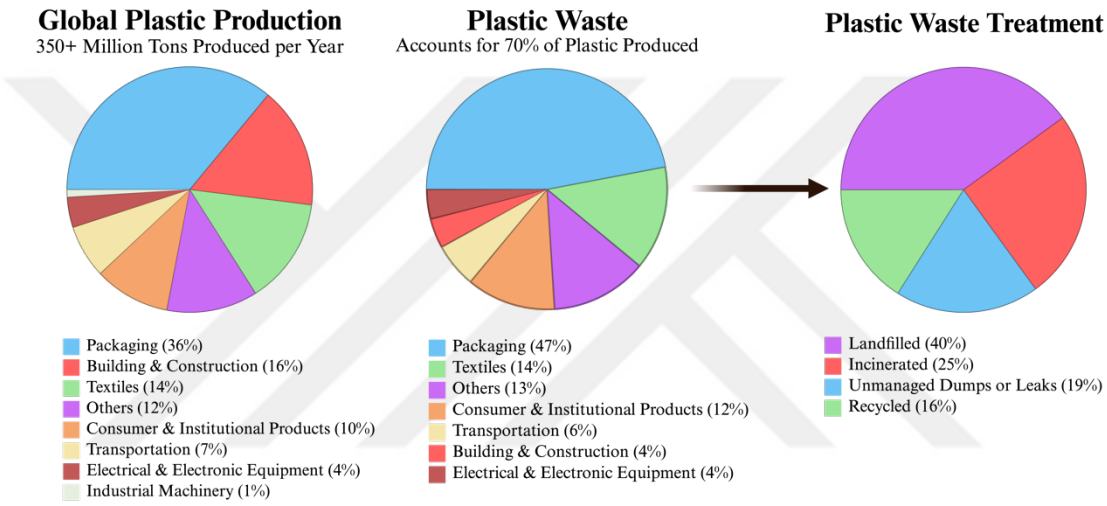

Figure 1. Plastic produced globally by sector. Upwards of 250 million tons of waste are produced annually. Most plastic waste is landfilled (40%) [12].

PET plastics might be a great convenience for daily purposes, which is evident by their widespread usage and substantial production rate, however they are also the culprit for major environmental issues. Not all PET can be recycled, a 2022 Zero Waste Europe report states that 1.8 million tons of recycled PET (rPET) flakes are estimated to be produced annually [13] and when this number is contrasted with the estimated annual amount of PET produced (30 million tons), a stark difference is observed, only around 5 to 10% of all PET gets recycled. PET, along with all major synthetic polymer plastics,

is a major environmental pollutant. A 2022 OECD report [14] suggests that around 350 million tons of plastic waste is being generated annually around the globe. Although reports on this matter do not exactly focus specifically on the amount of PET waste, we do know that PET accounts for 6% of all plastics produced, we also know that only around 5-10% of PET gets recycled, and that most PET products are intended to be single use, so we can get an understanding of the alarming amount of PET waste being generated. What is more alarming is that, although there is a global effort to gather plastic waste in landfills and dumpsites, each year 20 million tons of plastics end up in the environment due to mishandling and natural effects such as wind and rain [15]. Furthermore, around 2 million tons of this waste ends up in the ocean [14].

PET, just like other synthetic plastics, does not biodegrade in any significant manner [11], instead exposure to sunlight and the harsh environmental conditions cause the discarded plastics to break down into fragments in the microscale which are called microplastics [11,16,17]. When microplastics start contaminating water sources, they tend to end up everywhere [18,19]. Samples taken from even the most remote parts of world such as Antarctica [20], Mount Everest [21] and even the Mariana Trench [22] have come up positive for microplastics. More importantly, microplastics have been encountered in various different parts of the human body. Liver tissue [23], cardiac tissue [24], testes [25], breast milk [26] and in fact human blood [27] are some examples of where microplastics have been uncovered. The cause for concern is that in a number of studies, presence of microplastics in human tissue has been correlated with toxicity and disease. For example, it was found that patients with cirrhotic liver tissue had significantly higher amounts of microplastics, including PET, in their livers when compared to healthy patients [23]. A study done on both human and canine testes

showed that increased PET microplastic amount led to smaller than normal testes which could also be linked to infertility among other problems [25]. Furthermore, carotid artery plaque patients who had microplastics present in their carotid artery were found to be at a greater risk of stroke and heart attack when compared to patients without microplastics, suggesting the detrimental effect of microplastics on cardiovascular health [28]. The effects of microplastics on human health is an emerging area of study so more extensive research is still needed to completely understand the significance of the subject, however early results indicate the potential adverse consequences of microplastic presence in human tissue. Moreover, the negative outcomes of macro/microplastic presence does not end with human health. Wildlife and large ecosystems are also negatively affected. Land and marine animals alike have been found to be choked to death due to either ingesting or getting tangled in plastic waste [29,30]. Microplastics also cause harm to wildlife. For instance, uptake of PET microplastics was found to cause extensive damage and scarring to the digestive tract of terrestrial snails (*Achatina fulica*) [31]. Another example is how microplastic exposure was also uncovered to cause reduced reproduction activity in zebrafish (*Danio rerio*) [32]. Due to the macroplastics in the ocean, invasive species like algae and barnacles can attach and accumulate on the plastics, thus leading to the rapid and unnatural buildup of these species [33]. Microplastics have also been found to alter the composition and properties of soils, which leads to change in plant root and leaf traits, biomass and performance [34]. Looking at the extensive adverse effects of plastics/microplastics on human, animal, and plant health as well as the major ecological implications they have it is safe to say that both plastic and microplastic pollution is a tremendous issue that is getting worse each day.

Major landfilled PET waste treatment methods can be summarized in 3 groups, incineration, mechanical recycling or chemical recycling [35,36]. Incineration of PET waste with the goal to recover energy and space is a serious source of greenhouse gasses. It is estimated that burning one ton of PET leads to the emission of 2300kg of CO_2 [37]. Incineration is not an environmentally friendly way to deal with PET waste and some governments have proposed plans to greatly reduce the amount of PET burned [38]. PET waste should be recycled as a more sustainable alternative. Mechanical recycling of PET consists of grinding down discarded PET into flakes and then melting the flakes into recycled PET (rPET) pellets which can then be used for downstream purposes [39]. During this process PET can undergo thermal decomposition which leads to changing thermal and mechanical properties as well as molecular weight reduction [39,40]. Due to these issues, rPET loses significant material quality each cycle when compared to virgin PET (vPET) [12]. Because of its lower quality, rPET cannot be used for every application and loses important value [41]. Another problem with mechanical recycling which is most of the time overlooked, is the release of microplastics. Due to the grinding and milling processes, wastewater from the mechanical recycling process is a source of PET microplastics [42]. Chemical recycling improves on these problems. The chemical recycling of PET involves using different chemical catalyst to depolymerize PET into its monomers or various oligomers. With the help of appropriate catalysts, PET molecules can be undergo hydrolysis [43], glycolysis [44], methanolysis [45], ammonolysis [46] and aminolysis [46] reactions with each reaction yielding different products. Thanks to chemical recycling, monomers and oligomers are attained which can either be used to produce other valuable products or reproduce virgin PET without any loss of material quality [36]. Chemical recycling of PET is not perfect either. Due to the use of expensive

chemicals and the more complex process involved, this method is much more costly and is not very viable for widespread commercial use [47]. Moreover, most of the chemical catalysts used are also known to be environmental hazards as they are composed of metals such as Zn and Mn [48]. PET waste is accumulating at a tremendous rate which makes the handling of this waste a major issue. The currently used common methods of PET recycling are insufficient and therefore a new method which is both environmentally friendly and economically sustainable is urgently required. Bioremediation of PET via biotechnological tools may be the answer.

1.2 Biotechnological Approach for the Remediation of PET

During the last decade, a new method for PET recycling has emerged. The bioremediation of PET using the newly discovered enzymes of microorganisms has the potential to be an effective, environmentally friendly, and commercially viable tool. Correctly utilizing these biological tools would mean that the concerns of other conventional methods would no longer be an issue and thus biological remediation could be the future of PET recycling and circular economy. Newly discovered enzymes in the esterase, hydrolase, keratinase and lipase classes [49] can be used to degrade PET into either its monomers or various other molecules. Synthetic biology tools can be used for the inexpensive utilization of these enzymes and since organic molecules are being used, there is no concern of environmental pollution. Also, the enzymes can break down microplastics so another problem is addressed [50].

There are numerous enzymes discovered that can breakdown PET, the enzymes differ in their reaction mechanisms and reaction products. Notable examples include: *Tf*H,

TfCut1and TfCut2, LCC, HiC and *Is*PETase. *Tf*H is a hydrolase enzyme discovered in the actinomycete, *Thermobifida fusca* [51]. Discovered in 2005, it has the ability to degrade PET films to the PET monomer terephthalic acid (TPA) at 55 ℃ [51]. TfCut1 and TfCut2 are cutinase enzymes discovered in the organism *Thermobifida* KW3, they are active at 65 ℃ and 70 ℃ respectively and can degrade PET into its monomers: TPA and ethylene glycol (EG) [52,53]. Leaf and branch compost cutinase (LCC) is a cutinase type enzyme discovered in 2011 with a metagenomic approach from a leaf-branch compost library [54]. LCC is known to have PET degrading ability at 70 ℃ [55]. HiC, a cutinase from *Humicola insolens*, was found to a be a fungi sourced PET degrading enzyme in 2009 [56]. The cutinase exerts its activity at 70 to 80 ℃ [49,57].

1.3 *Is*PETase and *Is*MHETase

Perhaps the most the renowned of the PET degrading enzymes, *Is*PETase is an esterase class enzyme discovered from the bacterium *Ideonella sakaiensis* which was discovered in PET landfills, in 2016 [58]. *Ideonella sakaiensis* employs PETase along with MHETase for its catabolic activities [59,60]. The two enzymes work in tandem, PETase breaks solid PET down to TPA, mono-(2-hydroxyethyl)terephthalic acid (MHET), and minor amounts of bis-(2-hydroxyethyl)terephthalic acid (BHET) and following PETase activity, MHETase hydrolases the remaining MHET into TPA and EG, the PET monomers [58]. Both enzymes have an optimal temperature of 30 ℃. After its discovery, the authors also characterized PETase activity. PETase was found to produce 0.3 mmol/L degradation product after 18 hours when 50 nM of PETase was incubated with PET film with 6 mm diameter [58].

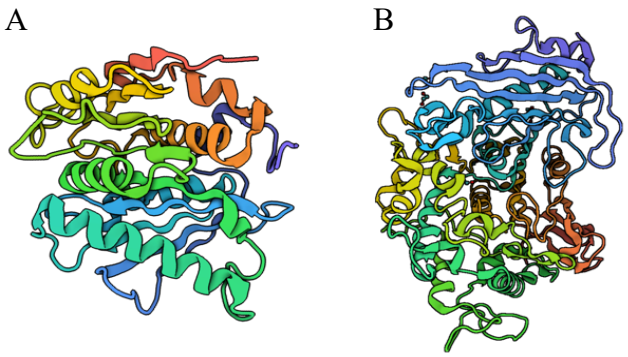

Figure 2. 3D crystal structure of A) PETase and B) MHETase [61].

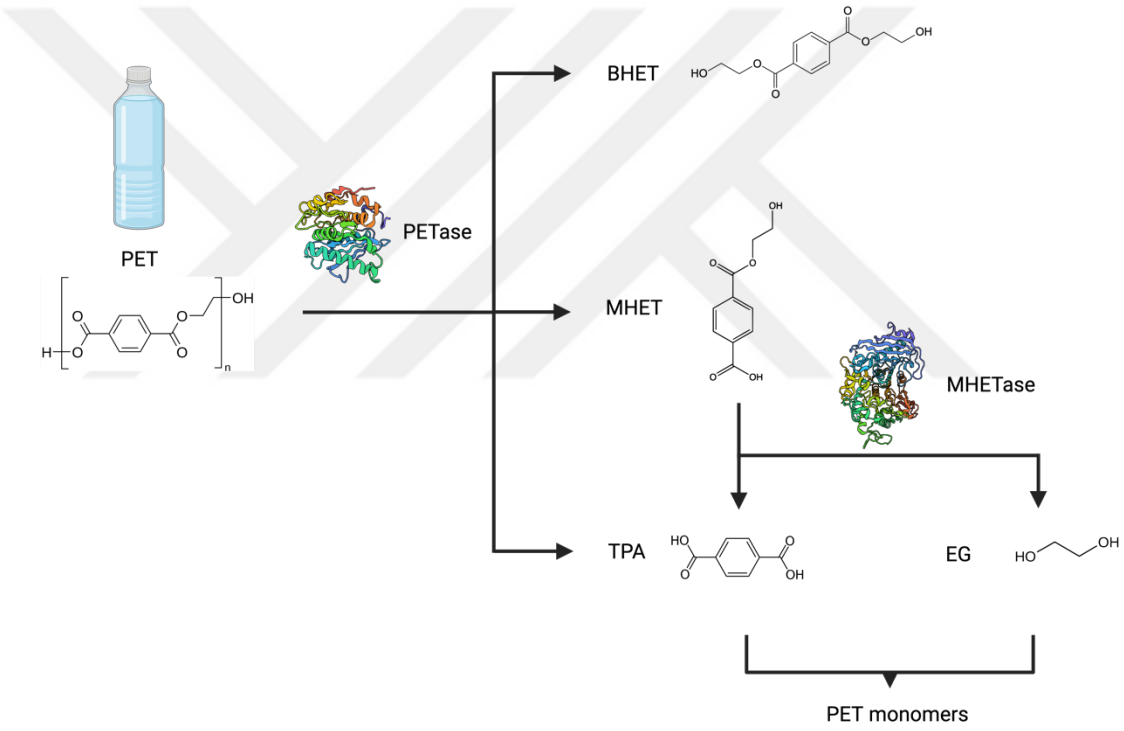

Figure 3. PET degradation pathway. PETase hydrolyses PET into BHET, MHET and TPA. MHETase hydrolyses MHET into TPA and EG. Illustration drawn using BioRender.com.

Out of the PET degrading enzymes, we believe that *Is*PETase has the greatest potential as a biotechnological tool. PETase has higher specificity against PET and more importantly the enzyme operates at moderate temperatures (30 °C) while still

maintaining a competitive degradation rate when compared to other enzymes [61]. Thanks to the ability to work at moderate temperatures, PETase is both beneficial for industrial use as there is no need for major heating and energy is conserved and as a biotechnological tool, where whole-cell bacterial systems can be constructed on model organisms such as *E. coli*, where the system can be kept at a temperature that is both viable for the cells and the enzyme. That being said, *Is*PETase also has two major drawbacks. The stability of the enzyme is very low, where a major loss of activity can be observed after 24 hours at 37 ℃ [62,63]. A second problem is the activity rate, considering the amount of PET waste that needs to be recycled, the activity of enzyme should be increased for viable use as an industrialized product [64]. A solution to both issues could potentially mean the industrialization of PETase for the bioremediation of PET.

Different tools, methods and approaches have been used in the search for solutions of the aforementioned problems. Protein engineering can be used to create more functional variants of PETase. ThermoPETase, a PETase variant created with rational protein engineering, was able to retain almost half of its activity after 48h at 40℃ showing success in increased thermal stability [65]. Another variant DuraPETase, designed with computational redesign tools, exhibited a 300-fold increase when compared to PETase regarding total product release over 10 days at mild conditions [66]. One final variant of note, FAST-PETase, created with the help of machine learning-aided engineering, was shown to catalyze the hydrolysis of PET at 50 ℃ with increased activity compared to native enzymes [67]. After designing the perfect protein, the next step is to develop a delivery system for the functional use of the protein. Synthetic biology tools have been previously used for this instance: bacterial [68] and fungal [69] surface display

systems, bacterial overexpression and secretion systems [70,71] as well as PETase expression in algae [72] are all examples of synthetic biology tools that are in development.

1.4 Aim of the Study

PETase and MHETase are two enzymes that work in tandem to degrade PET, PETase hydrolyses PET polymers into monomers (TPA) and oligomers (MHET, BHET) which then get further degraded into monomers (TPA, EG) by MHETase. When investigating the synergistic reaction activities of PETase and MHETase it is also seen that the activity of PETase is most likely the rate-limiting step [73]. PETase, arguably, is a more valuable tool for the bioremediation of PET and so, we can say that to create a platform for the remediation of PET, research should first focus on increasing the activity of PETase. With these in mind, this study aimed to create whole-cell systems which can efficiently hydrolyze PET polymers. First, we aimed to create a whole-cell catalyst in which PETase is displayed on the surface using the Ag43 autotransporter protein [74]. By the surface displaying of the enzyme, we sought to increase stability and thus activity. By immobilizing proteins, it is known that higher levels of stability can be achieved compared to free enzymes [75,76]. Furthermore, as "fresh" enzymes are constantly being translated and expressed in a living cell, stability concerns are once again addressed. Also, as the substrate for the system (PET polymers) cannot be ingested by cells, enzymes must be able to reach their intended target, making surface display systems a promising approach for our research. The Ag43 complex is composed of two subunits, where the alpha domain anchors the protein towards the environment

and the beta domain embeds itself into the outer membrane. For a second approach, we aimed to use the leaky outer membrane-based secretion system (iLOM-SS) [77] as our delivery tool. The constant secretion of newly produced PETase means a higher amount of stable and active enzymes are present in the environment and are interacting with the substrate at any time, once again addressing the concerns of loss of protein function due to instability. The iLOM-SS acts by expressing micL sRNA which in turn halts the production of Braun's lipoprotein (Lpp) thus disrupting the outer membrane of gram-negative bacteria. Braun's lipoprotein is a major molecule found in the outer membrane of gram-negative bacteria and is an important factor for the structural integrity of the outer membrane [78]. For both instances, we chose *E. coli* as our whole-cell platform for the ease of use, practicality, and compatibility of the given organism. Our research hopes to create an efficient and easy to use cellular catalyst which can aid in the urgent problem of PET plastic pollution.

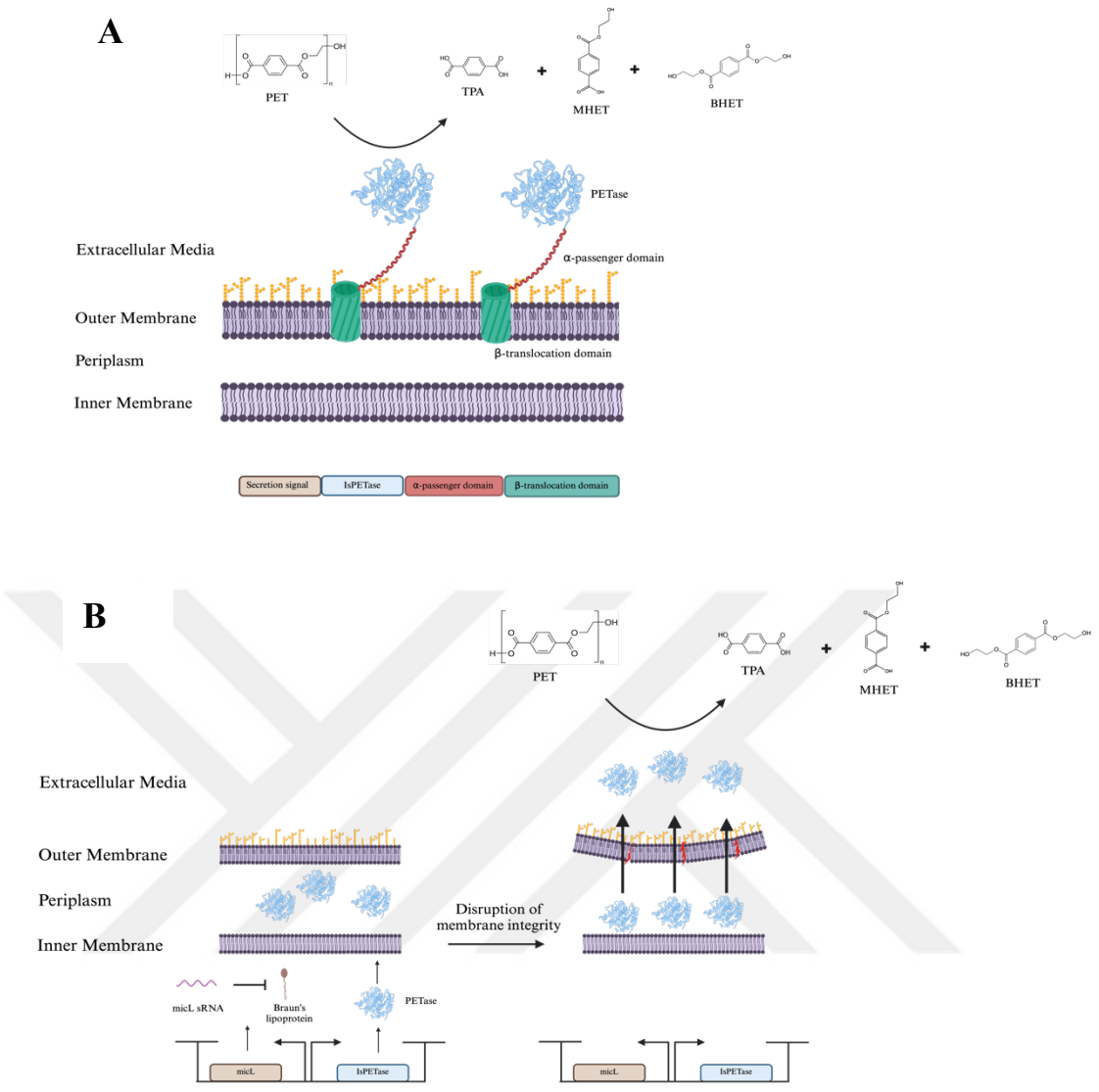

Figure 4. Illustration of the aim of the study. The two engineered constructs: A) The surface display of PETase on the surface of *E. coli*. The beta domain of Ag43 embeds itself to the outer membrane as a β barrel structure whereas PETase is attached via the alpha domain. B) The bacterial secretion of PETase. micL sRNA disrupts the expression of Braun's lipoprotein. The lack of Braun's lipoprotein creates a leaky outer membrane which allows for the free diffusion of PETase. Illustration drawn using BioRender.com.

CHAPTER II: MATERIALS AND METHODS

2.1 Cell Strains, Cell Maintenance, Cell Growth and Transformation

Escherichia coli (*E. coli*) DH5α Pro strain was used for the cloning of the constructs. Due to the mutations in recA1 and endA genes, the DH5α Pro strain allows for high yield, high insert stability and efficient cloning. The strain also contains the PRO DNA cassette, which encodes the constitutive expression of TetR and LacI repressors along with the spectinomycin antibiotic resistance gene. As for recombinant protein expression, the *E. coli* BL21 DE3 strains was utilized. BL21 DE3 is suitable for Isopropyl-β-d-1-thiogalactopyranoside (IPTG) induction due to the strain carrying the T7 polymerase gene under the control of the Lac promoter. BL21 DE3 is also deficient of OmpT and Lon proteases making the strain suitable for protein expression purposes. Cell stocks were taken as 25% glycerol in Lysogeny Broth (LB) growth medium (recipe given in Appendix E, Table E.1) and were kept at -80 °C.

For the transformation of the plasmids into the bacterial cells, chemical transformation was applied. For the preparation of chemically competent cells, the *E. coli* DH5α PRO and BL21 DE3 cells were inoculated from -80°C stocks into fresh LB medium containing their appropriate antibiotics. Following overnight growth, cells were diluted 1:100 into fresh LB and were allowed to reach between 0.3 – 0.5 OD600. The cells were then chilled on ice for 10 minutes and then centrifuged at 1000xg for 10 minutes at 4°C. The supernatant was discarded, and the cell pellet was resuspended in

Transformation and Storage (TSS) Buffer with a 1:10 dilution volume of the amount of the original overnight culture (TSS buffer recipe given in Appendix E, Table E.7). Aliquots containing 100 µL of the resuspended cells were stored at 80°C to be used for later transformations.

For the chemical transformation process, first the chemically competent cells were allowed to thaw on ice. Next, either 100 ng of the desired plasmid or the entire Gibson assembly mix (post reaction) were added to the cells. Following a 30-minute incubation on ice, cells were heat-shocked at 42°C for 45 seconds and then re-incubated on ice for another 2 minutes. 1 mL of fresh LB was then added to the cells and the cells were incubated at 37°C, 200 rpm for 60 minutes. After the incubation, the cells were centrifuged at 8000 rpm for 5 minutes and 1 mL of the supernatant was discarded. Using the remaining 100 µL supernatant, the cells were once again suspended and were spread onto LB-Agar plates (recipe given in Appendix E, Table E.1) containing appropriate antibiotics. The plates were incubated overnight at 37°C.

2.2 Construction of pET-22b(+) – PETase – 6xHis Vector

To construct the pET – 22b(+) – PETase – 6xHis vector, first the gene fragment encoding codon optimized PETase (GenBank: GAP38373.1, synthesized by Integrated DNA Technologies, US) was PCR amplified with the specific primer pair (including overhangs) using Q5 polymerase under appropriate conditions (PCR setup given in Appendix E, Table E.2, Table E.3). For the backbone, 3000 ng of pET-22b(+) – GRFT – 6xHis (plasmid previously available in our collection), was cut using the restriction enzymes, KpnI-HF (NEB) and XhoI (NEB) at 37°C for 3 hours (reaction setup given in Appendix E, Table E.4). Products from both the PCR reaction and the restriction

digestion reaction were loaded into a 1% agarose gel containing SYBR™ Safe DNA gel stain. Electrophoresis was run at 120V for 40 minutes. The DNA bands of interest were retrieved by cutting them out of the gel and using the Nucleospin Gel and PCR Clean-up kit (Macherey-Nagel) as per the manufacturer's instructions. The concentrations of the retrieved DNA were measured using a spectrophotometer (Thermo Scientific NanoDrop™ 2000). The obtained DNA parts (backbone and insert) were assembled using Gibson Assembly (homemade Gibson Assembly mix recipe given in Appendix E, Table E.5). A 3:1 molar ratio of insert to backbone was used for the reaction and the incubation time was 1 hour at 50°C. The post-reaction Gibson Assembly mixture was then transformed into chemically competent *E. coli* DH5α cells as described earlier. After overnight incubation of inoculated LB-Agar plates, colonies were picked for Next-Generation Sequencing (NGS) verification. Verified colonies were inoculated into fresh LB medium and after overnight growth at 200 rpm and 37°C, cell stocks were prepared and stored as previously explained.

2.3 Construction of pET-22b(+) –PelB - 6xHis – Ag43 – PETase Vector

To construct the pET-22b(+) –PelB - 6xHis – Ag43 – PETase vector, first DNA fragment encoding PETase was PCR amplified with Q5 polymerase (reaction conditions given in Appendix E, Table E.2, Table E.3) using appropriate primers. To use as a backbone for the construct, pET-22b – pelB – 6His – sfGFP – Ag43 plasmid (plasmid already found in our laboratory's possession, was digested using AflII (NEB) and BamHI-HF (NEB) at 37°C for 3 hours (reaction setup given in Appendix E, Table E.4). DNA fragments were loaded onto a 1% agarose gel containing SYBR Safe DNA

gel stain. After 45 minutes of electrophoresis at 130V, expected bands were cut out and retrieved with Nucleospin Gel and PCR Clean-up kit (Macherey-Nagel) by following the manufacturer's instructions. The concentrations of the DNA fragments were then measured using the Thermo Scientific NanoDrop™ 2000 spectrophotometer. Next, the fragments were used to construct the plasmid of interest using Gibson Assembly. After the Gibson Assembly reaction which was completed by incubation at 50°C for 1 hour, the reaction mix was transformed into chemically competent *E. coli* DH5α as previously described. After overnight incubation, colonies were picked from the LB-Agar plate for Sanger sequencing (Genewiz, USA). Sanger sequence verified colonies were then inoculated into fresh LB and after overnight growth, 25% glycerol stocks were taken and stored at -80°C.

2.4 Construction of pET-22b(+) – pLacO MicL + pNTetO PETase Vector

To construct the pET-22b(+) – pLacO MicL + pNTetO PETase plasmid, PETase gene was amplified with PCR, using Q5 polymerase and the appropriate primers. The resulting products were retrieved by agarose gel electrophoresis and Nucleospin Gel and PCR Cleanup Kit (MN) as previously stated. Next, to obtain the pET-22b(+) – pLacO MicL + pNTetO sfGFP plasmid (found in our laboratories depository), cells transformed with this plasmid were inoculated into LB and after overnight growth, Monarch Plasmid Miniprep Kit (New England Biolabs) was used according to the manufacturers protocol to isolate the vector. The obtained PCR product along with the isolated plasmid were digested in a double restriction enzyme digestion procedure using XbaI and BamHI. The appropriate fragments were once again obtained using the

Nucleospin Gel and PCR Cleanup Kit (MN) following agarose gel electrophoresis. The fragments were finally ligated using T4 ligase for 15 minutes at room temperature in appropriate conditions (reaction setup given in Appendix E, Table E. 12). Once ligation was done, the entire reaction product was transformed into chemically competent *E. coli* DH5α cells by following the previously explained heat-shock procedure. The cells were spread on agar plates for overnight growth. The next day, cell glycerol stocks were taken, and verification was done using Sanger sequencing.

2.5 Next-Generation Sequencing (NGS), Sanger Sequencing and *In Silico* Sequence Alignments

Cloned constructs were verified either with next-generation sequencing (NGS) or Sanger sequencing. To do so, first colonies were grown overnight in 3 mL of LB medium at 37°C at 200 rpm. The next day, cloned plasmids were isolated using GeneJet Plasmid Miniprep Kit (Thermo Scientific) according to the manufacturer's manual. DNA concentrations were measured using a spectrophotometer (Thermo Scientific).

For NGS, 20 µL of isolated plasmid at a 50 ng/µL concentration was sent to Intergen, Ankara. Geneious Prime (2021.1.1) software was used for analysis. Data received from Intergen were imported to the software along with the template sequences which were designed and obtained from Benchling.com. Parameters chosen were as followed: automatic determination of direction, 65% similarity and global alignment with free end gaps.

For Sanger sequencing purposes, 1000 ng of the plasmid was mixed with 5 µL of 5 µM appropriate sequencing primer and the final volume was adjusted to 15 µL by adding dH2O. Samples were sent to Genewiz (USA). Templates were once again exported from Benchling.com and sequencing data from Genewiz was mapped to the templates by using the Geneious application as previously described.

2.6 Expression, Purification and Quantification of PETase Enzyme

In order to facilitate the expression of PETase, the NGS-verified pET – 22b(+) – PETase – 6xHis plasmid was transformed into *E. coli* BL21 (DE3) cells. Since the gene encoding PETase is found downstream of the T7 promoter, protein expression can be induced using the lactose analog, Isopropyl-β-d-1-thiogalactopyranoside (IPTG). This is the case because the T7 RNA polymerase gene is regulated by the Lac promoter. Chemical transformation was done as previously explained, cell stocks were taken and stored as previously explained. From the glycerol stocks, cells were inoculated into fresh LB containing 100 µg/ml ampicillin and were incubated at 37 °C, 200 rpm. After allowing the cells to grow overnight, cells from the overnight culture were diluted 1:100 (v/v) into 1000 mL of fresh LB with ampicillin. The cell culture was once again incubated at 37 °C, 200 rpm until the cells reached mid-log phase (OD600 values must reach between 0.4-0.6) which is ideal for protein expression. Once desired OD600 values were obtained, IPTG was added to the culture to a final concentration of 1 mM and the culture was then incubated at 16 °C, 200 rpm for 16 hours. When the incubation was done, cells were centrifuged at 8000 xG for 5 minutes. The emerging pellet was resuspended in HisTrap binding buffer (recipe given in Appendix E, Table E.8) at an amount of 1:10 ratio to the original cell culture volume. Phenylmethylsulfonyl fluoride

(PMSF) was added to the sample to a final volume of 1 mM. PMSF is a protease inhibitor used in order to protect the protein of interest from protease degradation. The cells were then subjected to flash freezing with liquid nitrogen followed by thawing a water bath. This freeze-thaw cycle was repeated 5 times in order lyse the cells. Next, the sample was subjected to sonication to further lyse the cells. Sonication was done at a 30% amplitude with 10 seconds of pulse on and 10 seconds of pulse off cycle for 15 minutes. During sonication the cells were incubated on ice. The final lysate was done centrifuged at 4°C and 13000 xG for 45 minutes. The emerging supernatant was filtered using a 0.22 polyethersulfone (PES) syringe filter and. Once filtering was done, fast protein liquid chromatography (FPLC) was utilized for the isolation of his-tagged PETase. FPLC was done using the HisTrap™ HP (1 ml) (Cytiva) column coupled to the ÄKTA™ start (GE) system. For the FPLC process, first the column was washed using HisTrap binding buffer. Once 5 column volumes of binding buffer were used for washing, the filtered supernatant was run through the column. The protein of interest, PETase, was bound to the column due to being his-tagged. Next the column was once again washed with binding buffer in order to discard the unbound protein. Finally, HisTrap elution buffer (recipe given in Appendix E, Table E. 9) was used to elute the protein of interest. The flow rate during the entire process was 1 ml/min. The proteins were buffer exchanged using a Hi-Trap Desalting column (5 ml) (Cytiva). The HisTrap elution buffer high in imidazole concentration was replaced by 50 mM Glycine-NaOH buffer (pH 9) (recipe given Appendix E, Table E.11). For the buffer-exchange process, first the desalting column was washed 5 column volumes of water followed by 5 column volumes of 50 mM Glycine-NaOH buffer. The proteins were then applied to the column manually with the help of a syringe and were eluted with 50 mM Glycine-NaOH buffer. The flow rate for this process was 5 ml/min. All the buffers and solutions

used during the FPLC process were filtered with 0.45 µm PES filters and degassed. For the quantification of the amount of protein purified using FPLC, bicinchoninic acid (BCA) (Thermo Scientific) assay was performed. To use in the assay, bovine serum albumin (BSA) standards were prepared as: 1000 µg/ml, 750 µg/ml, 500 µg/ml, 250 µg/ml, 125 µg/ml, 62.5 µg/ml. To setup the assay, the working reagent was prepared by mixing 50 parts of Reagent A to 1 part of Reagent B. 200 µl of the working reagent was then distributed to wells in a 96-well plate. 10 µl of both protein samples and BSA standards as well as 10 µl of 50 mM Glycine-NaOH buffer (to use as a blank) was added to the wells. Following a 30-minute incubation at 37°C, absorbance of the wells were measured at 562 nm using a SpectraMax M5 Microplate Reader (Molecular Devices). Measurements were performed in triplicates; the average of the readings were used to plot a standard curve and the protein concentration of the sample was determined by this curve. In cases where concentrations were deemed too low, a 10 kDa molecular weight cut off spin filter (Merck Millipore) was used to concentrate the protein sample, per the manufacturer's instructions.

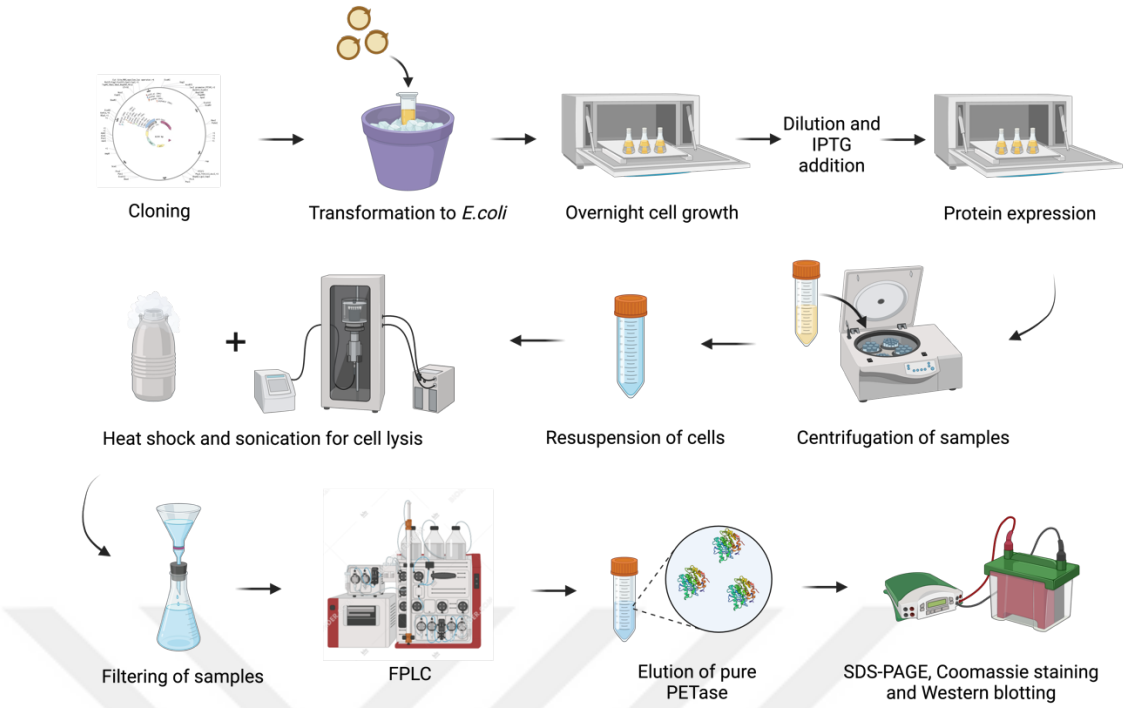

Figure 5. Illustration of the PETase expression and isolation workflow. Cloned vectors are transformed into *E. coli* BL21 (DE3) cells, after overnight growth and the following IPTG induction protein is expressed. To extract the protein, cells are resuspended with appropriate buffer and are lysed. Lysed cells are filtered and PETase is purified using FPLC. Purified protein is later used in downstream applications. Illustration drawn using BioRender.com.

2.7 Coomassie Staining and Western Blotting of Purified PETase

20 µL of the isolated protein were mixed with 4 µL of 6x SDS-PAGE loading dye and were incubated at 95°C for 5 minutes. The heated samples were then loaded into a 10% SDS-PAGE gel and run at 100 V for 30 minutes followed by 125 V for 1 hour. Once the run was complete, the gel was submerged into Coomassie brilliant blue dye solution

and heated in a microwave for 30 seconds. The gel was then removed from the dye and was incubated overnight with destaining solution (recipe given Appendix E, Table E.13) at room temperature with shaking. Imaging was done with Vilber Fusion Solo S.

For western blotting, samples were prepared, and SDS-PAGE protocols were run the same as previously explained. Next, the gel was blotted on to a PVDF membrane using Trans-Blot Turbo (Bio-Rad). The gel membrane was activated using methanol for 2 minutes followed by equilibration of both the membrane and gel in Towbin transfer buffer (recipe given Appendix E, Table E.14) for 10 minutes. The membrane and the gel were placed on top of one another and sandwiched by transfer papers before using the predefined transfer settings in the transfer system. After the transfer, the membrane was incubated with 5% milk powder in TBST buffer (recipe given Appendix E, Table E.15) at room temperature for 2 hours to block membrane surface from nonspecific binding. Next the membrane was incubated in 1:10000 primary anti-His mouse antibody containing 5% milk powder TBST solution, at 4°C for overnight. The next day, the membrane was washed in TBST for 10 minutes in shaking conditions. Washing was repeated three times. The membrane was then incubated in 5% milk powder in TBST containing 1:10000 horseradish peroxidase (HRP) conjugated goat anti-mouse antibodies (Abcam ab6789-1 MG) for 2 hours at room temperature with shaking. Once the incubation was completed the membrane was again washed with the same conditions as before. Finally, the membrane was treated with ECL substrates (Bio-Rad) by following the manufacturer's instructions. The membrane was imaged using the Vilber imaging system.

2.8 Expression of Surface-Displayed PETase

Cells from glycerol stocks were inoculated into fresh LB with appropriate antibiotics and overnight growth was observed. From the overnight culture, cells were 1:100 diluted into 10 mL of fresh LB supplemented with glucose to a final concentration of 1% w/v. Glucose was added to supplement the cells as the surface display of a protein can bear increased metabolic stress on bacteria. After incubation at 37°C, 200 rpm the OD600 values of the culture were observed and at 0.4-0.5 OD600 values, IPTG was added to the culture to a final concentration of 1 mM. After the addition of IPTG, the cells were incubated at 16°C and 200 rpm conditions.

2.9 Protein Precipitation and Western Blotting of Surface-Displayed PETase

Western blotting of the surface displayed proteins was done after the heat release and subsequent precipitation of the proteins. The non-covalent bonds between the two domains of the Ag43 complex can be disrupted by heat administration, resulting in the release of the complex to the environment. The cells from the IPTG induced culture were first incubated at 65°C for 10 minutes. Next, the heat-treated sample was centrifuged at 8000 xG for 5 minutes. To 200 µL of the supernatant, 1 ml of ice-chilled acetone was added. The mixture was incubated at -20°C for overnight to precipitate the proteins. The next day, the sample was centrifuged at 13000 xG at 4°C for 45 minutes. The supernatant was discarded, and the pellet was allowed to air dry. The resulting dry pellet was resuspended in 20 µL dH20 and 4 µL of 6x SDS-PAGE loading dye. Once the sample was heated at 95 °C for 5 minutes, the preparation of the sample for use in

western blotting was completed. SDS-PAGE and the following western blot analysis was performed as described above.

2.10 Immunocytochemistry (ICC) Labeling of Surface Displayed PETase

E. coli BL21 (DE3) cells transformed with the the pET-22b(+) –PelB - 6xHis – Ag43 – PETase vector were IPTG induced overnight at 16 °C. The next day, 250 µL of cells (OD600: 1.5) in LB were centrifuged at 8000 xG for 5 minutes. The supernatant was discarded, the pellet was washed with 1x PBS (recipe given Appendix E, Table E.16) and resuspended with 250 µL of 1% BSA dissolved in 1x PBS. The cells were incubated at room temperature for 2 hours for the blocking step, which was done to block cell surface from nonspecific binding. Once incubation was over, the cells were centrifuged, and the blocking solution was removed. The cells were washed with 1x PBS and suspended in anti-his antibody 1:250 diluted in 1% BSA dissolved in 1x PBS. The sample was incubated overnight at 4 °C. The following day, the cells were once again centrifuged and washed with 1x PBS. The washing step was repeated three times. The cells were then incubated in anti-mouse antibodies conjugated with DyLight550 dye diluted 1:500 in 1% BSA dissolved in 1x PBS. The incubation took place for 1.5 hours at room temperature. The cells were finally washed three times with 1x PBS before getting prepped on glass microscopy slides. The tagged cells were visualized using an epifluorescence microscope.

2.11 p-NPB Assay for Purified PETase Enzyme Activity

The p-nitrophenyl butyrate (pNPB) hydrolysis assay was utilized in order to test the esterase activity of PETase. First a 35 mM pNPB working stock was prepared by dissolving 6.33 mg of pNPB in 1 ml of methanol. Next, per the FPLC protocol previously explained, PETase was purified and desalted in glycine-NaOH (ph 9) buffer. Then, in a 96 well plate, pNPB was mixed with the enzyme for a total volume of 200 µL. In the final mixture, the enzyme concentration was 25 nM whereas the final pNPB concentrations were groups of 0.25 mM, 0.5 mM, 1 mM, 2 mM, and 4 mM. To compare with the autohydrolysis of the substrate, the same concentrations of pNPB were prepared without the addition of the enzyme. Once enzyme was added, the samples were incubated at 30 °C for 10 minutes. After the incubation, absorbance at 405 nm was measured using SpectraMax M5 Microplate Reader (Molecular Devices).

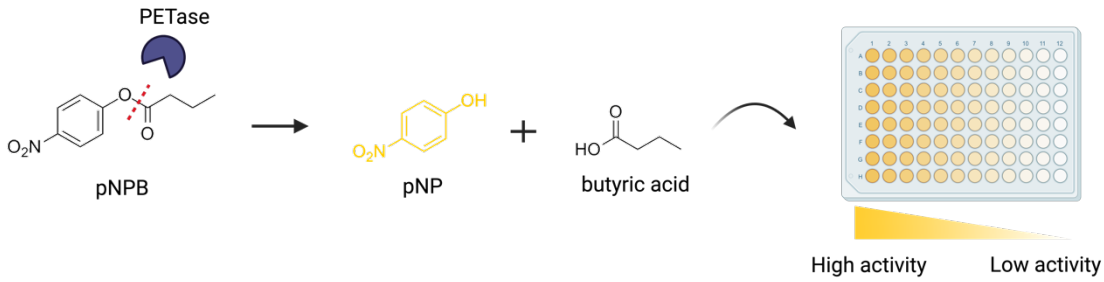

Figure 6. The principle of the pNPB assay. Illustration drawn using BioRender.com.

2.12 PET Degradation Assay for PETase

To test the PET degradation capabilities of PETase a degradation assay was designed. 75 mg of PET amorphous film (GF25214475, Goodfellow) was cut in circles and washed before being placed in a 6 well-plate. To wash the PET samples, first 70% ethanol was used, then the PET samples were washed using dH2O, finally the plastics were allowed to air dry. Different enzymes concentrations (150 μg/ml, 50 μg/ml) were added to the wells. Enzymes were purified and desalted as previously explained, the buffer used was 50 mM glycine-NaOH buffer. Enzymes were added to the wells for final volumes of 2 ml. As for the control group, 50 mM glycine-NaOH buffer without PETase was used. The samples were further split into two groups: the enzyme refresh group and the no refresh group. The no refresh group was incubated at 30 °C, no shaking, for 10 days. For the refresh group on other hand, PETase was isolated daily and the enzyme solutions in the wells were replaced with fresh enzyme every 24 hours, the discarded was enzyme solutions were collected as samples. Again, the refresh group samples were incubated at 30 °C, no shaking for 10 days. Once the 10-day incubation was over and the experiment was terminated, the collected samples were analyzed using high-performance liquid chromatography (HPLC) and quadrupole time of flight liquid chromatography/mass spectrometry (LC/MS QTOF). To prepare the samples, the collected enzyme solutions were first heat-treated at 85 °C for 10 minutes for the inactivation of the enzyme. Following heat treatment, the samples were centrifuged at 8000 xG for 5 minutes before being filtered with a 0.22 μm polytetrafluoroethylene (PTFE) syringe filter. The treated PET samples were analyzed using scanning electron microscope (SEM).

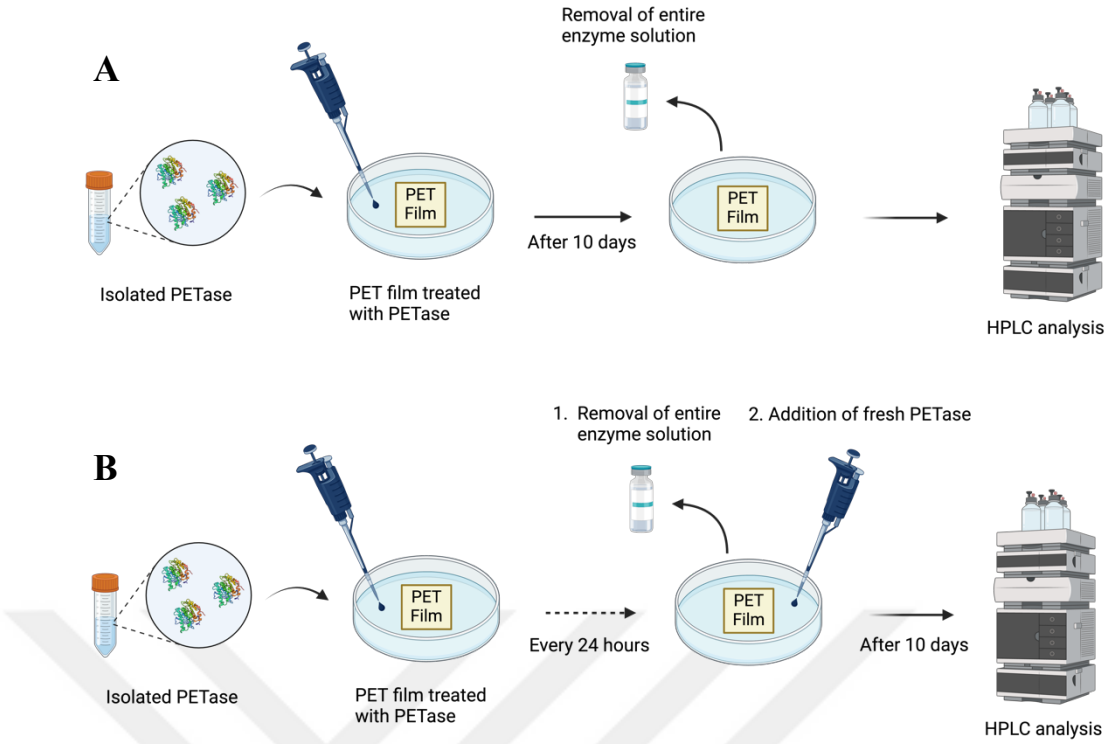

Figure 7. Illustration of isolated PETase activity assay. A) For the no refresh group samples, PET film and PETase solution are incubated for 10 days. After termination, samples are HPLC analyzed. B) For the enzyme refresh group samples, PET film and PETase solution incubated for a total of 10 days. Every 24 hours the solution is renewed with freshly isolated PETase. After termination, collected samples are HPLC analyzed. Illustration created in BioRender.com.

2.13 PET Degradation Assay for Surface-Displayed PETase

Transformed cells with the ability to display PETase were IPTG induced as previously mentioned. After induction, the cells were centrifuged at 8000 xG for 5 minutes. The supernatant was discarded, and the remaining pellet of cells were resuspended in either LB media (pH adjusted to 9 with the addition of NaOH), M9 minimal media (pH 9) (recipe given Appendix E, Table E. 10) or 50 mM glycine-NaOH buffer (pH 9). PET film was once again cut into 75 mg pieces, washed, and placed into 6 well-plates as stated above. For cells resuspended with 50 mM glycine-NaOH buffer, 2 ml of cells with an OD600 of 1.5 were added to the plastics along with the appropriate antibiotic to prevent contamination. Incubation took place at 30 °C, no shaking for 10 days. For the cells resuspended with either LB or M9 media, 2 ml of the cells (OD600: 0.3) were placed in the wells with the PET pieces. However, for these groups, 4/5 of the culture was discarded and replaced with fresh media every 3 days. The discarded media was collected to be used as samples. The appropriate antibiotics along with a final concentration of 1 mM IPTG was added to the cells. The samples were incubated at 30 °C, without shaking for 9 days. The samples collected were heat-treated at 85 °C for 10 minutes before centrifugation at 8000 xG for 5 minutes. The samples were filtered with 0.22 μm polytetrafluoroethylene (PTFE) syringe filters before being analyzed using HPLC.

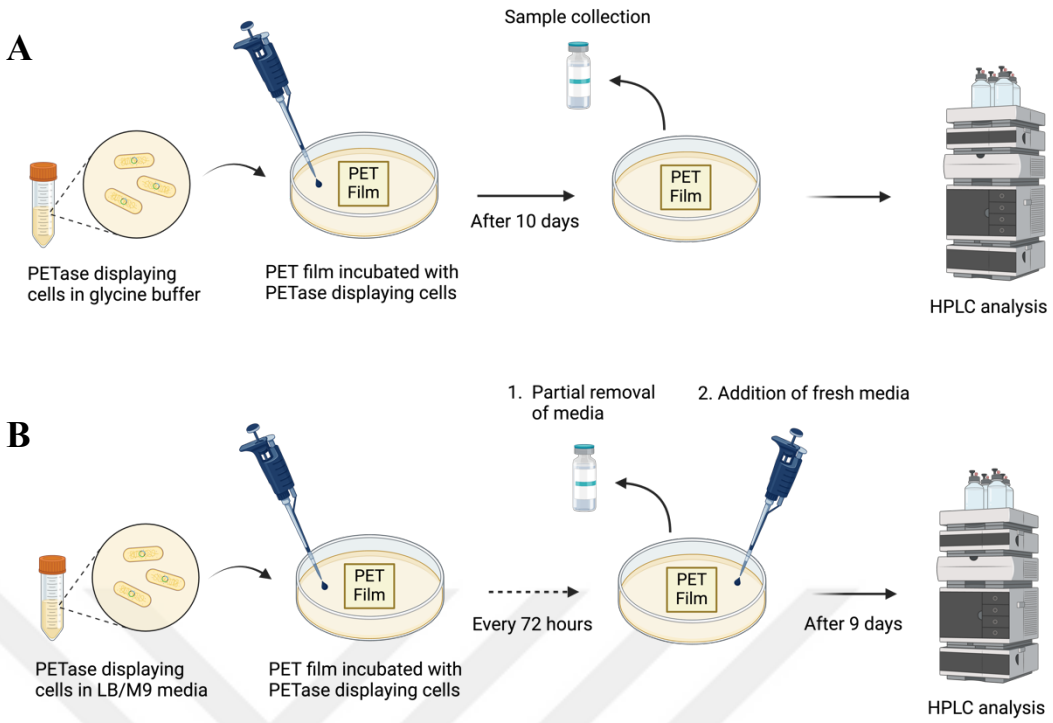

Figure 8. Illustration of surface displayed PETase activity assay. A) Assay for buffer group samples. Induced cells are suspended in 50 mM glycine-NaOH buffer and incubated with PET film. After 10 days, samples are collected for HPLC analysis. B) Assay for LB and M9 group samples. Induced cells are resuspended in respective media and incubated with PET film. Every 3 days fresh media is supplemented to the culture and samples are collected. Once the assay is terminated, samples are HPLC analyzed. Illustration created in BioRender.com.

2.14 Reverse Phase HPLC and LC/MS-QTOF Analysis of PET Degradation Assay Products

High performance liquid chromatography (HPLC) analysis was performed to the samples collected from the PET degradation assays. To do so, Agilent Technologies 1200 Series (Agilent) was used along with the Agilent ChemStation software. The system was coupled with an Agilent Zorbax 300SB C18 column. As for the mobile phases: 0.1% (v/v) formic acid in dH2O (A) and acetonitrile (B) was used. The mobile phase gradient was as the following: at 0-2 min: 95% A 5% B, 2-12 mins: 56% A 44% B, 12-15 mins: 30% A 70% B, 15-20 mins: 95% A 5% B. The flow rate was constant at 0.7 ml/min, 20 µl of sample was injected in the column and the experiment was conducted at room temperature. The multiwavelength detector (MWD) attached to the system was used to measure the 240 nm absorbance values of the samples. Terephthalic acid (TPA) (Thermo Scientific Chemicals) dissolved in dH20 was used to create a standard curve.

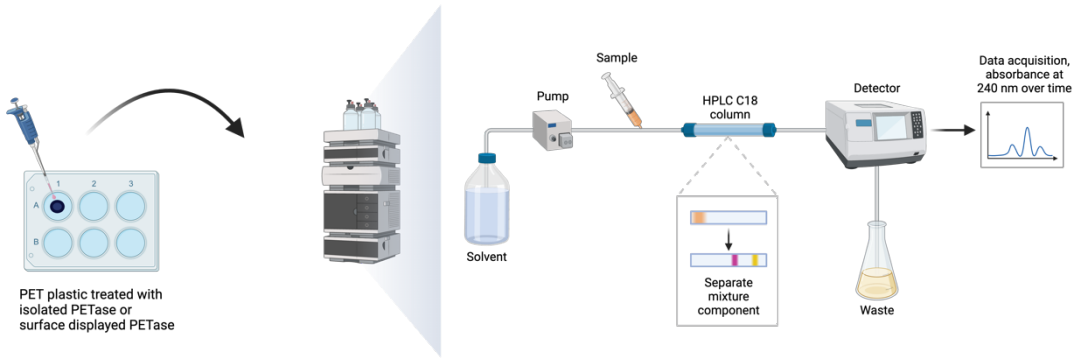

Figure 9. Working principle of HPLC analysis. Samples collected from the activity assays are run through a C18 column where the mixture components are separated. The components are analyzed for absorbance at 240 nm which accounts for PET degradation products (TPA, MHET, BHET). Illustration created using BioRender.com.

Samples in which TPA peaks were observed in their HPLC chromatogram were further analyzed using LC-MS QTOF. Agilent LC-MS QTOF 6530 was used, coupled to the Agilent Zorbax 300SB C18 column. The settings for the chromatography part of the procedure were the same as previously described. The rest of the operating conditions were: 125 V fragmentor, 3500 Vcap, 8 l/min drying gas flow, 6 l/min sheath gas flow, 300 °C gas temperature, 250 °C sheath gas temperature, electrospray ionization (ESI).

2.15 SEM Imaging of Enzyme Treated PET

For the samples where TPA peaks were observed in the HPLC analysis, the PET pieces were prepared and observed under the scanning electron microscope. First, the plastic samples were washed twice with dH2O followed by 25% ethanol, 50% ethanol, 75% ethanol and 100% ethanol in order to completely get rid of contaminants and dirt on the samples. After the samples were allowed to air dry, the surfaces of the plastic samples were covered with gold-palladium at a thickness of 5 nm. This coating allows the visualization of the surface of the samples under the SEM microscope. Finally, images were taken using FEI Quanta 200 FEG SEM with various electron energy voltages, between 5-20 keV.

CHAPTER III: RESULTS AND DISCUSSION

3.1 Cloning and Expression of PETase Protein

The genetic construct represented in Figure 10 was cloned to the pET22b vector which is a standard vector for recombinant protein expression. The construct includes a C terminal polyhistidine tag. This small tag consists of six histidine residues. This tag is primarily used for the purification and detection by the polyhistidine sequence's ability to bind nickel ions as well as anti-his antibodies, respectively. Furthermore, the 6xHis tag is known to increase solubility which aids to prevent aggregation of the tagged protein [79]. The tag was also seen not to interfere or alter the activity of PETase on either the C-terminal or N-terminal [80,81] which is the reason why this particular affinity tag was chosen. The tag and the protein are linked with a GS linker composing of Gly-Gly-Gly-Gly-Ser residues. The linker is used to increase flexibility and help with proper protein folding [82]. The expression of the protein of interest (PoI) is under the control of the T7 promoter which is in turn regulated by the Lac promoter. This allows for the IPTG inducible control of PETase expression.

Figure 10. Schematic illustration of the PETase expression construct. A polyhistidine tag is attached to PETase via a GS linker. Expression is under T7 promoter control. Illustration created using BioRender.com.

To clone the construct, Gibson assembly was utilized. The gene encoding PETase was synthesized by IDT. The gene was *E. coli* codon optimized before the purchase. Codon

optimization allows for the increased PETase protein production by making the sequence codons compatible with those which are frequently used by *E. coli*. [83] rather than the codons which are frequented by the native host, *I. sakaiensis*. The gene sequence was amplified by PCR and with the primers, CDP1 and CDP2. These specific primers were designed to attach overhangs to the insert gene which are required for the Gibson assembly process. PCR yielded the expected band of 941 base pairs, shown in Figure 11.

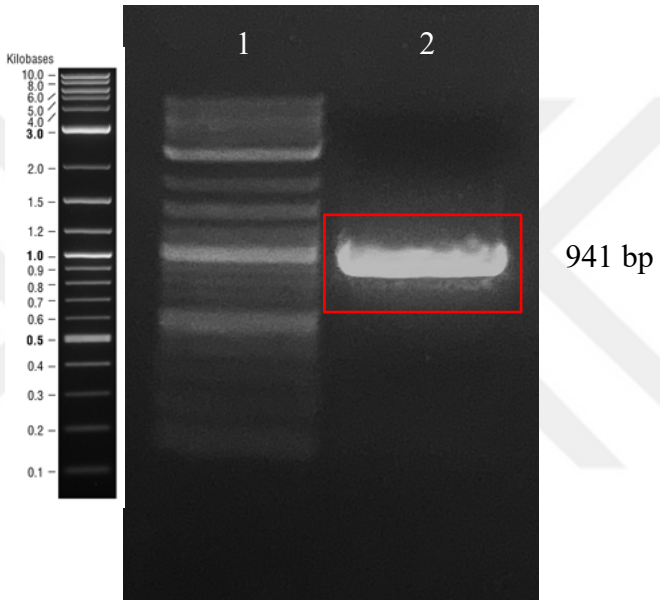

Figure 11. PCR amplification of PETase. Expected band is 941 bp. Lane 1 is the 1 kb plus DNA ladder (NEB).

To retrieve the backbone, the pET-22b(+) – GRFT – 6xHis vector was double restriction enzyme digested for an expected backbone size of 5298 base pairs (Figure 12).

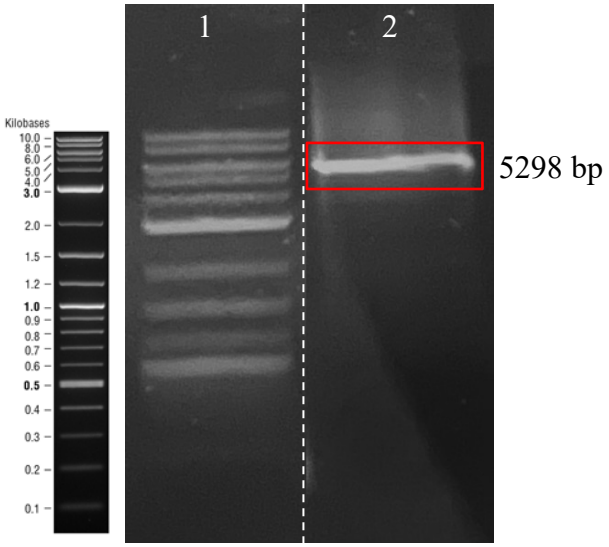

Figure 12. Restriction digestion to retrieve the pET-22b backbone. Expected band is 5298 bp. Lane 1 is the 1 kb plus DNA ladder (NEB). Dashed line indicates spliced gel image.

After retrieving both parts, the insert and the backbone were assembled using Gibson assembly at a 3:1 insert to backbone molar ratio. The schematic illustration of the final construct is given in Figure C.1 and the NGS sequence alignment of the construct is given in Figure D.1.

The cloning and the verification of the construct was performed in the *E. coli* DH5α cell strain, however for protein expression, the construct was transformed to the *E. coli* BL21 (DE3) strain. The BL21 (DE3) strain lacks the Ion and OmpT proteases, increasing protein expression efficiency and more importantly the lambda DE3 prophage which encodes the T7 RNA polymerase. The transformed cells were then induced by IPTG. For the induction, cells were grown until an OD600 of around 0.4-0.6 was reached and 1 mM of IPTG was added to the cells. The cells were then incubated overnight at 16 °C. 16 °C was selected as the induction temperature as

PETase is thermally unstable and is prone to loss of activity at prolonged exposure to ambient temperatures. Due to this issue both protein expression and protein isolation were performed at as cool temperatures as possible. Once induction and protein expression were ceased, PETase was isolated using the FPLC technique by taking advantage of the polyhistidine tag's affinity to nickel ions. Once the protein was bound to the nickel column, imidazole rich buffer was used for elution. Imidazole competes with the tagged protein for the binding of the column, allowing for elution. As stated earlier, the samples were kept as cool as possible on ice during the isolation process to avoid the loss of activity of PETase. Once the isolation of the protein was completed, the final isolate was loaded to a 10% SDS-PAGE gel for Western blot analysis (Figure 13). A 10% SDS-PAGE was selected for the proper resolution of the expected protein band, 31 kDa.

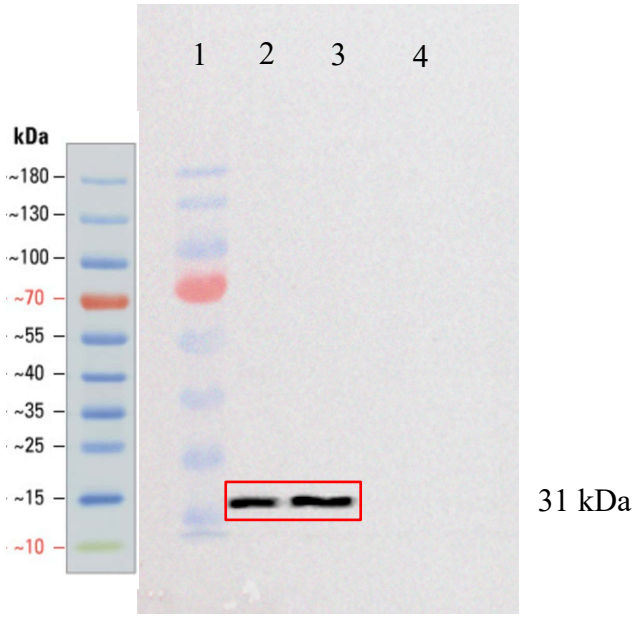

Figure 13. Western blot analysis of purified PETase. Lane 2 and lane 3 represent the elute from the FPLC protein isolation process. For lane 4, the same isolation process is

applied to empty BL21 cells as a control group. PageRuler prestained protein ladder (Thermo Scientific) is used as the marker, lane 1.

The Western blot analysis of the isolate revealed that PETase was successfully expressed by the cells and was successfully retrieved using the HisTrap affinity column in the FPLC procedure as the expected band of 31 kDa was observed. However, the Western blot image only reveals polyhistidine tagged proteins as the anti-His antibody is used in this blot. To reveal the entire protein content and to see if the protein is successfully isolated from other bacterial proteins, an SDS-PAGE electrophoresis followed by Coomassie blue staining was performed (Figure 14).

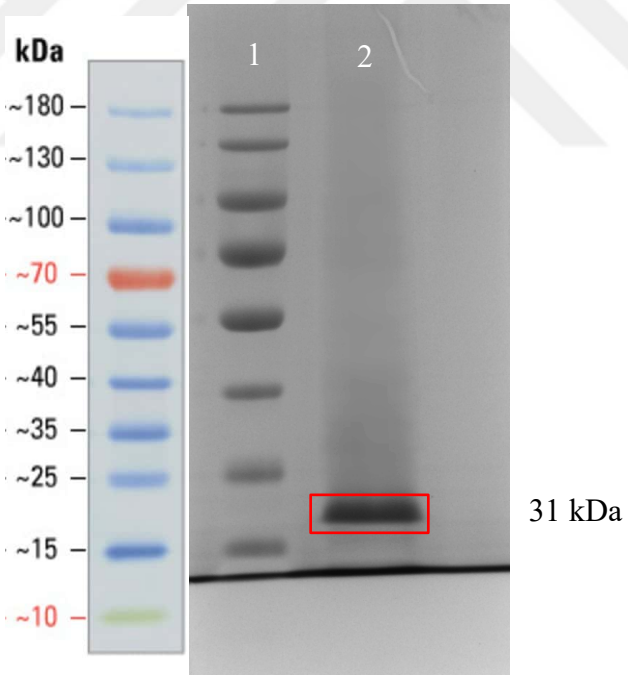

Figure 14. Coomassie staining of isolated PETase. The isolate from the FPLC process can be viewed in lane 2. PageRuler prestained protein ladder (Thermo Scientific) is used as a protein marker, lane 1.

As Coomassie blue binds to all proteins, this method of staining reveals the complete protein content of a sample. In Figure 14, the expected protein band, 31 kDa, corresponding to PETase can be clearly observed. Other than the expected band for PETase, no other protein can be observed in lane 2. This result suggests that not only PETase was able to be expressed and retrieved but also the protein was successfully purified using the above-mentioned processes.

3.2 Analysis of PETase Activity

To analyze the activity of isolated PETase, a p-nitrophenyl butyrate (pNPB) assay was performed. In this assay, the degradation of pNPB results in the formation of p-nitrophenol (pNP) and this product can be detected spectrophotometrically at 405 nm. As the bond between p-nitrophenol and butyrate is an ester bond and since PETase is an esterase class enzyme, this assay can be used to measure PETase activity. However, it should be noted that this substrate is not the preferred substrate of PETase and enzymatic activity against pNPB is lower compared to activity exerted against PET. Still, this assay provides a simple method to check PETase enzymatic activity. We performed the pNPB assay as a simple measurement to see if the enzyme we isolated in Chapter 3.1 has any viable enzymatic activity. The issue with this assay is the high amount of autohydrolysis pNPB shows when solved in 50 mM glycine-NaOH buffer and when incubated at 30 °C, the conditions which are required for PETase activity. The significant autohydrolysis of pNPB is a known issue [84]. So, to overcome this issue two groups were organized, the first group where a certain amount of pNPB was dissolved in buffer and was exposed to 30 °C for 10 minutes and second group where pNPB was dissolved in enzyme + buffer solution and again exposed to 30 °C for 10 minutes. For the first group, no enzyme group, only the autohydrolysis of pNPB was observed. For the second group, enzyme present group, autohydrolysis + enzymatic activity was observed. We expected that the second group would present higher absorbance readings and that the significant difference between the two groups would indicate PETase activity. The results of the pNPB assay are given in Figure 15.

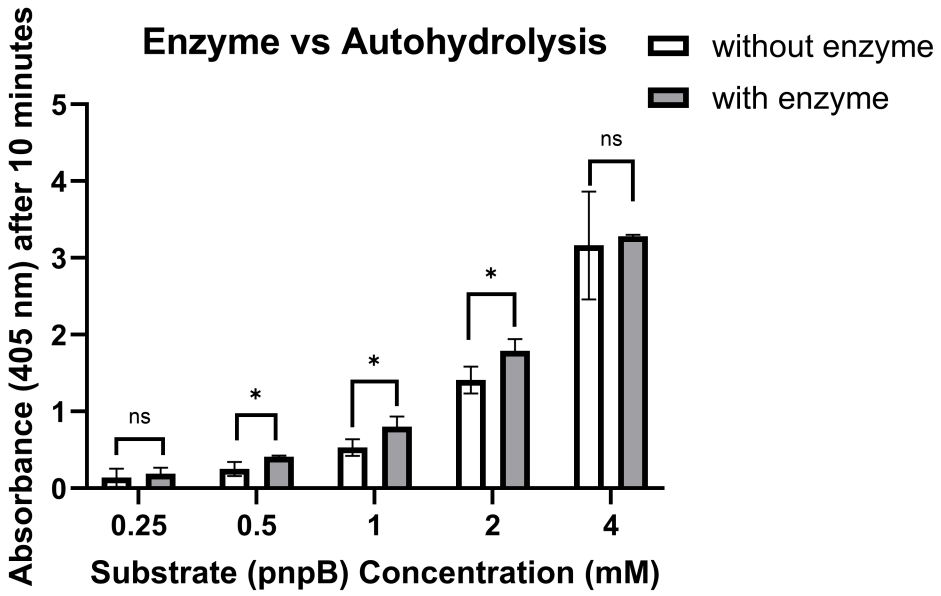

Figure 15. Enzyme vs Autohydrolysis results for the pnpB assay. 405 nm absorbances of the samples after treatment at different substrate concentrations. Enzyme concentrations used is constant. Analysis of the statistical significance was determined with student's t-test. ns indicates no significance, * indicates $p \leq 0.05$.

By observing Figure 15, it can be seen that there is a significant increase in released product in enzyme (+) groups compared to enzyme (-) groups when 0.5 mM, 1 mM and 2 mM concentration of the substrate is used. These were the expected results as enzymatic activity should result in higher hydrolysis of pNPB. However, contrary to the expected results, in the 0.25 mM and 4 mM substrate groups no significant difference was observed. We believe that for the 0.25 mM pNPB group, the unexpected results are due to the low amount of substrate. The low amount of substrate and thus low amount of product released might not have created a difference sensitive enough to change the recorded absorbance values. As for the 4 mM substrate concentration groups, this time the high amount of substrate might have caused the unexpected result. As the higher amount of substrate leads to higher amount of pNP released, the

absorbance values get to an amount where they reach the measuring limit of the spectrophotometer used (3.00 mAU). By looking at the expected results and explaining the unexpected results in Figure 15, it was concluded that the isolated PETase is active and exerts enzymatic activity.

Once the expressed and isolated PETase was shown to have the expected esterase activity, next an assay to show and characterize PETase enzymatic against PET itself was designed and performed. 75 mg PET film was treated with PETase in 50 mM glycine-NaOH buffer (pH 9.0) at 30 °C. Optimal buffer for PETase and the reaction temperature were chosen as described by Deng et al. [63]. Two setups for the assay were used. For the first setup, the initial enzyme solution was untouched, and no fresh enzyme was added (no refresh group). Samples were collected for HPLC analysis at the endpoint of the assay. For the second setup, the enzyme solution in which PET is treated was refreshed with freshly isolated enzyme every 24 hours (enzyme refresh group). Every 24 hours, the discarded enzyme solution was collected as a sample for HPLC analysis. Both experiments were terminated at 10 days. For both instances, two different enzyme concentrations were tested: 150 µg/ml and 50 µg/ml. For all experiments buffer containing no enzyme was used as the negative control. Products were analyzed with HPLC (coupled to a C18 column). Dilutions of TPA dissolved in 50 mM glycine-NaOH buffer were used as standards. TPA is one of three products produced by the PET hydrolysis reaction (TPA, MHET, BHET).

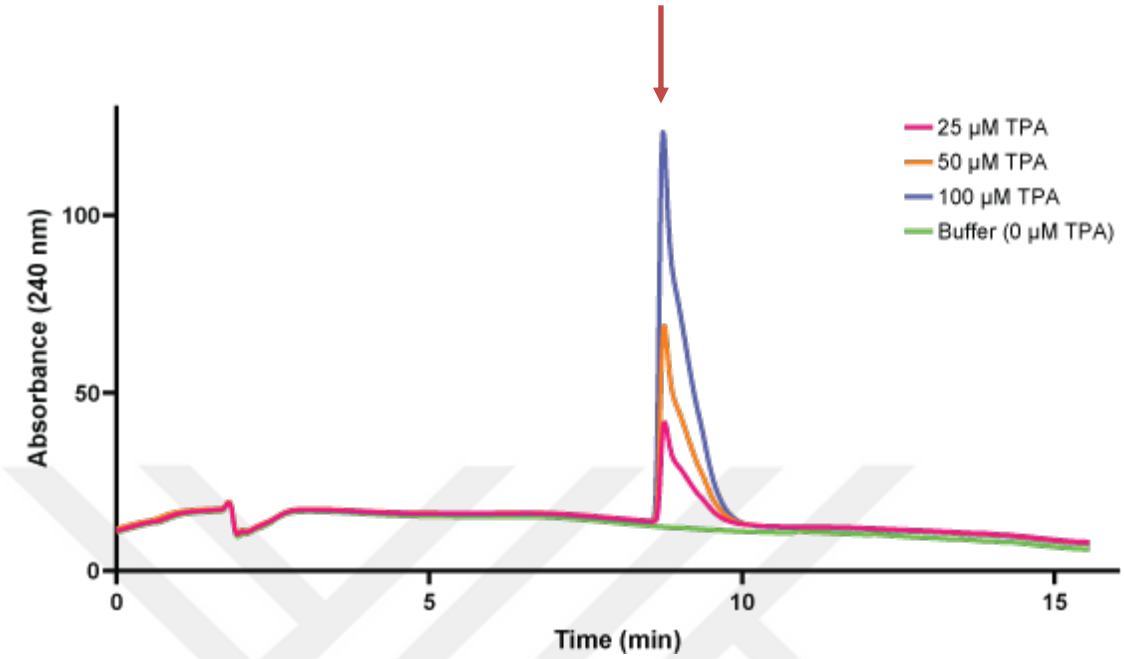

Figure 16. HPLC chromatogram of TPA standard dilutions. The TPA peaks are marked with a red arrow.

By first examining Figure 16, it can be seen that TPA is clearly detectable by measuring absorbance at 240 nm. Higher amount of TPA correlates to a higher peak as observed. Moreover, it is evident that peak describing TPA is at ~ 9 mins. From now on, the peak indicating TPA presence will be expected at around 9 mins. Next the previously described no refresh group samples were assayed.

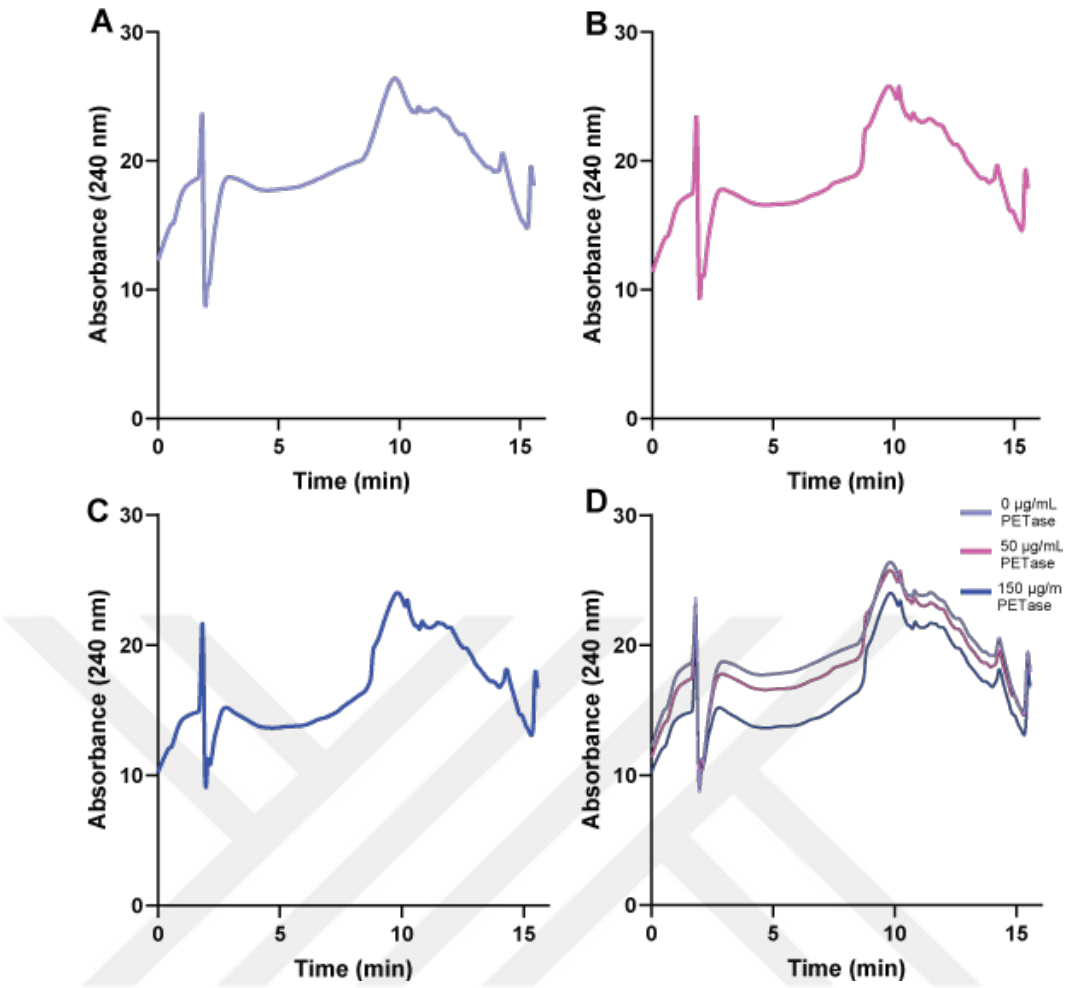

Figure 17. HPLC analysis of no refresh group samples. A) Chromatogram of no refresh group with 0 µg/ml PETase concentration (buffer only). B) Chromatogram of no refresh group with 50 µg/ml PETase concentration. C) Chromatogram of no refresh group with 150 µg/ml PETase concentration. D) Chromatograms in A, B and C are overlapped. Samples collected and analyzed after 10-day incubation.

Observing the no refresh group samples (Figure 17), no clearly distinguishable peaks at the expected timepoint of ~ 9 min can be seen, there seems to be no difference between the negative control (Figure 17.A) and the other groups (Figure 17.B and C). No TPA peaks mean no TPA production. The likely reason for this is the thermal unstability and the resulting loss of activity of PETase. PETase is known to lose activity even after 24 hours in mild conditions [62]. In the assay conducted, the enzyme most

likely does not retain activity long enough to produce significant amounts of TPA. To overcome this issue, the enzyme refresh group experiment was conducted as previously explained. As the enzyme is refreshed with fresh enzyme it is expected that enzymatic activity on the PET film will be constant and PET degradation will be observed.

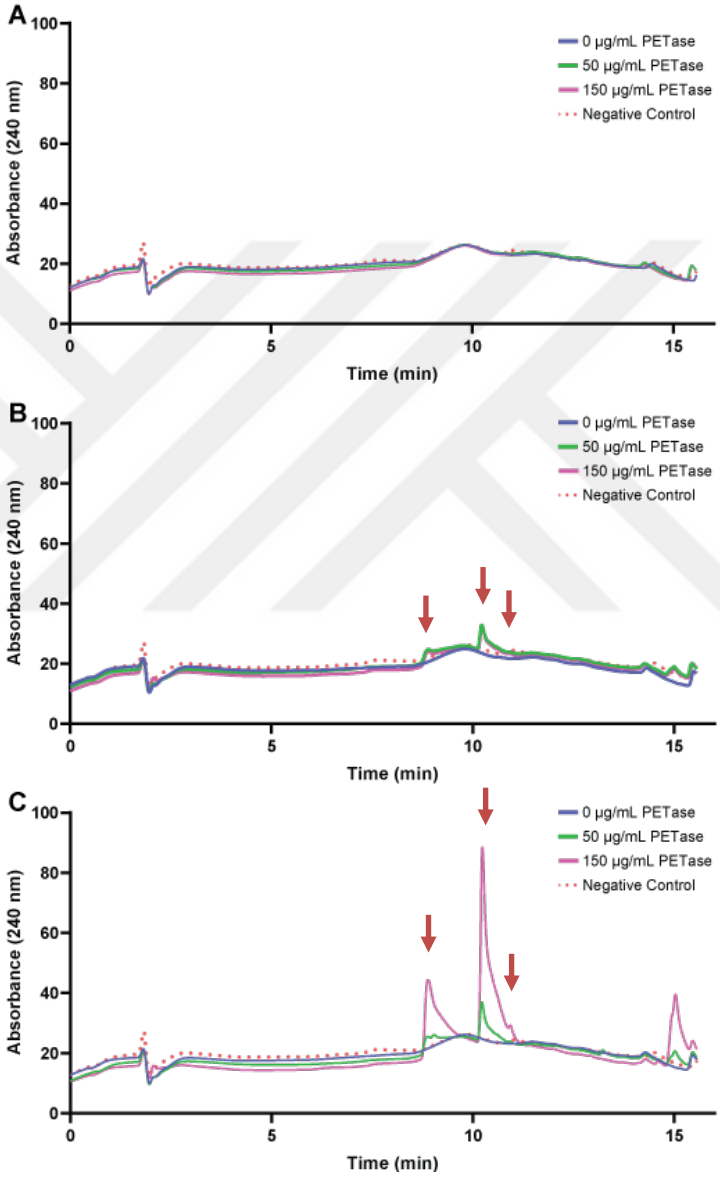

Figure 18. HPLC analysis of refresh group samples. A) Samples collected at day 1. B) Samples collected at day 5. C) Samples collected at day 10. Negative control is PETase only (no substrate). Peaks of interested are mark with red arrows.

Next, the enzyme refresh group experiments were conducted (Figure 18, Figure F.2, Figure F.3). In these results some trends can be observed, first it can be seen that higher amount of enzyme leads to higher TPA peaks which is expected. Higher concentrations of enzyme lead to higher product amounts and ultimately higher peaks. The second trend is that in each refresh, TPA peaks and thus TPA amount in the sample increases with the highest peaks observed in the day 10 samples (day 10 samples indicate reaction products for the interval between the 9^{th} day and the 10^{th} day), this trend can be most clearly observed in Figure F.3. This observation is likely due to the change in the substrate surface topology. As PET is degraded, imperfections on the surface are expected to occur which can increase surface area. The increase in surface area would likely offer more PETase binding leading to an increase in produced TPA.

The third and most important observation made from Figure 18 is the higher peak at ~10 min and a very small peak at around ~11 min. The mentioned peaks can be most prominently observed in the 150 µg/ml enzyme group at day 10 (Figure 18.C). The larger peak at ~10 mins is most likely MHET and the smaller peak at ~11 min is most likely BHET. Along with TPA these are the expected products of the PET hydrolyzation reaction. As MHET has a smaller molecular weight (210.18 g/mol) when compared to BHET (254.24 g/mol) it is expected that the peak indicating MHET would come earlier than the peak for BHET.

To analyze the unknown peaks at ~10 min and ~11 min, enzyme refresh group (150 µg/ml enzyme, day 10) samples were analyzed using mass spectrometry. These samples were selected for analysis as the mentioned unknown peaks were most prominent in this group. LC/MS QTOF allows for the exact detection of mass-to-charge ratio (m/z)

of components in a sample. The expected m/z values of the PET degradation products are as such, TPA: 165.13, MHET: 209.18, BHET: 253.24. The LC/MS QTOF was coupled with the same C18 column as used in the HPLC in order to separate the peaks of interest.

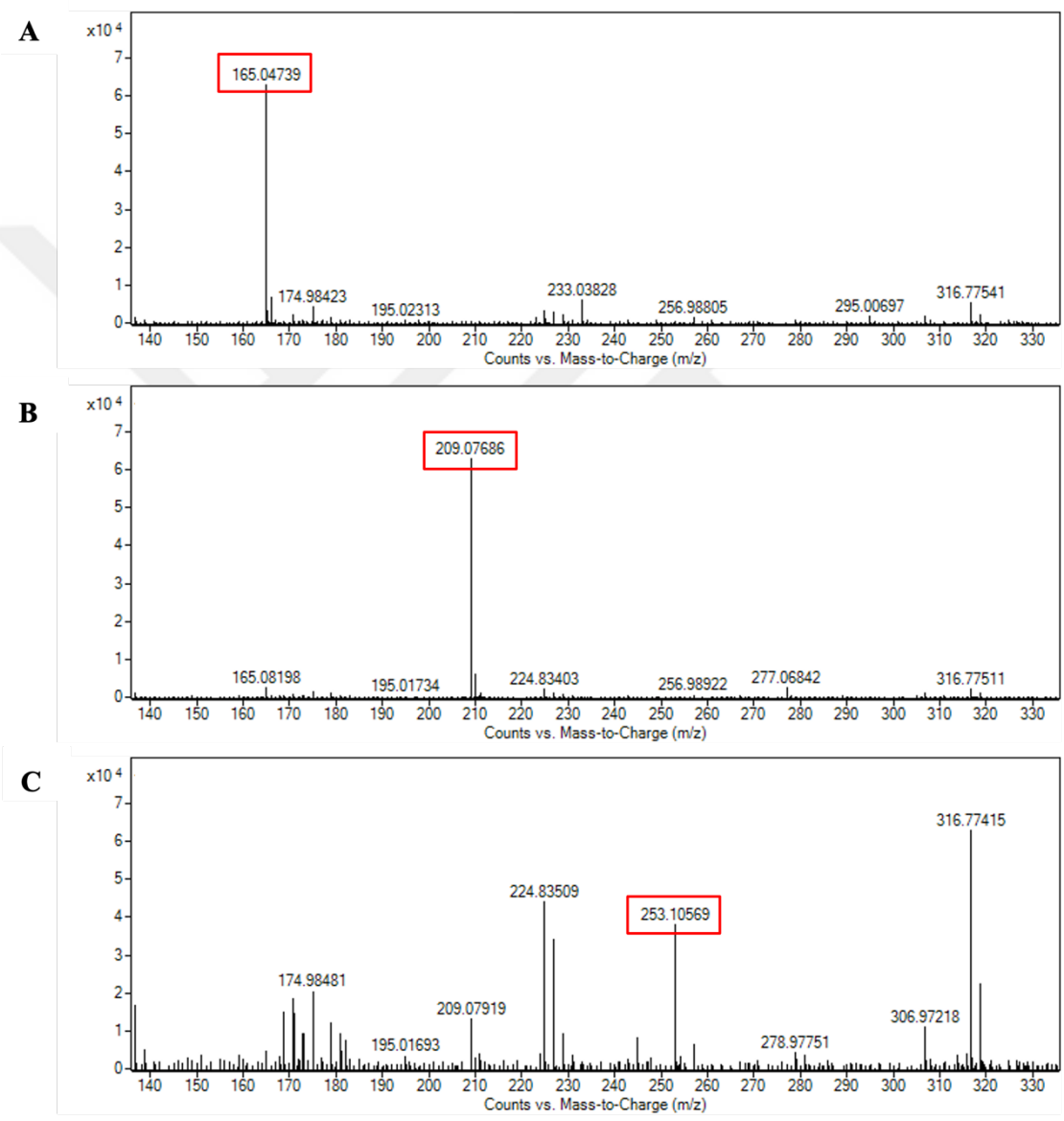

Figure 19. Mass spectrometry analysis of PET degradation products. A) Analysis of peaks at 9 min. B) Analysis of peaks at 10 min. C) Analysis of peaks at 11 min. Expected values are marked with red.

The LC/MS-QTOF analysis of the unknown peaks (Figure 19) revealed the peaks to be the expected molecules of MHET (Figure 19.B) and BHET (Figure 19.C). The expected m/z values of both MHET and BHET can be observed in 10 min and 11 min, respectively. Also, the TPA peak was once again confirmed as the expected m/z value was observed (Figure 19.A).

TPA, BHET and MHET are the expected products of the enzymatic degradation of PET. Since the presence of TPA, BHET and MHET is confirmed in the samples via both HPLC and LC/MS-QTOF analyses, it can be said that isolated PETase exhibits the expected PET degradation activity.

3.3 Visualization of Enzymatic PET Degradation

Once the PETase activity assays discussed in section 3.2 were completed, to further assess and visualize enzymatic activity, samples from the degradation assays were viewed using scanning electron microscopy (SEM). Enzyme-treated, buffer-treated and non-treated PET film samples were imaged. The surfaces of the samples were visually inspected to find any deformities on the surface and were compared. Images that were taken using SEM are given in Figure 20.

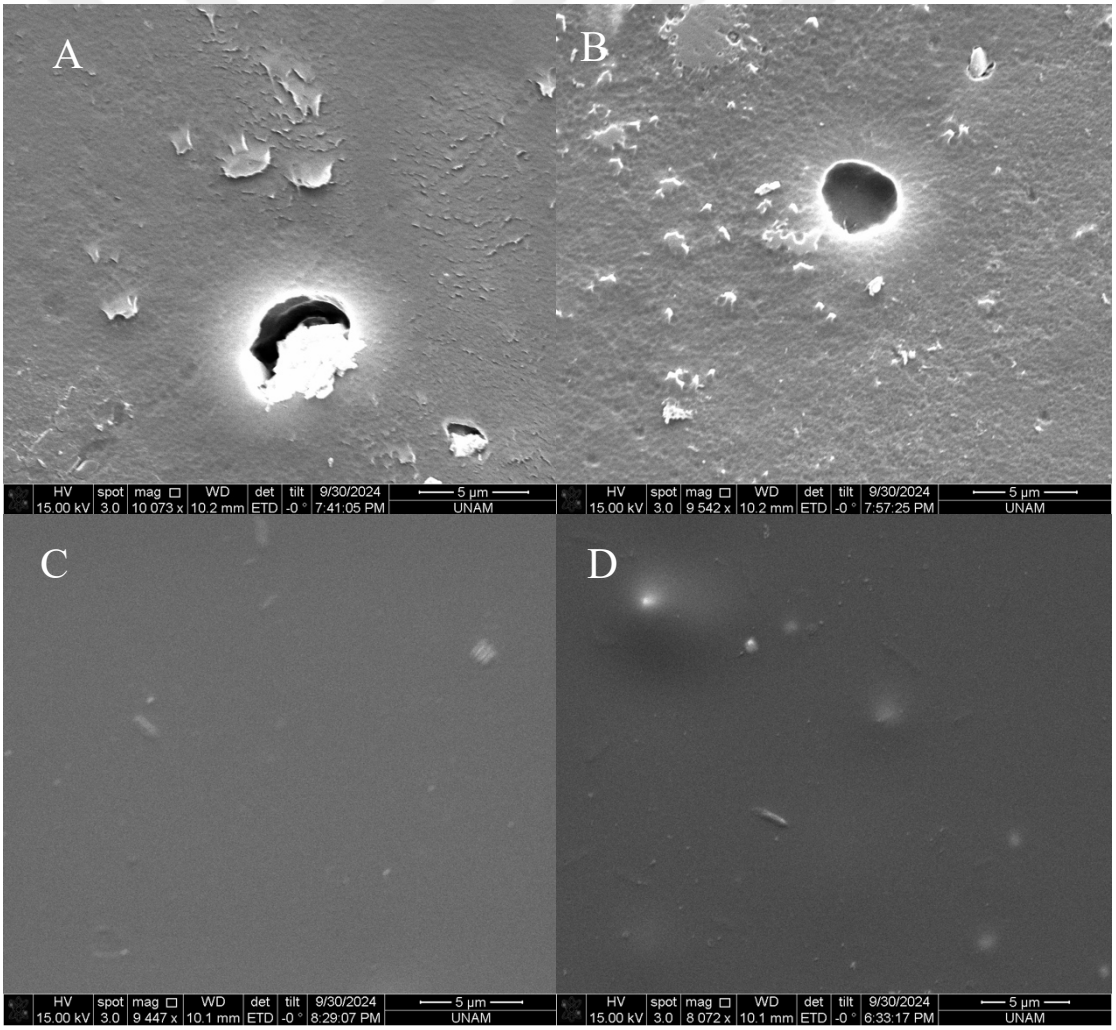

Figure 20. SEM images of treated PET film samples. A) PET film treated with 150 µg/ml every 24 hours. B) PET film treated with 50 µg/ml every 24 hours. C) PET film

treated with 0 μg/ml (only 50 mM glycine-NaOH buffer) every 24 hours. D) Untreated PET film.

PETase enzyme treated samples (Figure 20. A and B) seem to display obvious deformities on their surface when compared to the control groups (Figure 20. C and D). The control groups have smooth surfaces while the surfaces of the enzyme treated samples are eroded with micron scaled holes. Furthermore, the deformation on the surface of the 150 μg/ml enzyme per day sample seems to be more frequent and the holes seem to be larger and deeper when compared to the 50 μg/ml enzyme per day group. This observation is in line with the results of Chapter 3.2 as in the enzymatic activity assay done, it was observed that higher enzyme concentration led to a higher amount of degradation product. Moreover, as it is seen that PETase enzymatic activity results in holes and defects on the PET film surface, this also explains why degradation product amount increases each day for the results discussed in Chapter 3.2. As more holes and deformities form on the surface, the surface area of the substrate where PETase can bind to increases and as accessible substrate increases the amount of the product (TPA, MHET, BHET) increases. Although not a quantitative assay, SEM imaging reveals how PETase degrades PET and is further proof of its activity.

3.4 Cloning and Expression of Whole Cell System Displaying PETase Protein

For the surface display of PETase, the genetic circuit represented in Figure 21 was constructed. The construct once again features a polyhistidine tag on PETase. The tag offers the advantages explained in section 3.1. On the N-terminal of PETase the pelB leader sequence can be observed. This sequence consisting of 22 amino acids, acts as a guide for protein directing the tagged protein to the bacterial periplasm. Once the protein translocates to the periplasm the signal sequence is cleaved by peptidase enzymes. Furthermore, pelB has been shown to attune protein stability and aggregation [85], hence the reason this signal sequence was chosen. The pelB signal sequence is required for this construct as the protein needs to be directed to the periplasmic space so that it can be anchored to the cell surface. On the other flank of the PETase sequence, the Ag43 construct can be found. This construct consists of the α-passenger domain and the β-translocation domain. The α domain is a truncated version of the native sequence. The first 160 amino acids of the native α domain sequence have been deleted and is replaced by the sequence of the PoI to be carried as the cargo protein. While the α domain, along with the cargo protein, is secreted outwards of the cell, the β domain embeds itself into the outer membrane and folds into a β-barrel structure. The engineering of the Ag43 autotransporter protein into a bacterial cell surface display system was previously done in our lab [74]. We believed that using this system would be beneficial, as in previous work, proteins similar both in size and in enzymatic function to PETase were successfully expressed in this way [74].

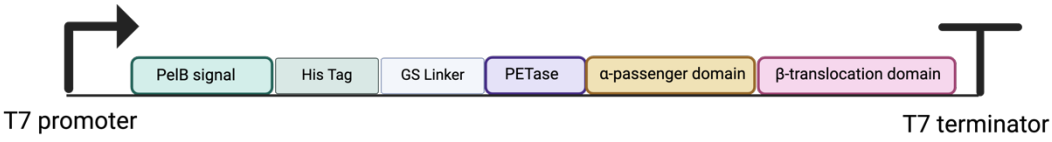

Figure 21. The schematic illustration of the Ag43-PETase expression construct. An N-terminal polyhistidine tag is linked to PETase via a GS linker. Flanking the his-tagged PETase, the pelB leader sequence can be found on the N-terminal. On the C-terminal, the Ag43 construct, passenger, and translocation domains, respectively, can be found. The expression cassette is under the control of the T7 promoter.

To clone the construct, first PETase was PCR amplified with overhangs appropriate for Gibson cloning. The expected band of 944 base pairs was observed in Figure 22.

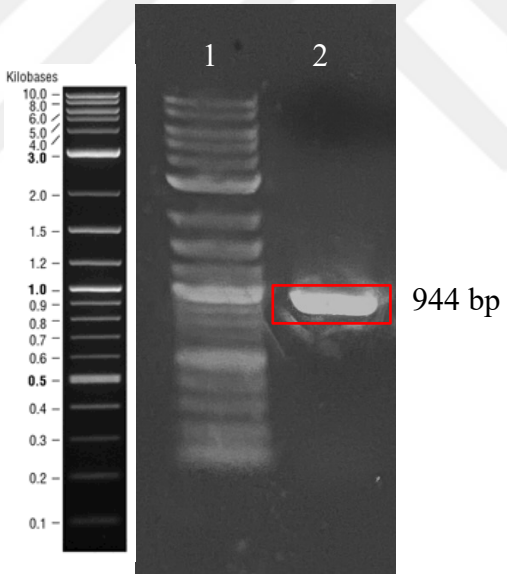

Figure 22. PCR amplification of PETase with overhangs. The expected band of 944 base pairs can be observed in lane 2. 1 kb plus DNA ladder (NEB) is used as a marker, lane 1.

To obtain the backbone, the vector pET-22b – pelB – 6His – sfGFP – Ag43 which was previously available in our lab was double digested using the AflII and BamHI-HF

restriction enzymes. The expected band of 8013 base pairs was observed and extracted from the gel image in Figure 23.

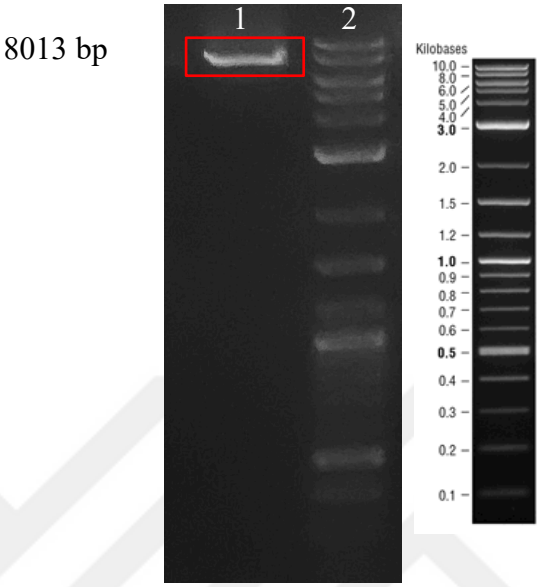

Figure 23. Digestion results of pET-22b – pelB – 6His – sfGFP – Ag43 plasmid. The expected band of 8013 base pairs can be observed in lane 1. 1 kb plus DNA ladder (NEB) is used as a DNA marker, lane 2.

Once the insert and the backbone were obtained, Gibson assembly was performed at a molar ratio of 3:1 insert to backbone. The plasmid map and the Sanger sequencing results of the construct can be viewed in Figure C.2 and Figure D.2, respectively.

After the construct was verified with Sanger sequencing, the newly obtained plasmid was transformed into *E. coli* Bl21 (DE3) strain for protein expression. Protein expression was again conducted with IPTG induction, overnight at 16 °C. Once again, 16 °C was chosen as the induction temperature so that PETase can retain enzymatic activity. However, this time, the cell culture was supplemented with 1% glucose.

Surface display is a costly metabolic activity for the cells and glucose aids cell viability. Before moving onto the Western blot analysis of the surface displayed proteins, the cell samples were subjected to heat treatment so that the surface display elements were released into the environment. Once heat treatment was completed, the cells were removed, and the remaining sample was subjected to acetone precipitation so that a more concentrated number of proteins could be retrieved. As the surface displayed proteins weren't isolated using FPLC, these extra steps were performed to gain a clearer image during Western blot analysis. Furthermore, an IPTG gradient was used to check expression efficiency based on IPTG concentration. IPTG conditions were selected as 1 mM, 0.5 mM, and 0.25 mM. Empty BL21 DE3 cells (1 mM IPTG) and 0 mM IPTG groups were selected as negative controls after being subjected to the same treatment. The result of the Western Blot analysis can be observed in Figure 24.

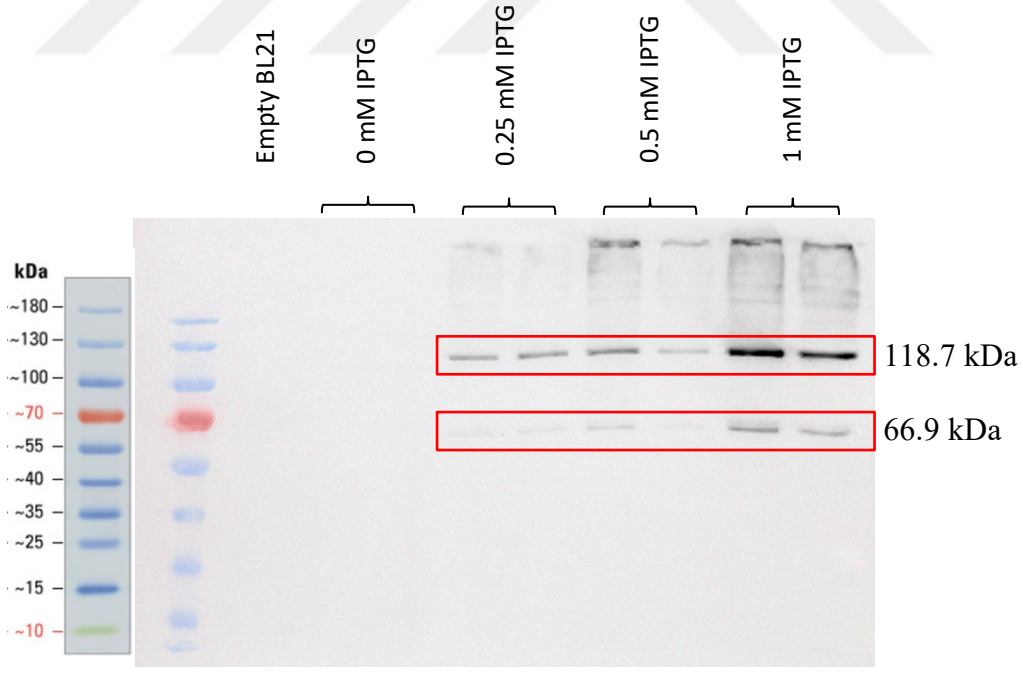

Figure 24. Western blot analysis of surface displayed PETase. Lane 2 is empty BL21 negative control. Lane 3 and 4 represents 0 IPTG negative control replicates. Lanes 5 and 6 represents 0.25 mM IPTG induced group replicates. Lanes 7 and 8 represent 0.5

mM IPTG induced group replicates. Lanes 9 and 10 represent 1 mM IPTG induced group replicates. PageRuler prestained protein ladder is used as the marker in lane 1.

Looking at the Western blot analysis in Figure X, in the induced groups 2 clear bands, 118.7 kDa and 66.9 kDa, can be observed. These were the expected bands. The 118.7 kDa band represents the entire Ag43 complex along with PETase: PETase (30kDa) + Ag43 α-passenger domain (33.7kDa) + Ag43 β-translocation domain (51.5kDa) + tags and linkers = 118.7 kDa. The α and β domains of the complex are linked with non-covalent bonds so they can get disrupted during the blotting process or by the heat treatment done to the cells before the Western Blot. So, the observed 66.9 kDa band is expected and represents: PETase (30kDa) + Ag43 α-passenger domain (33.7kDa) + tags and linkers = 66.9 kDa. From the Western Blot in Figure X, it can be interpreted that the surface display complex along with the his-tagged protein of interest are being successfully expressed by the transformed cells when induced by IPTG. Despite the expected results, a Western Blot analysis is not enough to verify the success of the proposed system. To make sure that the proteins are also displayed in a topologically correct manner on the surface of the cells, the complex was detected and visualized using immunocytochemistry (ICC).

For the ICC technique, the PETase displaying cells were labeled with an anti-his antibody conjugated with Dylight550, as the protein is his-tagged. To stain the nuclei of the cells, 4′,6-diamidino-2-phenylindole (DAPI) was used. DAPI is blue fluorescent, can pass through the intact cell membrane and binds to AT rich regions of dsDNA [86].

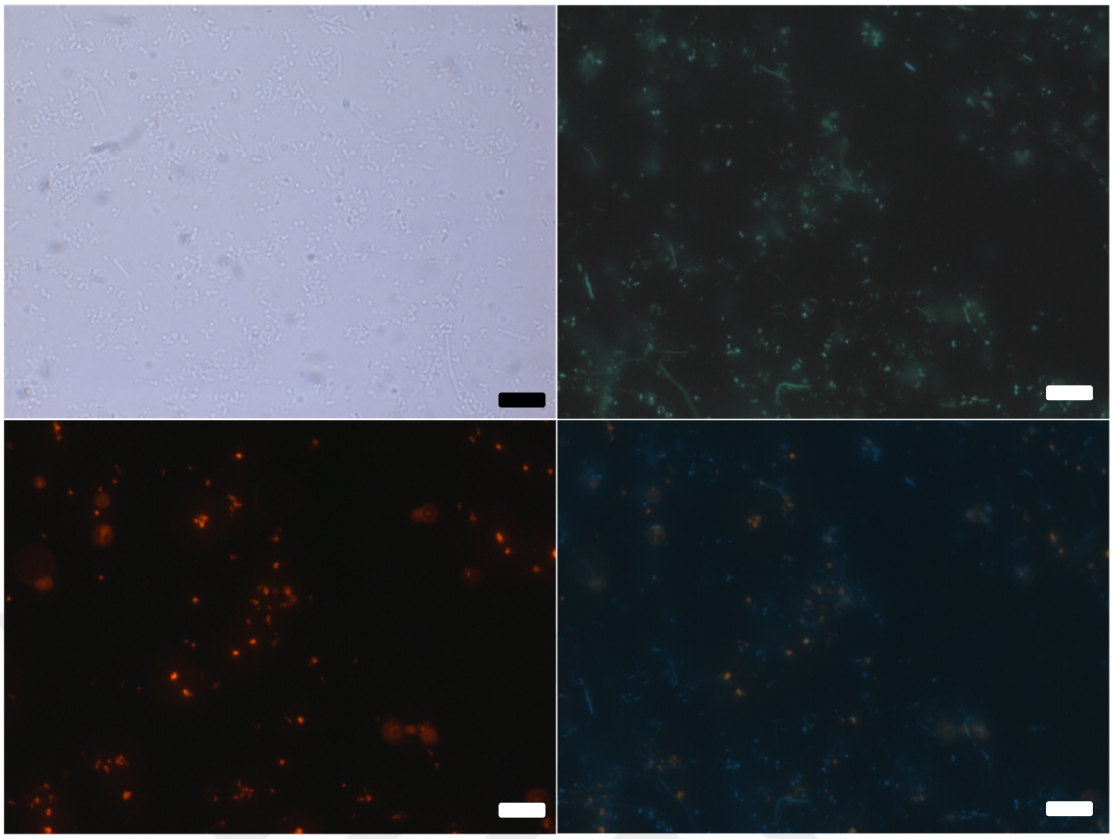

Figure 25. ICC staining of induced Ag43-PETase cells. Top left: Brightfield imaging of cells. Top right: blue light excited, for DAPI visualization. Bottom left: red-yellow light excited, for Dylight550 visualization. Scale bars represent 50 μm. Bottom right: all images merged.

Looking at Figure 25, the ICC labeled cells can be observed. The Dylight550 signal (red) can be clearly seen along surface of cells, indicating that his-tagged PETase is correctly displayed on the surface. Based on the observed bands in the Western blot data (Figure 24) and the observed Dylight 550 signals in the ICC data (Figure 25), it can be interpreted that PETase is correctly expressed and correctly displayed on *E. coli* cell surface using the Ag43 complex.

3.5 Analysis of Whole Cell System Activity

Once the proper surface display of PETase was verified via the analyses done in Chapter 3.4, next the PET degradation ability of the bacterial system was analyzed. To do so, PET degradation assays were performed. Different setups and conditions were tested. 3 different setups were drawn up. For the first setup (**buffer group**), IPTG induced PETase displaying cells were transferred to 50 mM glycine-NaOH buffer (pH 9.0). Similar to the no enzyme refresh group samples from Chapter 3.2, the cells were incubated with 75 mg PET film at 30 °C for 10 days in no shaking conditions. After 10 days, the assay was terminated, and samples were collected from the incubation for HPLC analysis. For the second setup (**LB group**), cells were once again IPTG induced however this time they were kept in LB media (pH 9.0). The cells were then incubated with 75 mg PET film at 30°C, non-shaking conditions. Every 3 days, a portion of the culture was removed and replaced with fresh media to create a continuous culture model and allow for new cellular growth and protein expression. This was done so that newly expressed "fresh" enzyme would replace the enzymes that have lost their activity due to thermal instability. The passaging was done every 3 days as this was the time required for the cells to reach confluency (OD600 = 1.5) under these conditions. The process involving the addition of fresh media was adapted from Jia et al. [75]. For the third and final setup (**M9 group**), cells were this time transferred to M9 minimal media (pH 9.0). Incubation conditions were once again 30°C, non-shaking and again cells were passaged every 3 days as explained for the second setup. During each passage, samples were taken for HPLC analysis. Samples were also taken at the endpoint of the assay which was determined to be 9 days. Both LB and M9 media were adjusted to pH

9.0 for optimal enzyme activity. For each assay, empty *E. coli* BL21 (DE3) was used as negative controls. Collected samples were then subjected to HPLC analysis.

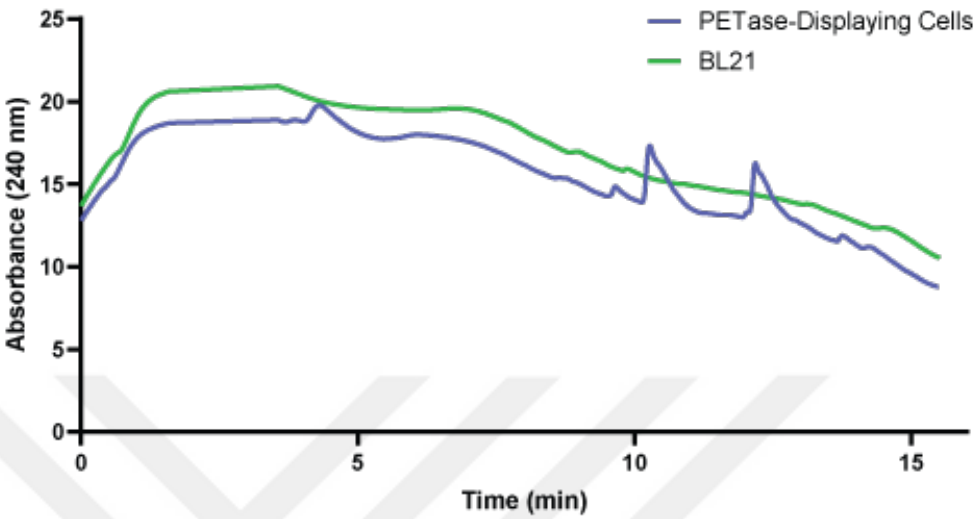

Figure 26. HPLC chromatogram for buffer group samples. Unknown bands of interest can be observed around the 10-minute mark. PET incubated with empty BL21 is used as the negative control group.

As discussed in Chapter 3.2, the expected products of the PET degradation reaction TPA, MHET, BHET are expected to generate HPLC chromatogram peaks at ~9 minutes, ~10 minutes and ~11 minutes, respectively. These are the expected peaks for the HPLC analysis of the buffer group assay in Figure 26. There seems to be a peak at ~10 min and ~11 min but not at ~9 min. However, although they are smaller, these peaks can be also observed in the negative control sample of empty cells. This would suggest that these peaks aren't representative of either MHET or BHET. Still, these samples were further analyzed using LC/MS QTOF.

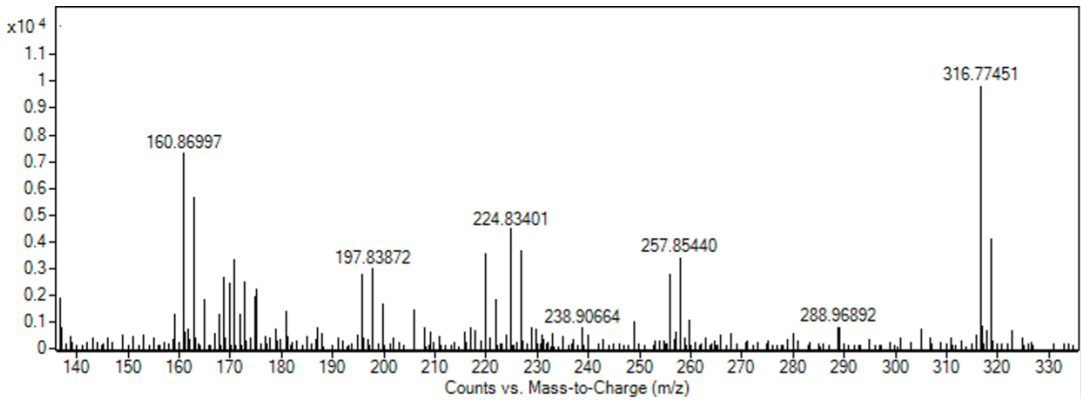

Figure 27. Mass spectrometry profile of the buffer group assay reaction products.

The LC/MS-QTOF analysis of the buffer group samples (Figure 27). revealed that in fact the unknown peaks were not of PET degradation products since the expected m/z values of neither product (TPA: 165.13, MHET: 209.18, BHET: 253.24) were observed in the mass spectrometry profile.

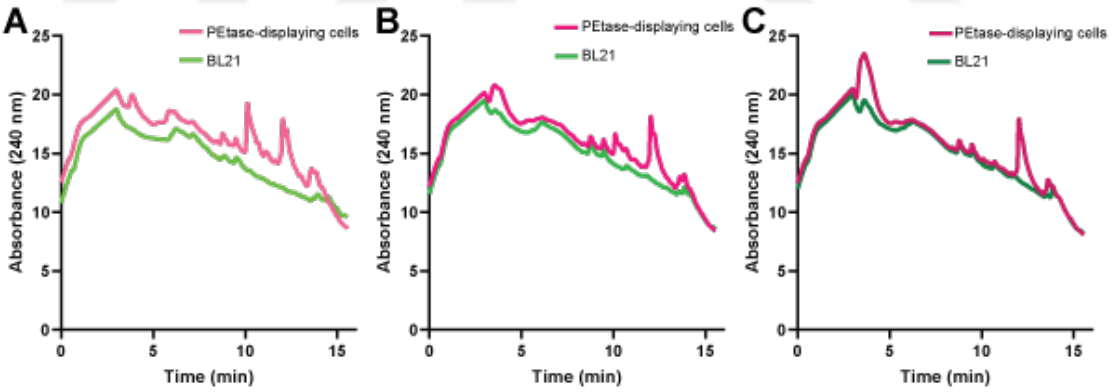

Figure 28. Chromatograms resulting from the HPLC analysis of LB group samples. A) Samples collected during day 3. B) Samples collected during day 6. C) Samples collected during day 9. PET incubated with empty BL21 cells are used as negative control. In each sample, unknown peaks around 9-10-11 minutes can be observed which are the expected minutes for the peaks of PET degradation products.

Next, the LB group samples were HPLC analyzed (Figure 28). Similarly, the expected bands indicating degradation product presence were at around 9, 10 and 11 minutes. Relatively small peaks were observed at the time of the expected products. The peaks were then analyzed with LC/MS QTOF (Figure 30).

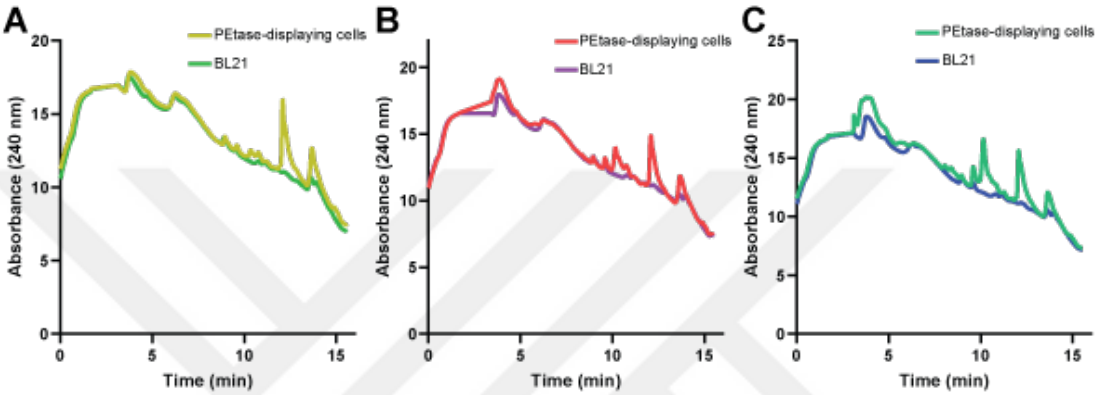

Figure 29. Chromatograms resulting from the HPLC analysis of M9 group samples. A) Samples collected during day 3. B) Samples collected during day 6. C) Samples collected during day 9. PET incubated with empty BL21 cells are used as negative control. In each sample, unknown peaks around 9-10-11 minutes can be observed which are the expected minutes for the peaks of PET degradation products.

Finally, the M9 group samples were HPLC analyzed in similar fashion (Figure 29). Again, the peaks suggesting TPA, MHET and BHET presence were expected at around 9, 10 and 11 minutes. Similar to the LB group, unknown small peaks could be observed around this time and further analysis was conducted with LC/MS QTOF (Figure 30).

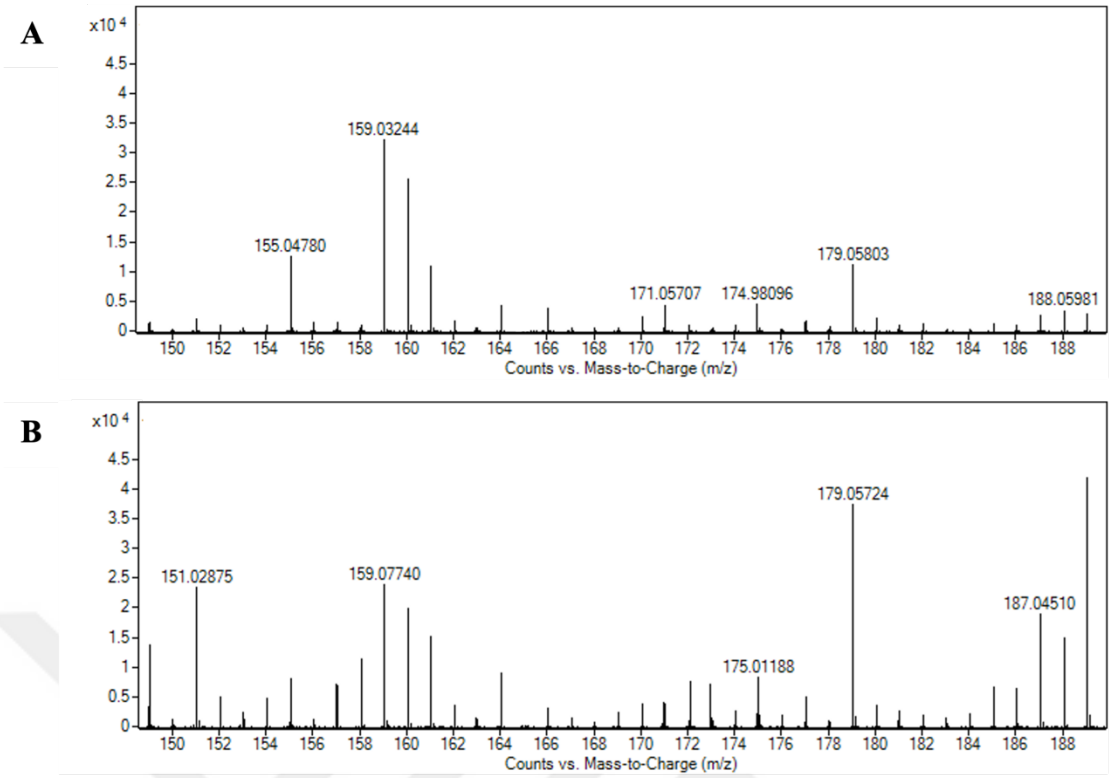

Figure 30. Mass spectrometry profiles of A) LB group and B) M9 group samples. Collected samples from day 3, day 6 and day 9 were mixed respectively for each group prior to analysis.

Unfortunately, the mass spectrometry of the unknown bands did not provide the expected values for the PET degradation products (Figure 30). This would indicate that that PET degradation products are not present in the samples.

Three different experimental conditions and groups were tested for the PET degradation activity of the PETase displaying cells. In neither condition the expected presence of PET degradation products (TPA, MHET and BHET) were observed. These initial unexpected results indicate that PET degradation via the constructed bacterial system in these conditions were unsuccessful. A couple of reasons might be behind the issue. One reason might be that the LB and M9 media complexions might be interfering with the proper folding of PETase on the surface of the cell or proper enzyme-substrate

interactions. Similarly, owing to the metabolic activity of the cells, one of the metabolites accumulating in the environment might be reason for the interference. Furthermore, the expression of the protein might not be enough to produce any meaningful catalytic activity. Similarly, the assay duration might have been insufficient as it was seen in Chapter 3.2 that each day greater amount of PET degradation products are observed and that in the first few days PETase activity might not be enough to produce significant products (Figure F. 1). In any case, more experiments, testing and trial and error is needed to understand the problem and a lot of optimization needs to be done. Different buffering conditions (different buffers, media, pH), induction and expression conditions (IPTG amount, induction temperature), assay setups (longer incubation time, greater cell amount) need to be tested and optimized.

3.6 Cloning of the iLOM-SS - PETase Construct

For the leaky outer membrane phenotype cells expressing PETase, the construct in Figure 31 was cloned. The plasmid includes two operons, micL sRNA expression is under the control of the Lac operator and PETase expression under the control of Tet operator. With this system, IPTG is used to induce expression of micL and thus induce the leaky outer membrane, whereas aTc is used to induce the expression of PETase. PETase is also tagged with the pelB secretion tag. The pelB sequence directs PETase to the periplasmic space. PETase which is in the periplasmic space can then get secreted by diffusing out of the outer membrane due to the micL sRNA disruption of the outer membrane.

Figure 31. Schematic illustration of the micL-PETase construct. micL sRNA expression is under the control of pLacO while PETase expression is controlled by pTetO. PETase is tagged with a 6xHis tag and the secretion tag, pelB.

To clone the construct in Figure 31, first PETase was amplified using PCR and then digested with XbaI and KpnI to create sticky ends. The expected band was 882 base pairs (Figure 32).

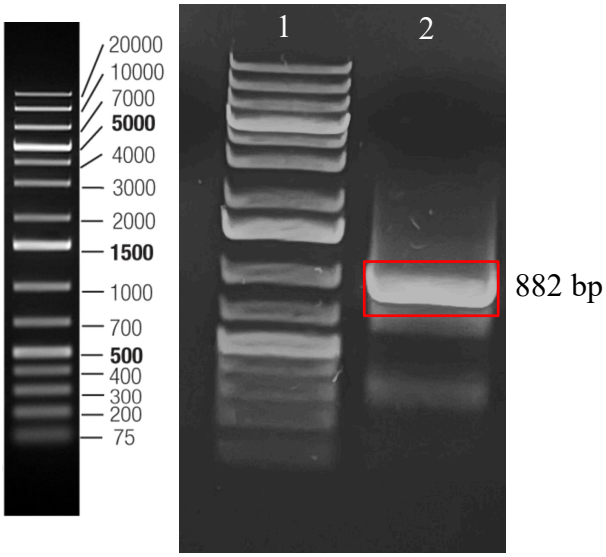

Figure 32. PCR amplification followed by XbaI and KpnI restriction digestion of PETase. GeneRuler 1 kb Plus DNA ladder (Thermo Scientific) is used as the marker in lane 1.

Next, the pET-22b(+) – pLacO MicL + pNTetO sfGFP plasmid was digested using XbaI and BamHI to obtain the backbone. The expected band of 6702 base pairs was retrieved after being observed as in Figure 33.

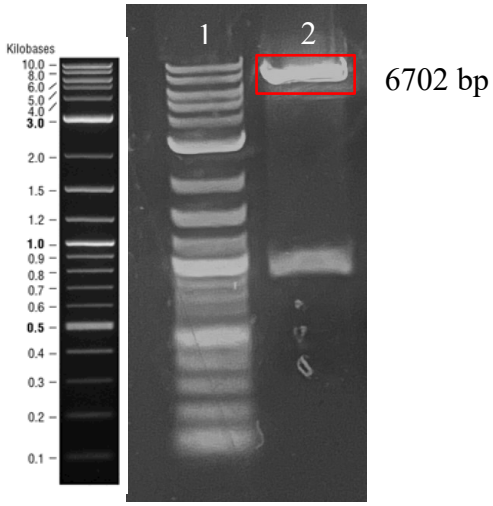

Figure 33. Double digestion of the pET-22b(+) – pLacO MicL + pNTetO sfGFP vector by XbaI and BamHI enzymes. 1 kb plus DNA ladder (NEB) is the marker used in lane 1.

Once both the insert and the backbone were obtained, the complementary sticky ends were ligated using T4 ligase to construct the pET-22b(+) – pLacO MicL + pNTetO PETase vector. The final construct (Figure C. 3) was verified with Sanger sequencing (Figure D. 3).

CHAPTER IV: CONCLUSION

As plastic usage has increased massively along the years, so has the consecutive accumulation of plastic waste and plastic pollution. This buildup of plastic waste has brought on many issues. The macro sized pollutants are the cause of issues for wildlife and a source of microplastics. Microplastics can cause major health problems for both animals and humans alike. Polyethylene terephthalate is a primary contributor to plastic pollution. The biological remediation of PET has presented itself as promising solution for this problem.

In this thesis, we aimed to engineer bacteria as tools for PET plastic bioremediation. For this system we used two approaches, for the first approach, the Ag43 autotransporter protein was utilized for the surface display of PETase. For the second approach, we aimed to utilize micL sRNA to disrupt the outer bacterial membrane for the secretion of PETase.

Before the construction of the proposed systems, we initially tested recombinant PETase activity. To do so, we first isolated recombinant PETase and verified the PET degradation activity of the enzyme. We performed a pNPB assay followed by the HPLC analysis of degradation products. In these results we observed that PETase needs to be isolated freshly and the enzyme solution to treat PET needs to be refreshed. This observation was in line with previous knowledge that PETase has low thermal stability and tends to lose activity in 24 hours at room temperature. We verified the enzymatic reaction products to be the expected PET degradation products with LC/MS QTOF. As further analysis of PETase activity, we examined degraded PET films with scanning electron microscopy. In the SEM images, we observed holes and scratches indicative

of PETase activity. These results showed us that the recombinant PETase produced and isolated in our laboratory had the expected PET degradation activity.

Once we were certain of the free PETase activity, we constructed the *E. coli* cells which are able to display PETase on their surface. We verified the surface display of PETase via immunocytochemistry staining. The staining of the cells revealed PETase on the surface of the cells as expected. Next, to assess the PET degradation activity of the PETase displaying cells, the cells were incubated with PET film. After incubation, HPLC and LC/MS QTOF analyses was performed to check the reaction products. Unfortunately, the expected reaction products were not observed. In future works, to solve this issue, we will focus on optimizing reaction parameters. We will focus on different buffering conditions as we suspect that the conditions used might be interfering with the proper folding of PETase. We will also be optimizing expression conditions. Higher amount of expression might lead to increase in activity where a significant amount of product might be detected with HPLC analysis. One other optimization will be done with the incubation settings. The incubation times as well as cell amounts will be optimized to find the correct working conditions for surface displayed PETase. While the initial results of the surface displayed PETase activity was not as expected, the construction of the second proposed bacteria where PETase is secreted was completed. This system was designed as an alternative system to degrade PET. The cloning of the plasmid was successfully verified. For future research, we will first perform secretion assays to show the successful expression and secretion of PETase using this system. Then we will once again complete activity assays by incubating PET film with PETase secreting cells under different conditions. Again, many optimizations will be done, different buffers with different pH values will be

used, different expression optimizations will be done and various assay setups, incubations times, cell densities will be tested.

All in all, we believe in the potential of PETase as the solution of PET recycling. With the knowledge gained from this study and the planned future research, we are hopeful that we can create a platform which can work as a useful tool in PET bioremediation.

BIBLIOGRAPHY

[1] M.M. Trescott, Pioneer Plastic: The Making and Selling of Celluloid. By Robert Friedel. (Madison: University of Wisconsin Press, 1983. xix + 153 pp. $19.95.), Bus. Hist. Rev. 58 (1984) 284–285. https://doi.org/10.2307/3115060.

[2] L.H. Baekeland, The synthesis, constitution, and uses of Bakelite., Ind. Eng. Chem. 1 (1909) 149–161.

[3] G. Kannan, S.E. Grieshaber, W. Zhao, Thermoplastic polyesters, Handb. Thermoplast. 41 (2016) 319.

[4] N.C. Wyeth, Inventing the PET Bottle, Res.-Technol. Manag. 31 (1988) 53–55. https://doi.org/10.1080/08956308.1988.11670536.

[5] R.J. Crawford, P.J. Martin, Plastics engineering, Butterworth-Heinemann, 2020.

[6] A.W. Birley, Plastics materials: properties and applications, Springer Science & Business Media, 2012.

[7] A.L. Andrady, M.A. Neal, Applications and societal benefits of plastics, Philos. Trans. R. Soc. B Biol. Sci. 364 (2009) 1977–1984. https://doi.org/10.1098/rstb.2008.0304.

[8] Plastics Europe, Plastics - the Facts 2023, (2023).

[9] Maria Tsakona, Elaine Baker, Ieva Rucevska, Thomas Maes, Lars Rosendahl Appelquist, Miles Macmillan-Lawler, Peter Harris, Karen Raubenheimer, Romain Langeard, Heidi Savelli-Soderberg, Kei Ohno Woodall, Jost Dittkrist, Tabea Anna Zwimpfer, Ruta Aidis, Clever Mafuta, Tina Schoolmeester, Drowning in Plastics - Marine Litter and Plastic Waste Vital Graphics, 2021.

[10] Plastics Europe, Plastics - the Facts 2022, (2022).

[11] R. Geyer, J.R. Jambeck, K.L. Law, Production, use, and fate of all plastics ever made, Sci. Adv. 3 (2017) e1700782. https://doi.org/10.1126/sciadv.1700782.

[12] Y.-H.V. Soong, M.J. Sobkowicz, D. Xie, Recent Advances in Biological Recycling of Polyethylene Terephthalate (PET) Plastic Wastes, Bioengineering 9 (2022) 98. https://doi.org/10.3390/bioengineering9030098.

[13] Andy Grant, Vera Lahme, Toby Connock, Leyla Lugal, How Circular Is PET?, (n.d.).

[14] OECD, Global Plastics Outlook: Economic Drivers, Environmental Impacts and Policy Options, OECD, 2022. https://doi.org/10.1787/de747aef-en.

[15] IUCN, ISSUES BRIEF - Plastic Pollution, (2024). https://iucn.org/resources/issues-brief/plastic-pollution (accessed November 14, 2024).

[16] D. Mentes, G. Nagy, T.J. Szabó, E. Hornyák-Mester, B. Fiser, B. Viskolcz, C. Póliska, Combustion behaviour of plastic waste – A case study of PP, HDPE, PET, and mixed PES-EL, J. Clean. Prod. 402 (2023) 136850. https://doi.org/10.1016/j.jclepro.2023.136850.

[17] C. Ioakeimidis, K.N. Fotopoulou, H.K. Karapanagioti, M. Geraga, C. Zeri, E. Papathanassiou, F. Galgani, G. Papatheodorou, The degradation potential of PET bottles in the marine environment: An ATR-FTIR based approach, Sci. Rep. 6 (2016) 23501. https://doi.org/10.1038/srep23501.

[18] A. Chamas, H. Moon, J. Zheng, Y. Qiu, T. Tabassum, J.H. Jang, M. Abu-Omar, S.L. Scott, S. Suh, Degradation Rates of Plastics in the Environment, ACS Sustain. Chem. Eng. 8 (2020) 3494–3511. https://doi.org/10.1021/acssuschemeng.9b06635.

[19] J. Brahney, M. Hallerud, E. Heim, M. Hahnenberger, S. Sukumaran, Plastic rain in protected areas of the United States, Science 368 (2020) 1257–1260. https://doi.org/10.1126/science.aaz5819.
[20] C.L. Waller, H.J. Griffiths, C.M. Waluda, S.E. Thorpe, I. Loaiza, B. Moreno, C.O. Pacherres, K.A. Hughes, Microplastics in the Antarctic marine system: An emerging area of research, Sci. Total Environ. 598 (2017) 220–227. https://doi.org/10.1016/j.scitotenv.2017.03.283.
[21] I.E. Napper, B.F.R. Davies, H. Clifford, S. Elvin, H.J. Koldewey, P.A. Mayewski, K.R. Miner, M. Potocki, A.C. Elmore, A.P. Gajurel, R.C. Thompson, Reaching New Heights in Plastic Pollution—Preliminary Findings of Microplastics on Mount Everest, One Earth 3 (2020) 621–630. https://doi.org/10.1016/j.oneear.2020.10.020.
[22] S. Gangadoo, S. Owen, P. Rajapaksha, K. Plaisted, S. Cheeseman, H. Haddara, V.K. Truong, S.T. Ngo, V.V. Vu, D. Cozzolino, A. Elbourne, R. Crawford, K. Latham, J. Chapman, Nano-plastics and their analytical characterisation and fate in the marine environment: From source to sea, Sci. Total Environ. 732 (2020) 138792. https://doi.org/10.1016/j.scitotenv.2020.138792.
[23] T. Horvatits, M. Tamminga, B. Liu, M. Sebode, A. Carambia, L. Fischer, K. Püschel, S. Huber, E.K. Fischer, Microplastics detected in cirrhotic liver tissue, eBioMedicine 82 (2022) 104147. https://doi.org/10.1016/j.ebiom.2022.104147.
[24] Y. Yang, E. Xie, Z. Du, Z. Peng, Z. Han, L. Li, R. Zhao, Y. Qin, M. Xue, F. Li, K. Hua, X. Yang, Detection of Various Microplastics in Patients Undergoing Cardiac Surgery, Environ. Sci. Technol. 57 (2023) 10911–10918. https://doi.org/10.1021/acs.est.2c07179.
[25] C.J. Hu, M.A. Garcia, A. Nihart, R. Liu, L. Yin, N. Adolphi, D.F. Gallego, H. Kang, M.J. Campen, X. Yu, Microplastic presence in dog and human testis and its potential association with sperm count and weights of testis and epididymis, Toxicol. Sci. 200 (2024) 235–240. https://doi.org/10.1093/toxsci/kfae060.
[26] A. Ragusa, V. Notarstefano, A. Svelato, A. Belloni, G. Gioacchini, C. Blondeel, E. Zucchelli, C. De Luca, S. D'Avino, A. Gulotta, O. Carnevali, E. Giorgini, Raman Microspectroscopy Detection and Characterisation of Microplastics in Human Breastmilk, Polymers 14 (2022) 2700. https://doi.org/10.3390/polym14132700.
[27] H.A. Leslie, M.J.M. Van Velzen, S.H. Brandsma, A.D. Vethaak, J.J. Garcia-Vallejo, M.H. Lamoree, Discovery and quantification of plastic particle pollution in human blood, Environ. Int. 163 (2022) 107199. https://doi.org/10.1016/j.envint.2022.107199.
[28] R. Marfella, F. Prattichizzo, C. Sardu, G. Fulgenzi, L. Graciotti, T. Spadoni, N. D'Onofrio, L. Scisciola, R. La Grotta, C. Frigé, V. Pellegrini, M. Municinò, M. Siniscalchi, F. Spinetti, G. Vigliotti, C. Vecchione, A. Carrizzo, G. Accarino, A. Squillante, G. Spaziano, D. Mirra, R. Esposito, S. Altieri, G. Falco, A. Fenti, S. Galoppo, S. Canzano, F.C. Sasso, G. Matacchione, F. Olivieri, F. Ferraraccio, I. Panarese, P. Paolisso, E. Barbato, C. Lubritto, M.L. Balestrieri, C. Mauro, A.E. Caballero, S. Rajagopalan, A. Ceriello, B. D'Agostino, P. Iovino, G. Paolisso, Microplastics and Nanoplastics in Atheromas and Cardiovascular Events, N. Engl. J. Med. 390 (2024) 900–910. https://doi.org/10.1056/NEJMoa2309822.
[29] A. Garcês, I. Pires, The Detrimental Impacts of Plastic Pollution on Wildlife, Res. Ecol. (2024) 42–46. https://doi.org/10.30564/re.v6i2.6294.

[30] M. Sigler, The Effects of Plastic Pollution on Aquatic Wildlife: Current Situations and Future Solutions, Water. Air. Soil Pollut. 225 (2014) 2184. https://doi.org/10.1007/s11270-014-2184-6.
[31] Y. Song, C. Cao, R. Qiu, J. Hu, M. Liu, S. Lu, H. Shi, K.M. Raley-Susman, D. He, Uptake and adverse effects of polyethylene terephthalate microplastics fibers on terrestrial snails (Achatina fulica) after soil exposure, Environ. Pollut. 250 (2019) 447–455. https://doi.org/10.1016/j.envpol.2019.04.066.
[32] B. Cormier, J. Cachot, M. Blanc, M. Cabar, C. Clérandeau, F. Dubocq, F. Le Bihanic, B. Morin, S. Zapata, M.-L. Bégout, X. Cousin, Environmental microplastics disrupt swimming activity in acute exposure in Danio rerio larvae and reduce growth and reproduction success in chronic exposure in D. rerio and Oryzias melastigma, Environ. Pollut. 308 (2022) 119721. https://doi.org/10.1016/j.envpol.2022.119721.
[33] M.R. Gregory, Environmental implications of plastic debris in marine settings—entanglement, ingestion, smothering, hangers-on, hitch-hiking and alien invasions, Philos. Trans. R. Soc. B Biol. Sci. 364 (2009) 2013–2025. https://doi.org/10.1098/rstb.2008.0265.
[34] A.A. De Souza Machado, C.W. Lau, W. Kloas, J. Bergmann, J.B. Bachelier, E. Faltin, R. Becker, A.S. Görlich, M.C. Rillig, Microplastics Can Change Soil Properties and Affect Plant Performance, Environ. Sci. Technol. 53 (2019) 6044–6052. https://doi.org/10.1021/acs.est.9b01339.
[35] J.Y. Jang, K. Sadeghi, J. Seo, Chain-Extending Modification for Value-Added Recycled PET: A Review, Polym. Rev. 62 (2022) 860–889. https://doi.org/10.1080/15583724.2022.2033765.
[36] T. Muringayil Joseph, S. Azat, Z. Ahmadi, O. Moini Jazani, A. Esmaeili, E. Kianfar, J. Haponiuk, S. Thomas, Polyethylene terephthalate (PET) recycling: A review, Case Stud. Chem. Environ. Eng. 9 (2024) 100673. https://doi.org/10.1016/j.cscee.2024.100673.
[37] T. Chilton, S. Burnley, S. Nesaratnam, A life cycle assessment of the closed-loop recycling and thermal recovery of post-consumer PET, Resour. Conserv. Recycl. 54 (2010) 1241–1249. https://doi.org/10.1016/j.resconrec.2010.04.002.
[38] R. Rosendal, Danish policy on waste management–Denmark without waste, Retrieved Res. Gate Httpswww Res. Netpublication287210935DANISHPOLICYONWASTEMANAGEMENT-Den. (2014).
[39] M. Frounchi, Studies on degradation of PET in mechanical recycling, Macromol. Symp. 144 (1999) 465–469. https://doi.org/10.1002/masy.19991440142.
[40] H. Wu, S. Lv, Y. He, J.-P. Qu, The study of the thermomechanical degradation and mechanical properties of PET recycled by industrial-scale elongational processing, Polym. Test. 77 (2019) 105882. https://doi.org/10.1016/j.polymertesting.2019.04.029.
[41] S. Dimitris, L.A. Achilias, Recent advances in the chemical recycling of polymers (PP, PS, LDPE, HDPE, PVC, PC, Nylon, PMMA), Mater Recycl Trends Perspect 3 (2014) 64.
[42] Y. Guo, X. Xia, J. Ruan, Y. Wang, J. Zhang, G.A. LeBlanc, L. An, Ignored microplastic sources from plastic bottle recycling, Sci. Total Environ. 838 (2022) 156038. https://doi.org/10.1016/j.scitotenv.2022.156038.
[43] K. Ragaert, L. Delva, K. Van Geem, Mechanical and chemical recycling of solid plastic waste, Waste Manag. 69 (2017) 24–58. https://doi.org/10.1016/j.wasman.2017.07.044.

[44] Q. Yue, L. Xiao, M. Zhang, X. Bai, The Glycolysis of Poly(ethylene terephthalate) Waste: Lewis Acidic Ionic Liquids as High Efficient Catalysts, Polymers 5 (2013) 1258–1271. https://doi.org/10.3390/polym5041258.
[45] Damayanti, H.-S. Wu, Strategic Possibility Routes of Recycled PET, Polymers 13 (2021) 1475. https://doi.org/10.3390/polym13091475.
[46] P. Gupta, S. Bhandari, Chemical Depolymerization of PET Bottles via Ammonolysis and Aminolysis, in: Recycl. Polyethyl. Terephthalate Bottles, Elsevier, 2019: pp. 109–134. https://doi.org/10.1016/B978-0-12-811361-5.00006-7.
[47] J.M. Garcia, M.L. Robertson, The future of plastics recycling, Science 358 (2017) 870–872. https://doi.org/10.1126/science.aaq0324.
[48] Y. Liu, X. Yao, H. Yao, Q. Zhou, J. Xin, X. Lu, S. Zhang, Degradation of poly(ethylene terephthalate) catalyzed by metal-free choline-based ionic liquids, Green Chem. 22 (2020) 3122–3131. https://doi.org/10.1039/D0GC00327A.
[49] J. Yao, Y. Liu, Z. Gu, L. Zhang, Z. Guo, Deconstructing PET: Advances in enzyme engineering for sustainable plastic degradation, Chem. Eng. J. 497 (2024) 154183. https://doi.org/10.1016/j.cej.2024.154183.
[50] Y. Zhang, W.O. Hancock, Measuring PETase enzyme kinetics by single-molecule microscopy, Biophys. J. 123 (2024) 3669–3677. https://doi.org/10.1016/j.bpj.2024.09.016.
[51] R. Müller, H. Schrader, J. Profe, K. Dresler, W. Deckwer, Enzymatic Degradation of Poly(ethylene terephthalate): Rapid Hydrolyse using a Hydrolase from *T. fusca*, Macromol. Rapid Commun. 26 (2005) 1400–1405. https://doi.org/10.1002/marc.200500410.
[52] R. Wei, D. Breite, C. Song, D. Gräsing, T. Ploss, P. Hille, R. Schwerdtfeger, J. Matysik, A. Schulze, W. Zimmermann, Biocatalytic Degradation Efficiency of Postconsumer Polyethylene Terephthalate Packaging Determined by Their Polymer Microstructures, Adv. Sci. 6 (2019) 1900491. https://doi.org/10.1002/advs.201900491.
[53] R. Wei, T. Oeser, W. Zimmermann, Synthetic Polyester-Hydrolyzing Enzymes From Thermophilic Actinomycetes, in: Adv. Appl. Microbiol., Elsevier, 2014: pp. 267–305. https://doi.org/10.1016/B978-0-12-800259-9.00007-X.
[54] S. Sulaiman, S. Yamato, E. Kanaya, J.-J. Kim, Y. Koga, K. Takano, S. Kanaya, Isolation of a Novel Cutinase Homolog with Polyethylene Terephthalate-Degrading Activity from Leaf-Branch Compost by Using a Metagenomic Approach, Appl. Environ. Microbiol. 78 (2012) 1556–1562. https://doi.org/10.1128/AEM.06725-11.
[55] A.N. Shirke, C. White, J.A. Englaender, A. Zwarycz, G.L. Butterfoss, R.J. Linhardt, R.A. Gross, Stabilizing Leaf and Branch Compost Cutinase (LCC) with Glycosylation: Mechanism and Effect on PET Hydrolysis, Biochemistry 57 (2018) 1190–1200. https://doi.org/10.1021/acs.biochem.7b01189.
[56] Å.M. Ronkvist, W. Xie, W. Lu, R.A. Gross, Cutinase-Catalyzed Hydrolysis of Poly(ethylene terephthalate), Macromolecules 42 (2009) 5128–5138. https://doi.org/10.1021/ma9005318.
[57] R. Hong, Y. Sun, L. Su, L. Gu, F. Wang, J. Wu, High-level expression of Humicola insolens cutinase in Pichia pastoris without carbon starvation and its use in cotton fabric bioscouring, J. Biotechnol. 304 (2019) 10–15. https://doi.org/10.1016/j.jbiotec.2019.07.011.
[58] S. Yoshida, K. Hiraga, T. Takehana, I. Taniguchi, H. Yamaji, Y. Maeda, K. Toyohara, K. Miyamoto, Y. Kimura, K. Oda, A bacterium that degrades and

assimilates poly(ethylene terephthalate), Science 351 (2016) 1196–1199. https://doi.org/10.1126/science.aad6359.
[59] G.J. Palm, L. Reisky, D. Böttcher, H. Müller, E.A.P. Michels, M.C. Walczak, L. Berndt, M.S. Weiss, U.T. Bornscheuer, G. Weber, Structure of the plastic-degrading Ideonella sakaiensis MHETase bound to a substrate, Nat. Commun. 10 (2019) 1717. https://doi.org/10.1038/s41467-019-09326-3.
[60] T. Burgin, B.C. Pollard, B.C. Knott, H.B. Mayes, M.F. Crowley, J.E. McGeehan, G.T. Beckham, H.L. Woodcock, The reaction mechanism of the Ideonella sakaiensis PETase enzyme, Commun. Chem. 7 (2024) 65. https://doi.org/10.1038/s42004-024-01154-x.
[61] S. Joo, I.J. Cho, H. Seo, H.F. Son, H.-Y. Sagong, T.J. Shin, S.Y. Choi, S.Y. Lee, K.-J. Kim, Structural insight into molecular mechanism of poly(ethylene terephthalate) degradation, Nat. Commun. 9 (2018) 382. https://doi.org/10.1038/s41467-018-02881-1.
[62] M. Furukawa, N. Kawakami, A. Tomizawa, K. Miyamoto, Efficient Degradation of Poly(ethylene terephthalate) with Thermobifida fusca Cutinase Exhibiting Improved Catalytic Activity Generated using Mutagenesis and Additive-based Approaches, Sci. Rep. 9 (2019) 16038. https://doi.org/10.1038/s41598-019-52379-z.
[63] B. Deng, Y. Yue, J. Yang, M. Yang, Q. Xing, H. Peng, F. Wang, M. Li, L. Ma, C. Zhai, Improving the activity and thermostability of PETase from Ideonella sakaiensis through modulating its post-translational glycan modification, Commun. Biol. 6 (2023) 39. https://doi.org/10.1038/s42003-023-04413-0.
[64] T. Fecker, P. Galaz-Davison, F. Engelberger, Y. Narui, M. Sotomayor, L.P. Parra, C.A. Ramírez-Sarmiento, Active Site Flexibility as a Hallmark for Efficient PET Degradation by I. sakaiensis PETase, Biophys. J. 114 (2018) 1302–1312. https://doi.org/10.1016/j.bpj.2018.02.005.
[65] H.F. Son, I.J. Cho, S. Joo, H. Seo, H.-Y. Sagong, S.Y. Choi, S.Y. Lee, K.-J. Kim, Rational Protein Engineering of Thermo-Stable PETase from *Ideonella sakaiensis* for Highly Efficient PET Degradation, ACS Catal. 9 (2019) 3519–3526. https://doi.org/10.1021/acscatal.9b00568.
[66] Y. Cui, Y. Chen, X. Liu, S. Dong, Y. Tian, Y. Qiao, R. Mitra, J. Han, C. Li, X. Han, W. Liu, Q. Chen, W. Wei, X. Wang, W. Du, S. Tang, H. Xiang, H. Liu, Y. Liang, K.N. Houk, B. Wu, Computational Redesign of a PETase for Plastic Biodegradation under Ambient Condition by the GRAPE Strategy, ACS Catal. 11 (2021) 1340–1350. https://doi.org/10.1021/acscatal.0c05126.
[67] H. Lu, D.J. Diaz, N.J. Czarnecki, C. Zhu, W. Kim, R. Shroff, D.J. Acosta, B.R. Alexander, H.O. Cole, Y. Zhang, N.A. Lynd, A.D. Ellington, H.S. Alper, Machine learning-aided engineering of hydrolases for PET depolymerization, Nature 604 (2022) 662–667. https://doi.org/10.1038/s41586-022-04599-z.
[68] S.A.H. Heyde, J. Arnling Bååth, P. Westh, M.H.H. Nørholm, K. Jensen, Surface display as a functional screening platform for detecting enzymes active on PET, Microb. Cell Factories 20 (2021) 93. https://doi.org/10.1186/s12934-021-01582-7.
[69] Z. Chen, Y. Wang, Y. Cheng, X. Wang, S. Tong, H. Yang, Z. Wang, Efficient biodegradation of highly crystallized polyethylene terephthalate through cell surface display of bacterial PETase, Sci. Total Environ. 709 (2020) 136138. https://doi.org/10.1016/j.scitotenv.2019.136138.
[70] L. Aer, Q. Jiang, I. Gul, Z. Qi, J. Feng, L. Tang, Overexpression and kinetic analysis of Ideonella sakaiensis PETase for polyethylene terephthalate (PET)

degradation, Environ. Res. 212 (2022) 113472. https://doi.org/10.1016/j.envres.2022.113472.
[71] H. Seo, S. Kim, H.F. Son, H.-Y. Sagong, S. Joo, K.-J. Kim, Production of extracellular PETase from Ideonella sakaiensis using sec-dependent signal peptides in E. coli, Biochem. Biophys. Res. Commun. 508 (2019) 250–255. https://doi.org/10.1016/j.bbrc.2018.11.087.
[72] J.W. Kim, S.-B. Park, Q.-G. Tran, D.-H. Cho, D.-Y. Choi, Y.J. Lee, H.-S. Kim, Functional expression of polyethylene terephthalate-degrading enzyme (PETase) in green microalgae, Microb. Cell Factories 19 (2020) 97. https://doi.org/10.1186/s12934-020-01355-8.
[73] B.C. Knott, E. Erickson, M.D. Allen, J.E. Gado, R. Graham, F.L. Kearns, I. Pardo, E. Topuzlu, J.J. Anderson, H.P. Austin, G. Dominick, C.W. Johnson, N.A. Rorrer, C.J. Szostkiewicz, V. Copié, C.M. Payne, H.L. Woodcock, B.S. Donohoe, G.T. Beckham, J.E. McGeehan, Characterization and engineering of a two-enzyme system for plastics depolymerization, Proc. Natl. Acad. Sci. 117 (2020) 25476–25485. https://doi.org/10.1073/pnas.2006753117.
[74] R.E. Ahan, B.M. Kırpat, B. Saltepe, U.Ö.Ş. Şeker, A Self-Actuated Cellular Protein Delivery Machine, ACS Synth. Biol. 8 (2019) 686–696. https://doi.org/10.1021/acssynbio.9b00062.
[75] Y. Jia, N.A. Samak, X. Hao, Z. Chen, Q. Wen, J. Xing, Hydrophobic cell surface display system of PETase as a sustainable biocatalyst for PET degradation, Front. Microbiol. 13 (2022) 1005480. https://doi.org/10.3389/fmicb.2022.1005480.
[76] A. Gennari, R. Simon, N.D.D.M. Sperotto, C.V. Bizarro, L.A. Basso, P. Machado, E.V. Benvenutti, A. Da Cas Viegas, S. Nicolodi, G. Renard, J.M. Chies, G. Volpato, C.F. Volken De Souza, One-step purification of a recombinant beta-galactosidase using magnetic cellulose as a support: Rapid immobilization and high thermal stability, Bioresour. Technol. 345 (2022) 126497. https://doi.org/10.1016/j.biortech.2021.126497.
[77] R.E. Ahan, C.E. Ozcelik, I.N. Cagil, U.O.S. Seker, A Synthetic Protein Secretion System for Living Bacterial Therapeutics, (2023). https://doi.org/10.1101/2023.06.14.544856.
[78] A. Konovalova, T.J. Silhavy, Outer membrane lipoprotein biogenesis: Lol is not the end, Philos. Trans. R. Soc. B Biol. Sci. 370 (2015) 20150030. https://doi.org/10.1098/rstb.2015.0030.
[79] J.A. Bornhorst, J.J. Falke, [16] Purification of proteins using polyhistidine affinity tags, in: Methods Enzymol., Elsevier, 2000: pp. 245–254. https://doi.org/10.1016/S0076-6879(00)26058-8.
[80] J. Hu, Y. Chen, Constructing Escherichia coli co-display systems for biodegradation of polyethylene terephthalate, Bioresour. Bioprocess. 10 (2023) 91. https://doi.org/10.1186/s40643-023-00711-x.
[81] H.P. Austin, M.D. Allen, B.S. Donohoe, N.A. Rorrer, F.L. Kearns, R.L. Silveira, B.C. Pollard, G. Dominick, R. Duman, K. El Omari, V. Mykhaylyk, A. Wagner, W.E. Michener, A. Amore, M.S. Skaf, M.F. Crowley, A.W. Thorne, C.W. Johnson, H.L. Woodcock, J.E. McGeehan, G.T. Beckham, Characterization and engineering of a plastic-degrading aromatic polyesterase, Proc. Natl. Acad. Sci. 115 (2018). https://doi.org/10.1073/pnas.1718804115.
[82] X. Chen, J.L. Zaro, W.-C. Shen, Fusion protein linkers: Property, design and functionality, Adv. Drug Deliv. Rev. 65 (2013) 1357–1369. https://doi.org/10.1016/j.addr.2012.09.039.

[83] M.C. Jenkins, C. Parker, C. O'Brien, P. Campos, M. Tucker, K. Miska, Effects of codon optimization on expression in Escherichia coli of protein-coding DNA sequences from the protozoan Eimeria, J. Microbiol. Methods 211 (2023) 106750. https://doi.org/10.1016/j.mimet.2023.106750.
[84] V. Pirillo, L. Pollegioni, G. Molla, Analytical methods for the investigation of enzyme-catalyzed degradation of polyethylene terephthalate, FEBS J. 288 (2021) 4730–4745. https://doi.org/10.1111/febs.15850.
[85] P. Singh, L. Sharma, S.R. Kulothungan, B.V. Adkar, R.S. Prajapati, P.S.S. Ali, B. Krishnan, R. Varadarajan, Effect of Signal Peptide on Stability and Folding of Escherichia coli Thioredoxin, PLoS ONE 8 (2013) e63442. https://doi.org/10.1371/journal.pone.0063442.
[86] R.K. Goel, A.M. Motlagh, Biological Phosphorus Removal, in: Compr. Water Qual. Purif., Elsevier, 2014: pp. 150–162. https://doi.org/10.1016/B978-0-12-382182-9.00051-7.

APPENDIX A

DNA SEQUENCES OF CONSTRUCTS

Table A. 1: Gene sequences used in this study.

Gene Name	**Sequence**
PETase (Optimized for *E. coli*)	ATGAATTTTCCCAGGGCTTCAAGACTAATGCAAGCAGCG GTGCTGGGTGGTCTGATGGCTGTGTCTGCTGCGGCGACC GCGCAGACCAACCCATACGCGCGCGGTCCGAACCCGAC GGCCGCGTCGTTAGAGGCGAGCGCTGGCCCTTTCACTGT GCGTAGTTTTACCGTCAGCCGTCCGTCCGGTTACGGCGC GGGTACCGTTTATTACCCGACCAATGCTGGCGGCACGGT AGGTGCAATCGCGATTGTCCCGGGTTACACCGCCCGTCA AAGCTCGATCAAGTGGTGGGGTCCACGTCTGGCCTCTCA CGGCTTCGTGGTGATCACCATTGACACCAATTCGACCCT GGATCAGCCGTCTTCCAGAAGTTCTCAGCAGATGGCAGC GCTGCGTCAAGTTGCGAGCTTGAATGGCACGTCAAGCAG CCCGATCTATGGTAAAGTTGATACCGCACGCATGGGCGT TATGGGTTGGTCCATGGGAGGCGGTGGCAGCTTGATTAG CGCTGCGAACAACCCGAGCTTGAAGGCAGCCGCGCCGC AAGCTCCGTGGGATAGCTCCACCAACTTCAGCAGCGTTA CCGTGCCGACGCTGATCTTCGCCTGCGAAAACGACAGCA TTGCGCCGGTTAACTCCTCTGCTCTGCCGATCTACGACTC CATGTCCCGTAATGCGAAACAGTTTCTGGAAATTAACGG CGGTAGCCATAGCTGCGCGAACTCCGGTAACTCTAATCA GGCGCTCATCGGTAAAAAGGGCGTGGCCTGGATGAAAC GCTTCATGGACAACGACACTCGCTATTCGACCTTTGCAT GCGAGAACCCGAATTCAACGCGTGTTAGCGATTTTCGTA CCGCGAATTGTAGC
Ag43 – Alpha Subunit	CGCACAACCATCAATAAAAACGGTCGCCAGATTGTGAGA GCTGAAGGAACGGCAAATACCACTGTGGTTTATGCCGGC GGCGACCAGACTGTACATGGTCACGCACTGGATACCACG CTGAATGGGGGATACCAGTATGTGCACAACGGCGGTACA GCGTCTGACACTGTTGTGAACAGTGACGGCTGGCAGATT GTCAAAAACGGGGGTGTGGCCGGGAATACCACCGTTAAT CAGAAGGGCAGACTGCAGGTGGACGCCGGTGGTACAGC CACGAATGTCACCCTGAAGCAGGGCGGCGCACTGGTTAC CAGTACGGCTGCAACCGTTACCGGCATAAACCGCCTGGG AGCATTCTCTGTTGTGGAGGGTAAAGCTGATAATGTCGT ACTGGAAAATGGCGGACGCCTGGATGTGCTGACCGGAC ACACAGCCACTAATACCCGCGTGGATGATGGCGGAACGC TGGATGTCCGCAACGGTGGCACCGCCACCACCGTATCCA TGGGAAATGGCGGTGTACTGCTGGCCGATTCCGGTGCCG

	CTGTCAGTGGTACCCGGAGCGACGGAAAGGCATTCAGTA TCGGAGGCGGTCAGGCGGATGCCCTGATGCTGGAAAAA GGCAGTTCATTCACGCTGAACGCCGGTGATACGGCCACG GATACCACGGTAAATGGCGGACTGTTCACCGCCAGGGGC GGCACACTGGCGGGCACCACCACGCTGAATAACGGCGC CATACTTACCCTTTCCGGGAAGACGGTGAACAACGATAC CCTGACCATCCGTGAAGGCGATGCACTCCTGCAGGGAGG CTCTCTCACCGGTAACGGCAGCGTGGAAAAATCAGGAAG TGGCACACTCACTGTCAGCAACACCACACTCACCCAGAA AGCCGTCAACCTGAATGAAGGCACGCTGACGCTGAACG ACAGTACCGTCACCACGGATGTCATTGCTCAGCGCGGTA CAGCCCTGAAGCTGACCGGCAGCACTGTGCTGAACGGTG CCATTGAC
Ag43 – Beta Subunit	CCCACGAATGTCACTCTCGCCTCCGGTGCCACCTGGAAT ATCCCCGATAACGCCACGGTGCAGTCGGTGGTGGATGAC CTCAGCCATGCCGGACAGATTCATTTCACCTCCACCCGC ACAGGGAAGTTCGTACCGGCAACCCTGAAAGTGAAAAA CCTGAACGGACAGAATGGCACCATCAGCCTGCGTGTACG CCCGGATATGGCACAGAACAATGCTGACAGACTGGTCAT TGACGGCGGCAGGGCAACCGGAAAAACCATCCTGAACC TGGTGAACGCCGGCAACAGTGCGTCGGGGCTGGCGACC AGCGGTAAGGGTATTCAGGTGGTGGAAGCCATTAACGGT GCCACCACGGAGGAAGGGGCCTTTGTCCAGGGGAACAG GCTGCAGGCCGGTGCCTTTAACTACTCCCTCAACCGGGA CAGTGATGAGAGCTGGTATCTGCGCAGTGAAAATGCTTA TCGTGCAGAAGTCCCCCTGTATGCCTCCATGCTGACACA GGCAATGGACTATGACCGGATTGTGGCAGGCTCCCGCAG CCATCAGACCGGTGTAAATGGTGAAAACAACAGCGTCCG TCTCAGCATTCAGGGCGGTCATCTCGGTCACGATAACAA TGGCGGTATTGCCCGTGGGGCCACGCCGGAAAGCAGCG GCAGCTATGGATTCGTCCGTCTGGAGGGTGACCTGATGA GAACAGAGGTTGCCGGTATGTCTGTGACCGCGGGGGTAT ATGGTGCTGCTGGCCATTCTTCCGTTGATGTTAAGGATGA TGACGGCTCCCGTGCCGGCACGGTCCGGGATGATGCCGG CAGCCTGGGCGGATACCTGAATCTGGTACACACGTCCTC CGGCCTGTGGGCTGACATTGTGGCACAGGGAACCCGCCA CAGCATGAAAGCGTCATCGGACAATAACGACTTCCGCGC CCGGGGCTGGGGCTGGCTGGGCTCACTGGAAACCGGTCT GCCCTTCAGTATCACTGACAACCTGATGCTGGAGCCACA ACTGCAGTATACCTGGCAGGGACTTTCCCTGGATGACGG TAAGGACAACGCCGGTTATGTGAAGTTCGGGCATGGCAG TGCACAACATGTGCGTGCCGGTTTCCGTCTGGGCAGCCA CAACGATATGACCTTTGGCGAAGGCACCTCATCCCGTGC CCCCCTGCGTGACAGTGCAAAACACAGTGTGAGTGAATT ACCGGTGAACTGGTGGGTACAGCCTTCTGTTATCCGCAC CTTCAGCTCCCGGGGAGATATGCGTGTGGGGACTTCCAC TGCAGGCAGCGGGATGACGTTCTCTCCCTCACAGAATGG CACATCACTGGACCTGCAGGCCGGACTGGAAGCCCGTGT CCGGGAAAATATCACCCTGGGCGTTCAGGCCGGTTATGC

	CCACAGCGTCAGCGGCAGCAGCGCTGAAGGGTATAACG GTCAGGCCACACTGAATGTGACCTTC
MicL	ATGGCCGGAGCAGGAGTCCGTGCAGAAAACCTGCACCA CTTCCTCGATGCCGGAGTGCTGGAAGTCCATAGCTCCGC GGGAGCGTGGCAAGCCTCACCGATGCGTTATCGTAATCA AGGATTGTCCATGTCATCAGATGAACACGCGGACGAGTA TTCGCGTTATATCGTAGACGGGGCGGCGGTTGCTGAAAT GAAAGGAATCATTGAACGCCATCAGGCCAAATGATTTTT ACCGTTGCATCATGTCGCCCAATATGATGCTTGCTCGTAC CAGGCCCCTGCAATTTCAACAGGGGCCTTTTTTT
T7 promoter	TAATACGACTCACTATAG
T7 terminator	TAGCATAACCCCTTGGGGCCTCTAAACGGGTCTTGAGGG GTTTTTTG
Lac operator	AATTGTGAGCGGATAACAATTGACATTGTGAGCGGATAA CAAGATACT
Linker TEV	GGTGGCGGTGGTAGCGAAAACCTGTACTTTCAGGGCGGT GGCGGTGGTAGC
pelB signal sequence	ATGAAATACCTGCTGCCGACCGCTGCTGCTGGTCTGCTG CTCCTCGCTGCCCAGCCGGCGATGGCC
Ampicillin resistance gene	CACCCAGAAACGCTGGTGAAAGTAAAAGATGCTGAAGA TCAGTTGGGTGCACGAGTGGGTTACATCGAACTGGATCT CAACAGCGGTAAGATCCTTGAGAGTTTTCGCCCCGAAGA ACGTTTTCCAATGATGAGCACTTTTAAAGTTCTGCTATGT GGCGCGGTATTATCCCGTATTGACGCCGGGCAAGAGCAA CTCGGTCGCCGCATACACTATTCTCAGAATGACTTGGTTG AGTACTCACCAGTCACAGAAAAGCATCTTACGGATGGCA TGACAGTAAGAGAATTATGCAGTGCTGCCATAACCATGA GTGATAACACTGCGGCCAACTTACTTCTGACAACGATCG GAGGACCGAAGGAGCTAACCGCTTTTTTGCACAACATGG GGGATCATGTAACTCGCCTTGATCGTTGGGAACCGGAGC TGAATGAAGCCATACCAAACGACGAGCGTGACACCACG ATGCCTGCAGCAATGGCAACAACGTTGCGCAAACTATTA ACTGGCGAACTACTTACTCTAGCTTCCCGGCAACAATTA ATAGACTGGATGGAGGCGGATAAAGTTGCAGGACCACTT CTGCGCTCGGCCCTTCCGGCTGGCTGGTTTATTGCTGATA AATCTGGAGCCGGTGAGCGTGGGTCTCGCGGTATCATTG CAGCACTGGGGCCAGATGGTAAGCCCTCCCGTATCGTAG TTATCTACACGACGGGGAGTCAGGCAACTATGGATGAAC GAAATAGACAGATCGCTGAGATAGGTGCCTCACTGATTA AGCATTGGTAA
TetR gene	ATGATGTCTAGATTAGATAAAAGTAAAGTGATTAACAGC GCATTAGAGCTGCTTAATGAGGTCGGAATCGAAGGTTTA ACAACCCGTAAACTCGCCCAGAAGCTAGGTGTAGAGCA GCCTACATTGTATTGGCATGTAAAAAATAAGCGGGCTTT

	GCTCGACGCCTTAGCCATTGAGATGTTAGATAGGCACCA TACTCACTTTTGCCCTTTAGAAGGGGAAAGCTGGCAAGA TTTTTTACGTAATAACGCTAAAAGTTTTAGATGTGCTTTA CTAAGTCATCGCGATGGAGCAAAAGTACATTTAGGTACA CGGCCTACAGAAAAACAGTATGAAACTCTCGAAAATCA ATTAGCCTTTTTATGCCAACAAGGTTTTTCACTAGAGAAT GCATTATATGCACTCAGCGCTGTGGGGCATTTTACTTTAG GTTGCGTATTGGAAGATCAAGAGCATCAAGTCGCTAAAG AAGAAAGGGAAACACCTACTACTGATAGTATGCCGCCAT TATTACGACAAGCTATCGAATTATTTGATCACCAAGGTG CAGAGCCAGCCTTCTTATTCGGCCTTGAATTGATCATATG CGGATTAGAAAAACAACTTAAATGTGAAAGTGGGTCTTA A
TetO gene	TCCCTATCAGTGATAGAGA
GS linker	GGTGGCGGTGGATCC
His-tag	CACCACCACCACCACCAC

APPENDIX B

LIST OF PRIMERS

Table B. 1: Primer sequences used in this study.

Primer Name	Sequence (5'-3')
pCDP1	AACAATTCCCCTCTAGATTAACTTTAAGAAGGAGGGTACCATGAATTTTCCCAGGGCTTCAAGAC
pCDP2	GATCTCAGTGGTGGTGGTGGTGGTGCTCGAGGGATCCACCGCCACCGCTACAATTCGCGGTACGAAAATC
pCDP3	CTCGAGCACCACCACCACC
pCDP4	GGTACCCTCCTTCTTAAAGTTAATCTAGAGG
pCDP8a	GAAAGTACAGGTTTTCGCTACCACCGCCACCGCTACAATTCGCGGTACGAAAATCG
pCDP8b	GTGCGCTTAAGGCTACCACCGCCACCGCCCTGAAAGTACAGGTTTTCGCTACCA
pCDP9	GCATCGGGATCCATGAATTTTCCCAGGGCTTCAAG
pCDP10	ACCACAGTGGTATTTGCC
SEQ22R	CCTCCTTTCAGCAAAAAACCCC
SEQFWD22	CATACCCACGCCGAAACAAG
T7 Term. P	CAAAAAACCCCTCAAGACCCG

APPENDIX C

PLASMID MAPS OF CONSTRUCTS

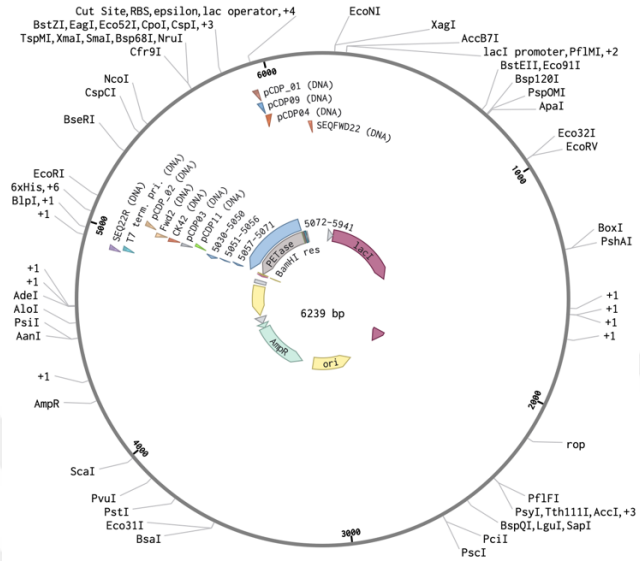

Figure C. 1. Plasmid map illustration of pET – 22b(+) – PETase – 6xHis vector

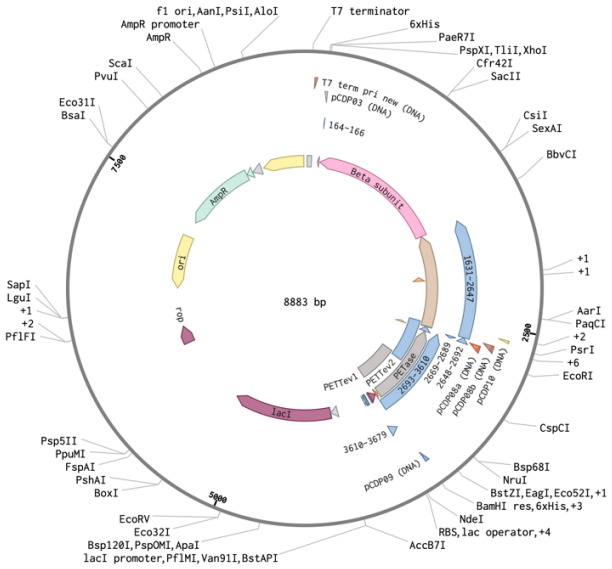

Figure C. 2. Plasmid map illustration of pET-22b(+) –PelB - 6xHis – Ag43 – PETase vector.

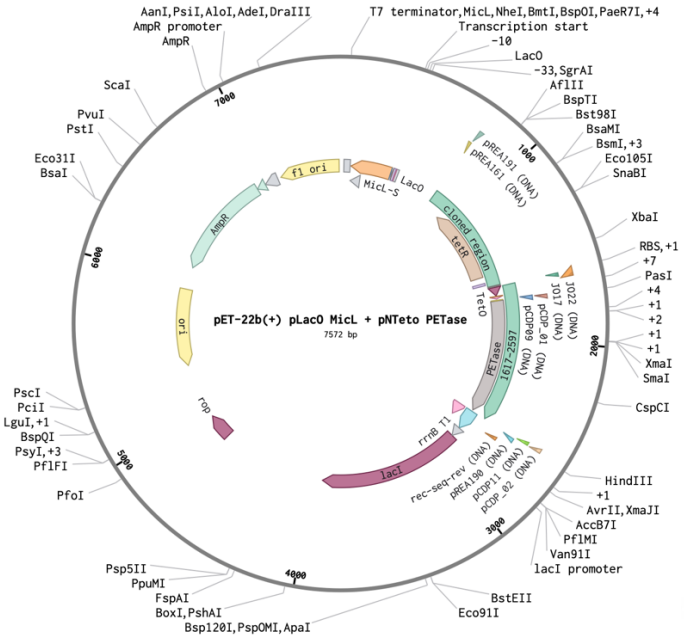

Figure C. 3. Plasmid map illustration of pET-22b(+) – pLacO MicL + pNTetO PETase vector

APPENDIX D

SEQUENCING RESULTS

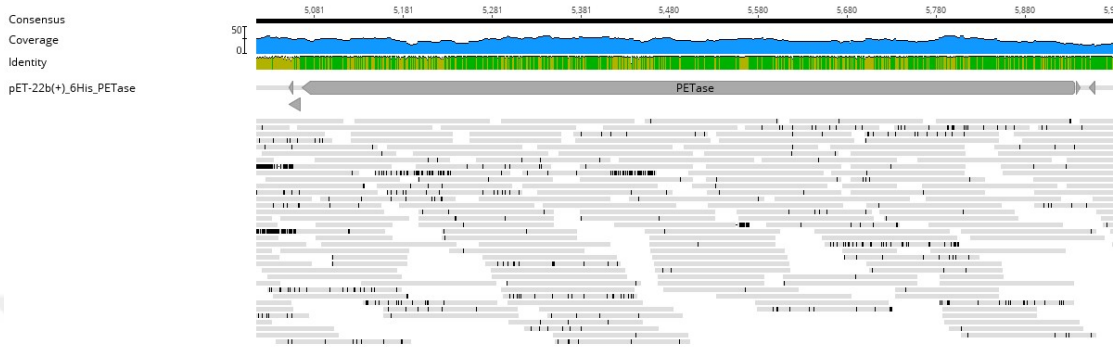

Figure D. 1. Sequence alignment of pET22b - PETase - 6xHis construct. Alignment done in Geneious software.

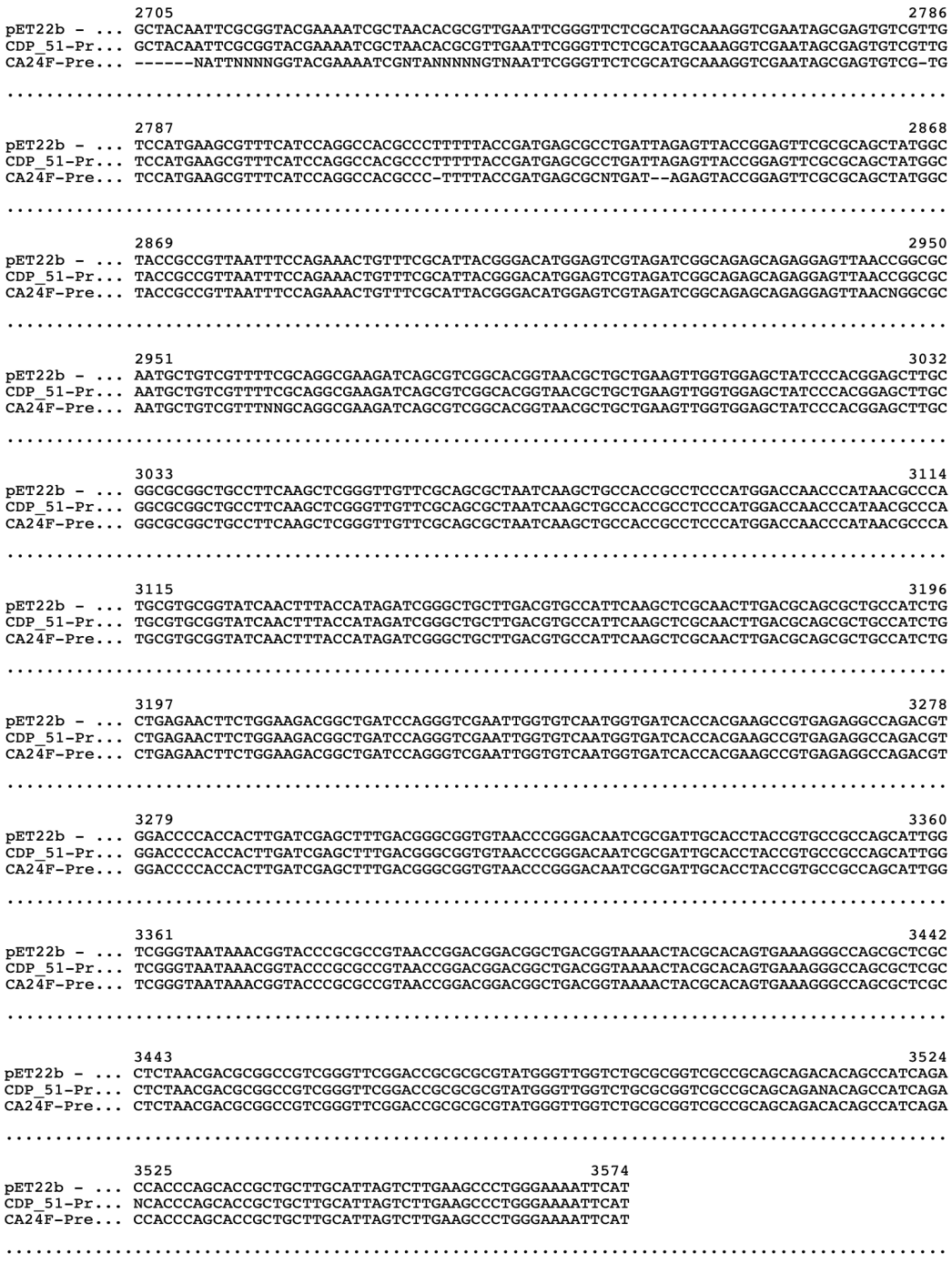

Figure D. 2. Sanger sequencing result for pET-22b(+) –PelB - 6xHis – Ag43 – PETase. Alignment shows the sequencing of the insert, PETase. Alignment done and image retrieved from Benchling.com.

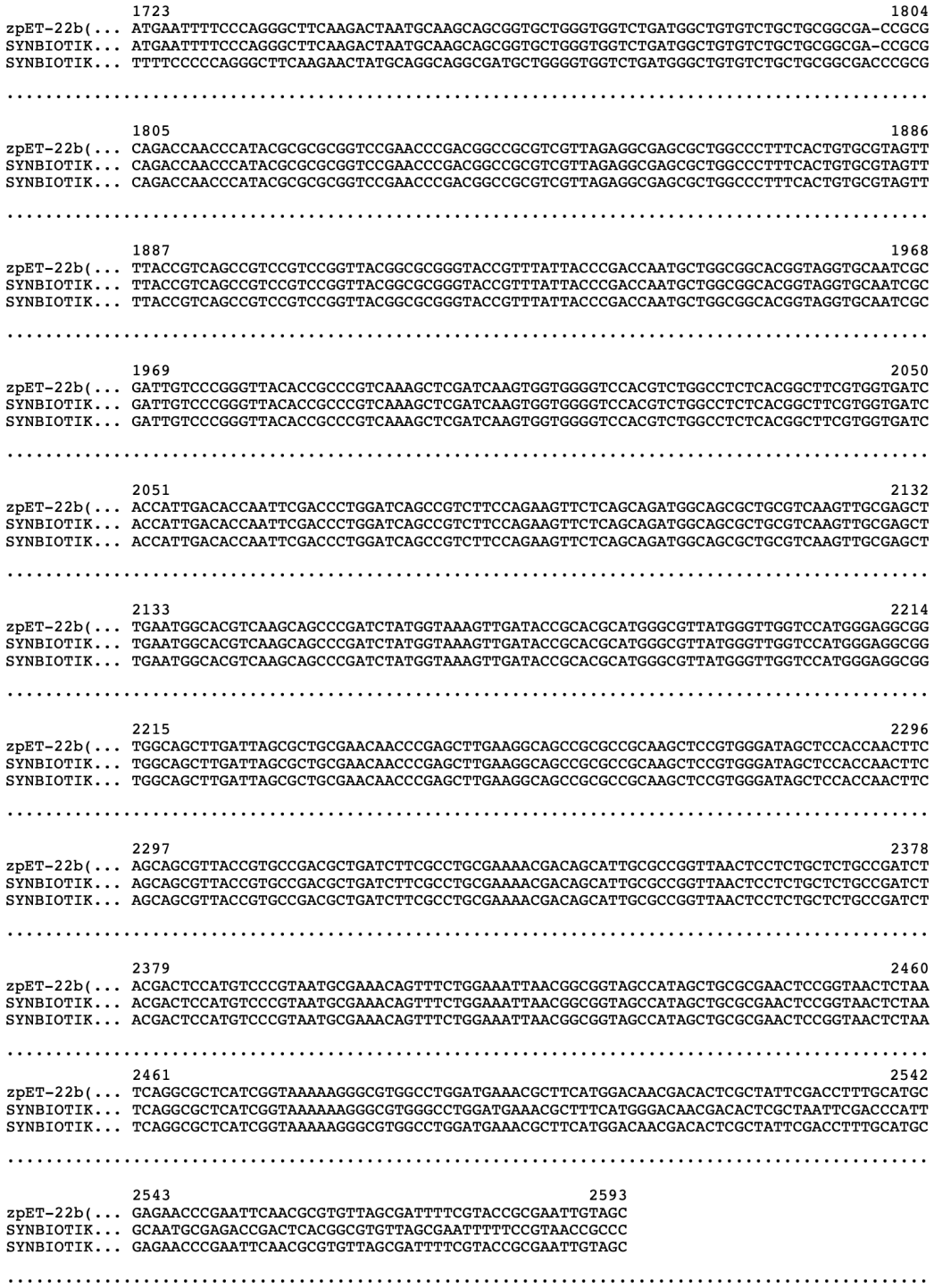

Figure D. 3. Sanger sequencing result for pET-22b(+) – pLacO MicL + pNTetO PETase. Alignment shows the sequencing of the insert, PETase. Alignment done and image retrieved from Benchling.com.

APPENDIX E

ADDITIONAL REACTION RECIPES

Table E. 1. Recipes of LB growth medium and LB agar

Reagent	**Amount**
Tryptone	10 g
Yeast Extract	5 g
NaCl	10 g
Agar (for LB agar)	15 g
dH2O	To 1 L

Table E. 2. Reagent amounts for Q5 Polymerase reactions.

Reagent	**Amount for 25 µL Reaction Volume (Final Concentration)**
Q5 Reaction Buffer (5X)	5 µl (1X)
10 µM Forward Primer	1.25 µl (0.5 µM)
10 µM Reverse Primer	1.25 µl (0.5 µM)
10 mM dNTP	0.5 µl (200 µM)
Template DNA	50 ng
Q5 Polymerase (NEB)	0.5 µl (0.02 U/µl)
Nuclease-free H2O	To 25 µl

Table E. 3. Thermal cycler settings for Q5 Polymerase reactions.

Reaction Step	**Temperature**	**Time**
Initial Denaturation	98 ºC	30 seconds
Polymerization (25 to 35 cycles)	98 ºC	5-10 seconds
	60 – 72 ºC	10-30 seconds
	72 ºC	30 seconds/kb
Final Extension	72 ºC	2 minutes
Hold	4 ºC	∞

Table E. 4. Double restriction enzyme reaction set-up.

Reagent	**Amount for 50 µl Reaction**
DNA	1000 to 3000 ng
10X Cut Smart Buffer	5 µl
Restriction Enzyme #1	1 µl
Restriction Enzyme #2	1 µl
Nuclease-free H2O	To 50 µl

Table E. 5. Recipe for homemade Gibson assembly mixture (1.33X).

Reagent	**Amount**
5X Isothermal Buffer	100 µl
Taq Ligase (40 U/µl)	50 µl
Phusion Polymerase (2 U/µl)	6.25 µl
T5 Exonuclease (1 U/µl)	2 µl
Nuclease free h2O	216.75 µl

Table E. 6. Recipe for 5X Isothermal Buffer.

Reagent	**Final Concentration**
Tris-HCl	500 mM
MgCl2	50 mM
DTT	50 mM
NAD	5 mM
PEG-8000	25%
dNTPs	1 mM from each
Dissolved in dH2O	

Table E. 7. Transformation and Storage (TSS) buffer recipe.

Reagent	**Amount**
1M MgCl2	1.5 ml
DMSO	2.5 ml
PEG 8000	5 g
LB Medium	To 50 ml

Table E. 8. Recipe for HisTrap Binding Buffer (pH 7.4).

Reagent	**Final Concentration**
Sodium Phosphate	20 mM
NaCl	500 mM
Imidazole	20 mM
Dissolved in dH2O	

Table E. 9. Recipe for HisTrap Elution Buffer (ph 7.4).

Reagent	**Final Concentration**
Sodium Phosphate	20 mM
NaCl	500 mM
Imidazole	500 mM
Dissolved in H2O	

Table E. 10. Recipe for M9 Minimal Growth Media.

Reagent	**Amount**
5X M9 Salts	200 ml
1M MgSO4	2 ml
1M CaCl2	0.1 ml
40% Glucose	10 ml
dH2O	To 1 L

Table E. 11. Recipe for 50 mM Glycine-NaOH Buffer (pH 9.0).

Reagent	**Amount**
Glycine	3.75 g
NaOH	0.35 g
dH2O	1 L

Table E. 12. Setup for T4 ligation reaction.

Reagent	**Amount**
Vector DNA	50 ng
Insert DNA	1:1 Molar ratio to vector DNA
T4 DNA Ligase	1 µl
10X T4 DNA Ligase Buffer	2 µl
Nuclease free dH2O	To 20 µl

Table E. 13. Recipe for Coomassie destaining solution

Reagent	**Amount**
Acetic Acid (Glacial)	100 ml
Methanol	500 ml
dH2O	400 ml

Table E. 14. Recipe for 1X Towbin Buffer.

Reagent	**Concentration**
TRIS base	0.025 M
Glycine	1.92 M
Methanol	20% (v/v)
Dissolved in dH2O	

Table E. 15. 1x TBST recipe.

Reagent	**Amount**
NaCl	8.8 g
KCl	0.2 g
TRIS base	3 g
Tween-20	1 ml
dH20	To 1 L

Table E. 16. Recipe for 10x PBS (pH 7.4).

Reagent	**Amount**
Na2HPO4	14.4 g
KH2PO4	2.4 g
NaCl	80 g
KCl	2 g
dH2O	To 1 L

APPENDIX F

ADDITIONAL RESULTS

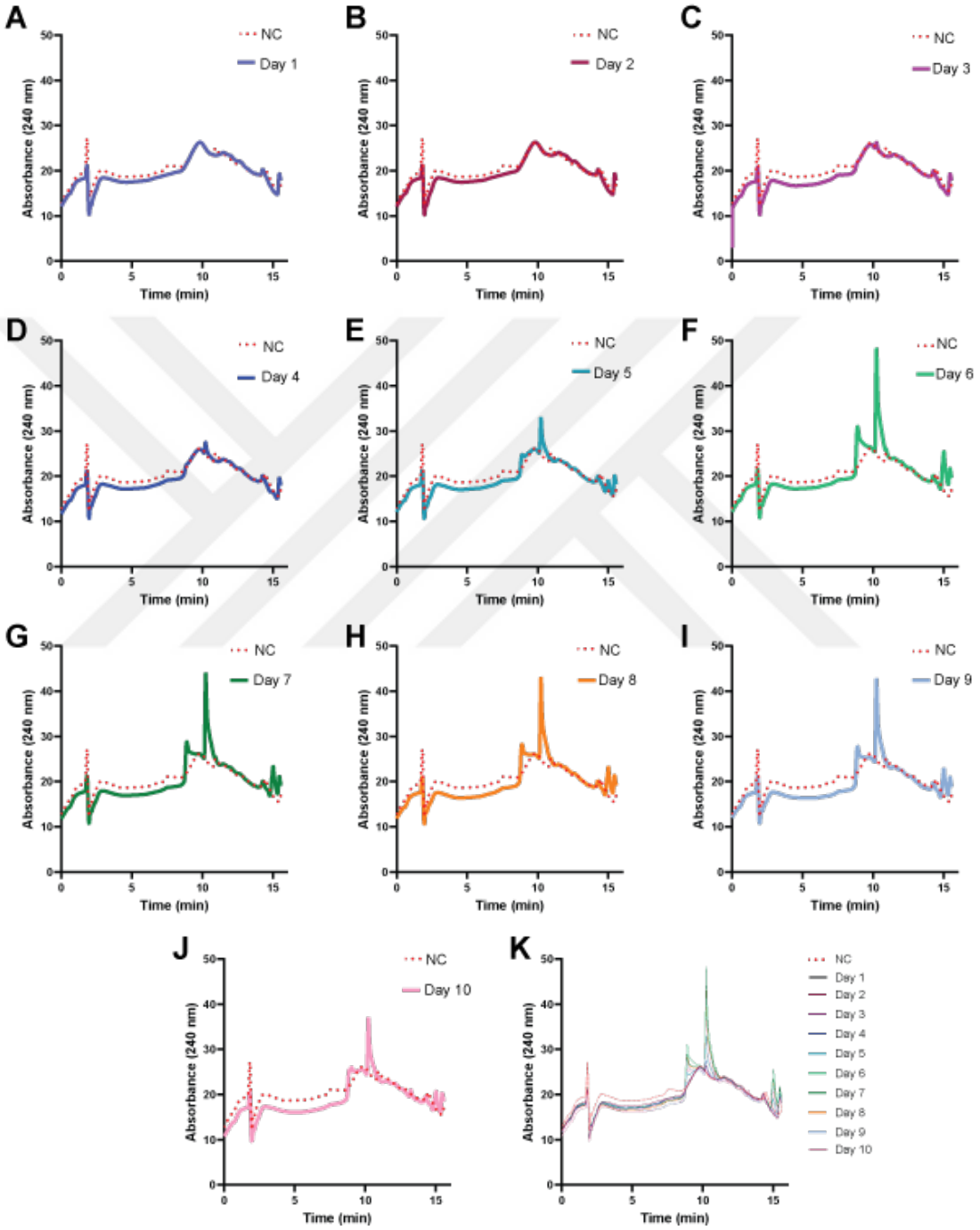

Figure F. 1. HPLC analysis of enzyme refresh group (50 µg/ml) assay. A-J are day 1 to 10 samples, respectively. K is all chromatograms overlapped.

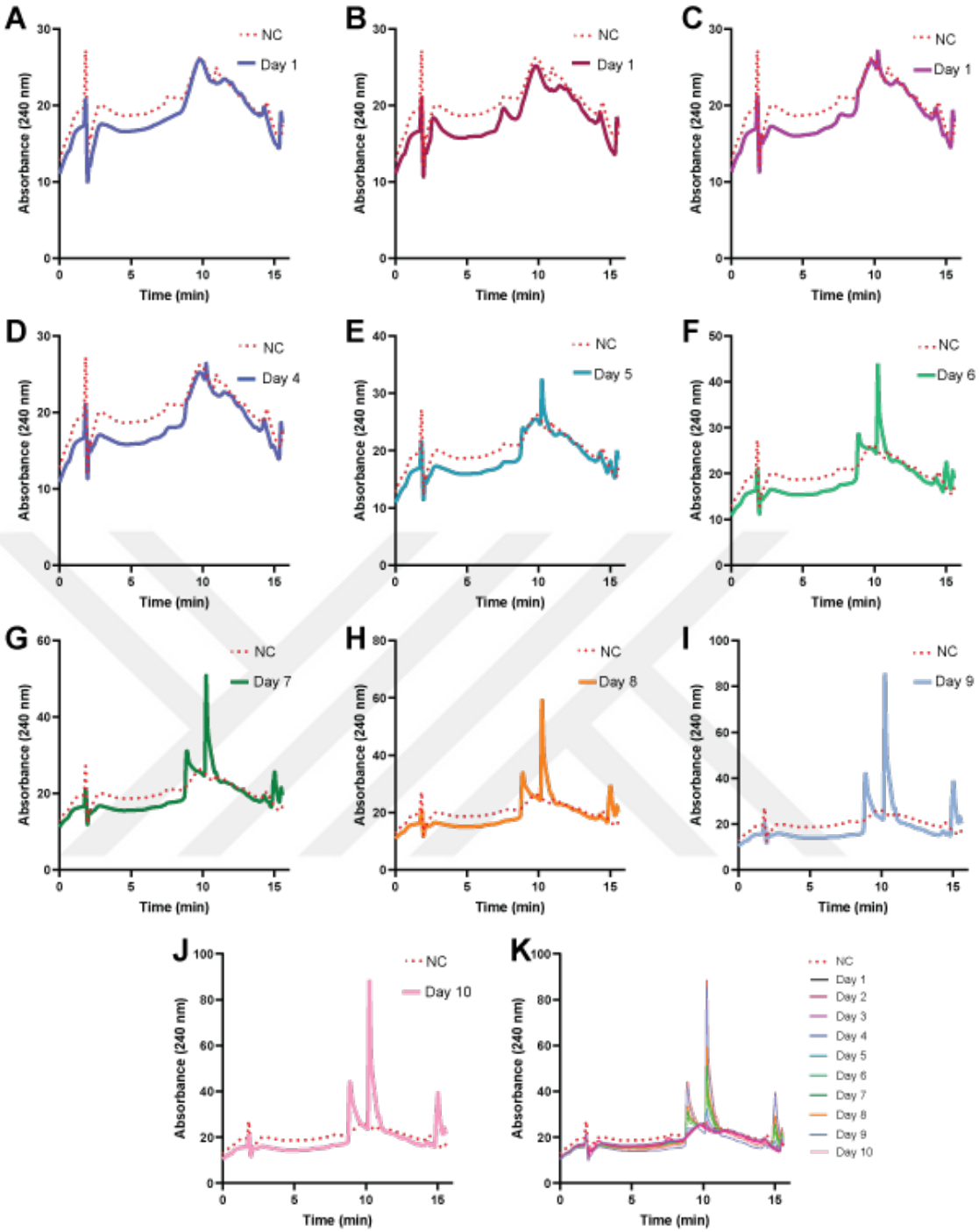

Figure F. 2. HPLC analysis of enzyme refresh group (150 µg/ml) assay. A-J are day 1 to 10 samples, respectively. K is all chromatograms overlapped.